Investigation of the molecular mechanisms of the neuronal differentiation in p2 domain in the spinal cord

Zur Erlangung des akademischen Grades eines

DOKTORS DER NATURWISSENSCHAFTEN

(Dr. rer. nat.)

von der KIT-Fakultät für Chemie und Biowissenschaften

des Karlsruher Instituts für Technologie (KIT)

genehmigte

DISSERTATION

von

Gökhan Cucun, M.Sc.

aus Izmir, Turkey

1. Referent: Dr. Sepand Rastegar

2. Referent: Prof. Dr. Lennart Hilbert

Tag der mündlichen Prüfung: 16.07.2024

Erklärung

Hiermit versichere ich, dass ich die vorliegende Arbeit selbständig verfasst und keine anderen als die angegebenen Quellen und Hilfsmittel verwendet. Die Satzung des Karlsruher Instituts für Technologie (KIT) zur Sicherung guter wissenschaftlicher Praxis wurde beachtet. Insbesondere habe ich wörtlich oder sinngemäß aus anderen Werken übernommene Inhalte als solche kenntlich gemacht. Die Richtigkeit der vorstehenden Erklärungen bestätige ich. Ich versichere an Eides statt, dass ich nach bestem Wissen die reine Wahrheit erklärt und nichts verschwiegen habe.

Datum: _____ Unterschrift: _____

Table of content

Acknowledgements

Firstly, I would like to express my deepest gratitude to my supervisor Dr. Sepand Rastegar for his guidance and encouragement. He always supported me to attend workshops and conferences.

I would like to sincerely thank Prof. Dr. Lennart Hilbert and Prof. Dr. Martin Bastmeyer for their valuable time in reading my thesis.

I would like to thank Dr. Thomas Dickmeis and Dr. Hector Sanchez-Iranzo for their valuable comments and scientific discussions during my PhD and being my thesis advisory committee members.

I am very grateful to my colleague Fushun Chen, for his friendship and contribution to my thesis by analyzing single-cell RNA sequencing data. I am thankful to Jincan Chen for his friendship and scientific discussions. I would like to thank all current and former members of Rastegar group Masa, Tanja, Anne, Melina, Sabrina, Marcel, and Agnes for the friendly environment and their support.

I would like to extend my profound appreciation to my family for supporting me from the beginning of my journey to be a scientist.

List of figures

List of tables

Abbreviations

CRM: Cis-regulatory modules

CSF-cNs: Cerebrospinal fluid contacting neurons

foxn4: Forkhead box N4

gata3: GATA binding protein 3

INs: Interneurons

islr2: Immunoglobulin superfamily containing leucine-rich repeat 2

KA cells: Kolmer-Agduhr cells

nkx1.2lb: NK1 transcription factor related 2-like b

RBs: Rohon Beard neurons

sc-RNA seq: Single-cell RNA sequencing

slc6a5: Solute carrier family 6 member 5

sox1a: SRY-box transcription factor 1a

vsx1: Visual system homeobox 1 homolog, chx10-like

Summary

In this thesis, the heterogeneity of V2s interneurons has been investigated in detail to decipher the transcriptional control of V2 interneurons and its heterogeneity. Single-cell RNA sequencing data with the screening experiments showed that the expression of *nkx1.2lb* gene is distinguished among the identified candidate markers. *Nkx1.2lb* is one of the enriched transcription factors that diversify the V2s populations with its partial expression in *sox1a*-positive V2s interneuron. Attenuation of *nkx1.2lb* gene leads to the reduction of known V2s interneuron markers, suggesting its function is required for the identity of V2s interneurons.

To characterize the transcriptional regulation of *nkx1.2lb*, putative cis-regulatory modules (CRMs) of the *nkx1.2lb* gene were identified with the assistance of ATAC-Seq approach. Six putative CRMs of nkx1.2lb have been identified and their activities were screened with enhancer screening assays. The expression of nkx1.2lb is regulated by CRM-4 exclusively in the heart, while CRM-5 and CRM-6 are sufficient to drive its expression specifically in the spinal cord. Therefore, the expression of *nkx1.2lb* gene is regulated by different putative cis-regulatory modules.

Zusammenfassung

In dieser Arbeit wurde die Heterogenität von V2s-Interneuronen im Detail untersucht, um die transkriptionelle Kontrolle von V2-Interneuronen und ihre Heterogenität zu entschlüsseln. Einzelzell-RNA-Sequenzierungsdaten mit Screening-Experimenten zeigten, dass die Expression des Gens nkx1.2lb unter den identifizierten Kandidatenmarkern hervorsticht. Nkx1.2lb ist einer der angereicherten Transkriptionsfaktoren, die die V2s-Populationen diversifizieren und teilweise in sox1a-positiven V2s-Interneuronen exprimiert werden. Die Abschwächung des nkx1.2lb-Gens führt zu einer Verringerung der bekannten V2s-Interneuron-Marker, was darauf hindeutet, dass seine Funktion für die Identität der V2s-Interneuronen erforderlich ist.

Um die Transkriptionsregulation von nkx1.2lb zu charakterisieren, wurden mit Hilfe des ATAC-Seq-Ansatzes putative cis-regulatorische Module (CRMs) des nkx1.2lb-Gens identifiziert. Es wurden sechs mutmaßliche CRMs von nkx1.2lb identifiziert und ihre Aktivitäten mit Enhancer-Screening-Assays untersucht. Die Expression von nkx1.2lb wird durch CRM-4 ausschließlich im Herzen reguliert, während CRM-5 und CRM-6 ausreichen, um die Expression speziell im Rückenmark zu steuern. Daher wird die Expression des nkx1.2lb-Gens durch verschiedene mutmaßliche cis-regulatorische Module reguliert.

1. Introduction

1.1 Development of Spinal cord

The spinal cord is the part of the central nervous system (CNS) with the brain. Appropriate spatial and temporal differentiation of cells is essential to produce cellular heterogeneity in the nervous system. After gastrulation, the neural keel is formed after the folding of the neural plate (Papan and Campos-Ortega, 1994). During development, the neural keel rounds up sequentially to form the neural rod and the cavitation of the neural rod leads to the formation of neurocoele in the neural tube (Figure 1).

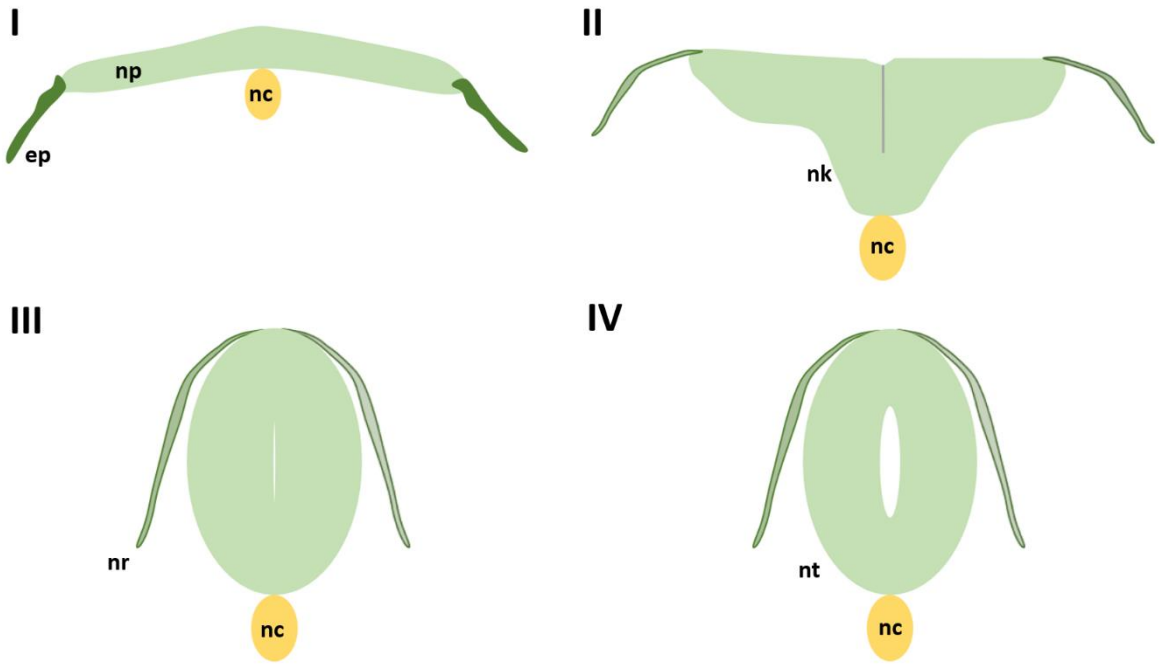

Figure 1: Consecutive stages for the formation of neural tube in zebrafish. ep: epidermis, np: neural plate, nc:notochord , nk: neural keel, nr: neural rod, nt: neural tube. Adapted from (Papan and Campos-Ortega, 1999, 1994)

The posterior neural tube is comprised of eleven distinct progenitor domains which are exposed to a combination of morphogens during development (Andrews et al., 2019; Cucun et al., 2024; Dessaud et al., 2008; Sagner and Briscoe, 2019). The morphogen gradients are primarily sourced from roof plate providing BMP and Wnt signaling dorsally, and floor plate with notochord is the main source of Shh signaling ventrally (Danesin et al., 2021; Farreny et al., 2018; Miller et al., 2004; Shinozuka and Takada, 2021; Xing et al., 2018). Dorso-ventral

morphogen gradients induce domain-specific transcription factors in each domain which leads to initiation of different transcriptional networks in each section (Figure 2).

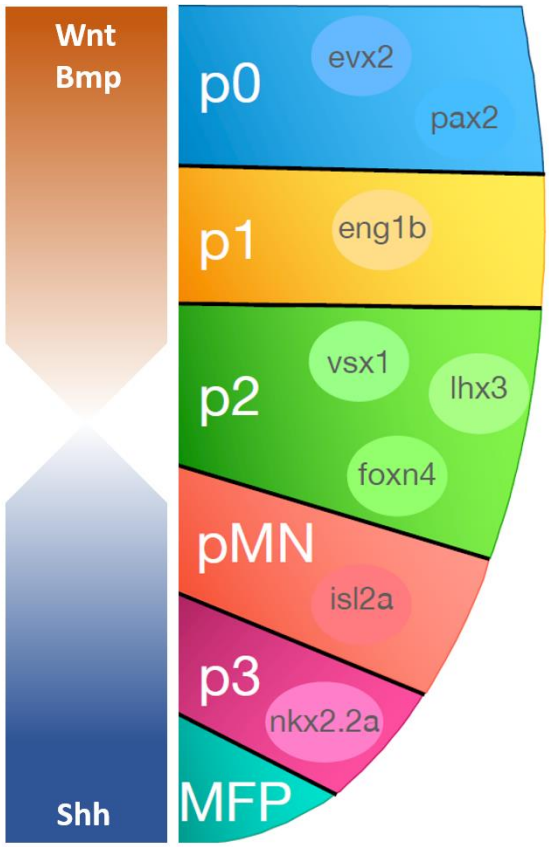

Figure 2: Dorso-ventral positions of the progenitor domains in the ventral spinal cord. Ventral interneurons consist of five distinct progenitor domains. Dorsally located P0 domain expressing *evx2* and *pax2* generates commissural V0 interneurons, p1 domain expressing *eng1b* is the source of V1 interneurons, p2 domain expressing *vsx1*, *foxn4*, and *lhx3* gives rise to V2 interneurons, pMN domain expressing *isl2a* produces motor neurons, ventrally located p3 domain generates V3 interneurons.

Later, each domain produces eleven distinct cell populations. These progenitors are mainly divided into two main domains; six dorsal domains (dI1, dI2, dI3, dI4, dI5, and dI6), and five ventral domains (p3, pMN, p2, p1, and p0). Dorsal progenitors produce sensory interneurons which are essential for detection of sensory information and information processing. Ventral progenitors are the central part of motor function and locomotion (Frank and Mendelson, 1990; Imai and Yoshida, 2018; Smith et al., 2012) . Spinal cord is the center of coordinated movement which requires a complex neuronal circuits between sensory neurons, interneurons and motor neurons (Rayon et al., 2021). Initiation of locomotion is triggered

primarily by external stimulus which served as an input for the propagation of signals detected by sensory neurons. In zebrafish, mechanosensory Rohon Beard (RB) neurons supply sensory input to dorsally located sensory interneurons (Katz et al., 2021; Williams and Ribera, 2020). These sensory neurons relay received signals to the interneurons. The interneurons process the signals and transmit signals to motor neurons through complex axonal processes (Umeda and Shoji, 2017). In ventral part, pMN domain contributes to production of both primary and secondary motor neurons that are modulated by the interneurons (Masahira et al., 2006; Todd et al., 2012; Xing et al., 2022).

1.2 Signaling pathways

1.2.1 BMP Signaling pathway

BMP signaling consists of target cells possessing type I and type II BMP receptors and a variety of secreted ligands including BMPs, transforming growth factor (TGFs), growth/differentiation factors (GDFs), anti-Müllerian hormone (AMH), and activins. Type I and type II receptors are transmembrane cell surface receptors with kinase activity (Kretzschmar et al., 1997; Mohedas et al., 2013). An efficient activation of the receptor complex for its activity necessitates a ligand dimer with two type I and type II receptors (Agnew et al., 2021; Mueller, 2015; Nickel and Mueller, 2019). Type I receptor contains a Glycine/Serine-rich domain that is phosphorylated by type II receptor for intracellular kinase activity which is required for the phosphorylation of downstream mediators known as SMADs (Tajer et al., 2021; Wine-Lee et al., 2004) . SMADs mainly consist of MH1 domain in N-terminus and MH2 domain in the C-terminus, these domains are connected with a proline rich linker (Dennler et al., 1999; Grishin, 2001; Ruiz et al., 2021). MH1 domain is required for its DNA-binding activity, while MH2 is essential for interaction between SMADs and their interacting partners such as Smurf1 (Attisano and Tuen Lee-Hoeflich, 2001; Hill, 2016; Yan et al., 2016). SMADs are divided into three subgroups: inhibitory SMADs, common mediator SMADs, and receptor-regulated SMADs (RSMADs) (Feng and Derynck, 2005; Massagué et al., 2005; Werner et al., 2000). Upon receptor activation, RSMADs interact with common mediator SMAD4, by forming a heteromeric complex to translocate into nucleus, where they bind either SMAD-binding elements (SBE) or transcription factor together with activators/repressors and histone modifying proteins to regulate target gene expression (Dennler et al., 1999; Koinuma et al., 2009; Pierreux et al.,

2000). Additionally, BMP receptors can activate SMAD-independent pathways such as MAPK, ERK and JNK pathways (Massagué et al., 2005; Miyazono et al., 2005; Mukai et al., 2007; Zhou et al., 2007). For instance, the Tak1/p38 pathway is activated by BMPs through the ubiquitination of Traf6 protein (Sorrentino et al., 2008; Yamashita et al., 1996). BMP signaling coordinates various developmental processes including embryonic patterning, morphogenesis, neuronal induction and cell differentiation (Beederman et al., 2013; Eldar et al., 2002; Fainsod et al., 1997; Merino et al., 1998). Phylogenetic analysis revealed the conservation of BMP receptors and its ligands in the animal kingdom (Lochab and Extavour, 2017; Nikaido et al., 1997; Samuel et al., 2001). The BMP5/6/7/8 are the orthologue of *Drosophila glass bottom boat* (Gbb/60A) and *Screw* (scw), while BMP2/4 show high similarity with *Drosophila Decapenthaplegic* (dpp) (Le Dréau and Martí, 2013; Schmierer and Hill, 2007). The BMPs are secreted from the roof plate cells to govern the development of both neural crests and dorsal neurons which have sensory function in the spinal cord during development and adulthood (Caspary and Anderson, 2003; Chizhikov and Millen, 2005, 2004). BMPs are involved in the generation of distinct dorsal interneurons. For instance, BMP7 regulates the production of dI1-dI3 and dI5 dorsal interneurons through Sma1 and Smad5 activity (Le Dréau and Martí, 2012). It has been demonstrated that BMP signaling is required for the formation and differentiation of dorsally located *tlx3* and *isl1*-expressing Rohon-Beard sensory neurons in the developing spinal cord (Appel et al., 1995; Korzh et al., 1993; Nguyen et al., 2000). In the dorsal region of the spinal cord, BMP signaling cooperates with Wnt signaling to harmonize the neurogenesis. (Kléber et al., 2005) showed that Wnt activity is antagonized by BMP2 in sensory neurogenesis. The regulatory role of BMP signaling is not only restricted to the dorsally located sensory neurons, however it is involved in the formation of proper architecture of motor circuits organized in pMN domain, through *atlastin 1* which regulates the type 1 receptor trafficking (Fassier et al., 2010).

1.2.2 Sonic Hedgehog signaling pathway

The Sonic Hedgehog pathway is divided into two major mechanisms depending on the involvement of Gli proteins; (1) Canonical Sonic Hedgehog pathway which requires ligand-binding activity to receptor associating with the activation of Gli protein, and (2) Non-canonical Sonic Hedgehog pathway also referred as Gli-independent mechanisms in which

cyclin B1 is essential and regulator for the pathway activity (Blotta et al., 2012; Polizio et al., 2011; Robbins et al., 2012). Canonical Sonic Hedgehog signaling mainly consists of Shh, Patched 1 (Ptch1), Smoothened (Smo), SUFU, and Gli proteins (Choudhry et al., 2014; Rimkus et al., 2016). Shh ligands undergo several posttranslational modifications which are crucial for their activities such as palmitoylation (Buglino and Resh, 2008; Chen et al., 2004). Palmitoylation of Shh ligands is an essential step for pathway activation (Resh, 2021). After posttranslational modifications of Shh ligands, firstly, the ligands (45 kDa) are synthesized as a precursor, after that the ligands undergo proteolytic cleavages on their both N-terminus and C-terminus giving rise to Shh-N (19 kDa) and Shh-C (26 kDa), respectively (Bumcrot et al., 1995; Resh, 2021; Roelink et al., 1995). Ptch1 is a 12-pass transmembrane protein that acts as a harbor for Shh ligands for the pathway activity (Fleet and Hamel, 2018; Lindström et al., 2006). Smo is another membrane protein with 7 transmembrane structures which is inhibited by Ptch1 protein in the absence of Shh ligands (Milenkovic et al., 2009). On the contrary, in the presence of Shh ligands, Ptch1 protein is internalized and targeted to endosomal degradation pathway therefore smo proteins are recruited to cilia (Bijlsma et al., 2012; Milenkovic et al., 2009). Shh signaling plays a central role in biological processes including tissue homeostasis, neural tube development, and nervous system repair (Bond et al., 2013; Patten and Placzek, 2000; Petrova and Joyner, 2014; van den Brink, 2007). Disrupted Shh signaling is linked to developmental disorders and diseases (Mangum et al., 2016; Ming et al., 1998; Rimkus et al., 2016). Shh signaling is provided by two main structures in the developing spinal cord; floor plate and notochord (Jeong and Epstein, 2003; Yu et al., 2013). Shh signaling is known to act as a primary signaling pathway which tailors and required for ventral spinal cord patterning mediated by both Gli2 and Gli3 (Jessell, 2000; Lee and Pfaff, 2001; Litingtung and Chiang, 2000). However, in contrast to mammalian ventral neurons, the generation of some of the ventral neurons (V2, V1 and, V0v interneurons) in zebrafish is not affected in the absence of Shh signaling, but solely the generation of motor neurons and V3 neurons are hampered (England et al., 2011). It has been also stated that the continuous gradient combination of *shh* with *tiggywinkle hedgehog (twhh)* determines the dorsoventral positioning of olig2-expressing motor neuron progenitors and propagation of oligodendrocyte progenitor cells (OPCs) (Farreny et al., 2018; Park et al., 2004; Xu et al., 2020).

1.2.3 Wnt signaling pathway

Wnt signaling is highly conserved and involves in various biological processes which are essential for development, tissue patterning and homeostasis (Pond et al., 2020; Steinhart and Angers, 2018; Wodarz and Nusse, 1998). Interaction between Wnt and receptors together with co-receptor is essential for the pathway activation. Its activation is initiated with binding of Wnt ligand to seven transmembrane receptor named Frizzled, together with a co-receptor, low-density lipoprotein receptor 5/6 (LRP5/6) (Grainger and Willert, 2018; Kikuchi et al., 2011; Wodarz and Nusse, 1998). Variety of Wnt ligands have been identified and their interactions with aforementioned receptors diversify the pathway functions. According to involvement of β-catenin, this pathway can be broady classified into two; Canonical Wnt signaling (β-catenin-dependent Wnt signaling), Non-canonical Wnt signaling (β-catenin independent Wnt signaling). β-catenin plays an essential role for transcriptional regulation of Canonical Wnt target genes. β-catenin protein possesses armadillo sequences which is necessary for its nuclear transportation (Funayama et al., 1995; Loureiro and Peifer, 1998). In Wnt off state, cytoplasmic β-catenin is degraded by the destruction complex which consists of adenomatous polyposis coli (APC), Glycogen Synthase Kinase 3-β (GSK3-β), Axin, and Casein kinase (CK1α) (Kim et al., 2012; Tacchelly-Benites et al., 2018). In Wnt-on state, binding of Wnt glycoprotein to receptors destabilize the destruction complex which leads to translocation of cytoplasmic β-catenin into nucleus (Shah and Kazi, 2022; Tacchelly-Benites et al., 2018) . After translocation, β-catenin interact with T-cell factor/Lymphoid enhancer factor (TCF/LEF) grumolato paper to induce cell-specific target gene expression. Canonical Wnt signaling has been associated with neuronal specification, determination of neuronal fate and maintenance of neuronal identity (Bonner et al., 2008; Ille et al., 2007; Muroyama et al., 2002; Shimizu et al., 2005) . Specifically, Wnt pathway plays essential role for the induction of markers genes in the dorsal spinal cord. Wnt3a induce the expression of *LH2*, *Islet1*, and Pax2 transcription factors which are the markers of D1, D2, and D3, respectively (Muroyama et al., 2002). In addition, mitogen activity of dorsal interneurons are regulated by Wnt signaling pathway through regulation of cyclin D1, ad cyclin D2 (Ille et al., 2007; Megason and McMahon, 2002).

1.2.4 Notch signaling pathway

Notch pathway is evolutionarily conserved signaling pathway which is involved in neurogenesis, neuronal differentiation (Cornell and Eisen, 2002; Diotel et al., 2020; Gerber et al., 2019; Mahler et al., 2010; Oliveira-Carlos et al., 2013; Shin et al., 2007). Notch ligands are transmembrane proteins containing DSL (Delta, LAG-2 and Serrate) domain that is pivotal for the pathway activity by interacting with Notch receptors (Cordle et al., 2008; Gazave et al., 2009; Wang, 2011). Extracellular portion of Notch receptors possess LIN repeats and RAM domain is located intracellular part together with nuclear localization signals (Kimble and Simpson, 1997; Ma et al., 2023; Zhou et al., 2022) . Activation of Notch pathway requires the binding of Delta ligand on one cell to Notch receptor on adjacent cell. The interaction between ligand and Notch receptor leads to the proteolytic cleavage of the receptor in two steps liberating Notch intracellular domain (NICD). After that, NICD translocates into the nucleus interacting with DNA-binding proteins such as LAG-1 to induce the expression of downstream target genes (Song et al., 1999). Notch signaling has been characterized in the determination of the neuronal cell fate decision in different ways. For instance, inhibition of Notch pathway through NOTCH1 reprograms astrocytes to become neurons in the spinal cord (Tan et al., 2022). The roles of Notch pathway are already examined in the development and fate cell specification of ventral neurons in the spinal cord (Gerber et al., 2019; Schäfer et al., 2007). Generation of lateral floor plate (LFP) progenitors and p3 cells depends of the Notch pathway (Schäfer et al., 2007). Notch activity is involved in the determination of the fate of LFP progenitors to differentiate into Kolmer-Agduhr" (KA") (Huang et al., 2012; Jacobs et al., 2022). In zebrafish, Notch mutant exhibits increased number of V2a interneurons at the expense of V2b interneurons. Combinatory functions of different Notch ligands (Delta A, Delta C, Delta D) with its receptors (Notch1a, Notch1b, and Notch3) possess essential roles in V2 interneuron specification. In detail, Mib1 activates Delta A and Delta D ligands to preserve P2 progenitors, and Delta A with Delta C control the fate of V2a and V2b interneurons redundantly. Notch1a, Notch1b, and Notch3 are involved in the proliferation of p2 progenitors and only Notch1a primarily contributes to the determination of V2a/V2b cells (Mizoguchi et al., 2020). Downstream effector, *her15.1* differentially expressed in V2 lineage. The maturation of V2b interneurons relies on transient expression of *her15.1*. Contrarily, decreased expression of *her15.1* is required for axon genesis in V2b interneurons (Mizoguchi

et al., 2020). In addition, the differentiation of V2s interneurons from V2b/V2s progenitor cells necessitates the activity of Notch pathway (Gerber et al., 2019).

1.3 Generation of V2 Interneuron Populations

1.3.1 V2a Interneurons

In p2 progenitor domain, *vsx1*$^{+}$ progenitors are the source of two temporally distinct intermediate progenitors; early-formed V2a/b sister pairs, which constitute 75% of intermediate progenitors, and V2b/s sister pairs constitute 25% of total intermediate progenitor. (Bello-Rojas and Bagnall, 2022; Del Barrio et al., 2007; Gerber et al., 2019; Peng et al., 2007) (Figure 3). V2a INs are generated from V2a/b sister pairs together with V2b INs (Kimura et al., 2008, 2006). V2a INs possess ipsilaterally descending projections and locates more dorsally compare with V2b INs (Kimura et al., 2006; Menelaou and McLean, 2019). V2a INs are marked by the expression of homeodomain-containing repressor, *visual system homebox 2 homolog (vsx2, also named Chx10)* transcription factor together with one of the glutamatergic excitatory markers named *solute carrier family 17 member 6b (slc17a6b)* genes (Batista et al., 2008; Kimura et al., 2008, 2006). *Vsx2* has a crucial role in the fate specification and differentiation of V2a interneurons (Clovis et al., 2016). V2a INs share some transcription factors with other ventral interneurons such as motor neuron progenitors even these two population is derived from separate progenitor domains, but dissimilar downstream effectors induce different molecular programs in cell-fate decision in these cells (Ericson et al., 1997; Thaler et al., 1999). For instance, *vsx2* specifies V2a interneurons by suppressing motor neuron fate through its transcriptional repressor activity in p2 progenitors, while one of the downstream LIM-homeodomain factor, lhx3 is expressed in both V2a interneuron and motor neurons, but *lhx3* interacts with *isl1* to acquire motor neuron identity in motor neuron progenitors (Clovis et al., 2016). In addition to *lhx3*, also single-strand DNA-binding proteins (*ssdp1 and ssdp2*) are expressed in both cell types. However, *ssdp1/2* induces transcriptional activity of LIM complexes which have a crucial role during differentiation stages of both motor neurons and V2a interneurons by forming hexameric and tetrameric complexes with *lhx3* and *NLI*, respectively (Thaler et al., 2002). Furthermore, *lhx3* is sufficient together with *lhx4* to promote the expression of *vsx2* in chick and required for differentiation of both V2a and V2b INs (Seredick et al., 2014; Tanabe et al., 1998; Thaler et al., 1999). (Skaggs et al., 2011) also

showed that Class B Basic Helix-Loop-Helix Protein 5 *(Bhlhb5)*, currently retitled *Bhlhe22*, promotes the expression of one of the ligands for Notch signaling, *delta like-4 (Dll4)* in V2a INs. Decreased expression level of *bhlhb5* leads to a reduced number of V2a INs and an increased number of V2b INs (Skaggs et al., 2011). Another vsx gene, *vsx1,* has been found as an essential transcription factor for the fate of V2a INs by binding *tal1* promoter directly to inhibit its transcriptional regulation, which results in an increased tal1-positive V2b cells (Zhang et al., 2020).

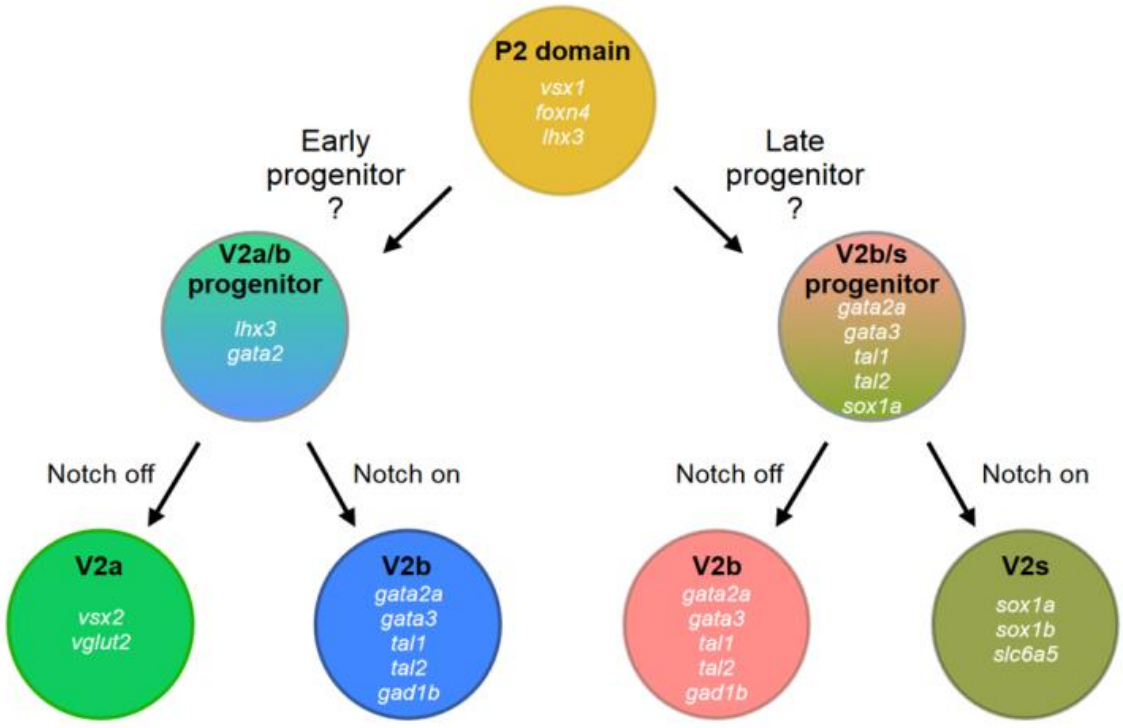

Figure 3: Development of V2 interneurons in the spinal cord. P2 domain gives rise to two temporarily distinct progenitors. P2 domain express *vsx1, foxn4,* and *lhx3* markers. V2a/V2b progenitor is an early produced progenitor and expresses *lhx3* and *gata2* marker genes generating V2a interneurons with V2b interneurons. V2a interneurons express *vsx2* and *vglut2* marker genes. V2b interneurons express *gata2a, gata3, tal1, tal2 and gad1b*. Lately produced progenitor named V2b/V2s progenitor expressing *gata2a, gata3, tal1, tal2, sox1a*. V2b/V2s progenitor generates V2b and V2s interneurons. V2s interneurons express *sox1a, sox1b* and *scl6a5*. (Adapted from (Cucun et al., 2024))

V2a INs are the part of locomotion and sensory signaling with its diverse subclasses, which have varying connections to sensory neurons and motor neurons to modulate the swimming

behaviour during diverse motions (Knafo et al., 2017; Pallucchi et al., 2022; Sengupta et al., 2021). Furthermore, the activation of circumferential descending (CiD) vsx2-positive V2a INs are triggered by Mauthner neurons during escape behavior (Berg et al., 2018). Also, they are the part of the module that is involved in mechanosensory feedback modulation pathway together with Rohon-Beard cells during escape movement (Knafo et al., 2017) (Figure 4).

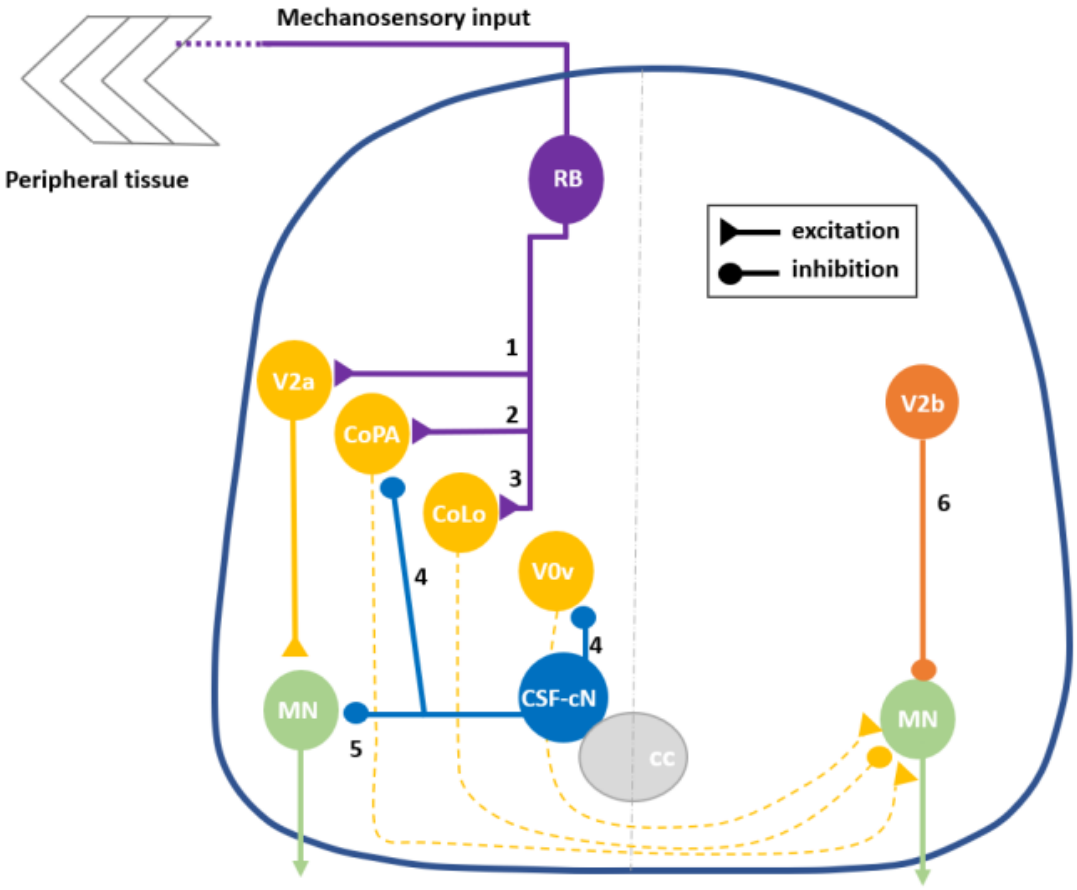

Figure 4: Sensory signaling and processing in the zebrafish spinal cord. Diagram showing the interaction between sensory neurons and interneurons with motor neurons. Rohon Beard neurons (RBs) and cerebrospinal fluid contacting neurons (CSF-cNs) receive sensory inputs from the peripheral tissues and the central canal (cc), respectively to relay sensory information through V2a interneuron (V2a), commissural primary ascending (CoPA), commissural local (CoLo), V0v and V2b interneuron during active locomotion. (1) Swim speed enhancement (2) Sensorymotor gating and escape behaviour (3) Modulation of motor neuron excitability (4) Locomotor output modulation (5) Direct modulation of motor neuron activity (6) Speed specific circuit. MN: motor neuron, dashed lines: commissural axons. Adapted from (Henderson et al., 2019).

Additionally, their function is known in speed modulation that slow-type V2a INs are involved in the regulation of locomotion speed by being target of inhibitory V1 INs (Kimura and Higashijima, 2019). Thereby, this heterogeneity of V2a IN with their different target neurons provides a rich repertoire of locomotion. However, the classification of heterogeneity of V2a INs is under debate, since it is not possible to classify them according to their anatomical differences, but instead it is possible to grouped them into different subgroups with the help of their electrophysiological properties with neuronal tracing approaches; Type I and Type II V2a INs (Ampatzis et al., 2014; Pallucchi et al., 2022). Type I V2a INs contact solely to caudal primary motor neurons via chemical synapses, while Type II V2a INs are connected widely to pMNs regardless of their innervation via mixed chemical and electrical synapses (Pallucchi et al., 2022). Recent single-cell transcriptomic study proposed that these two types of V2a INs are distinct at the transcriptional level, too. Type I V2a INs express strongly *vsx2* together with *shox2* gene, while *vsx2* is weakly expressed in Type II V2a INs with no *shox2* expression (Kelly et al., 2023). In addition to their roles in the locomotion and sensory information processing, they mediate cholinergic input despite their glutamatergic identity to modulate the proliferation of neural stem/progenitor cells (NSPCs) by connecting both monosynaptically and polysynaptically during exercise controlled neurogenesis in adult zebrafish spinal cord (Chang et al., 2021).

1.3.2 V2b Interneurons

V2b INs are generated by the final division of pair producing *vsx1*$^{+}$ p2 progenitors (Bello-Rojas and Bagnall, 2022; Del Barrio et al., 2007; Karunaratne et al., 2002; Kimura et al., 2008; Okigawa et al., 2014; Peng et al., 2007). V2b cells are a group of interneurons possessing ipsilateral descending projections (Batista et al., 2008). Transcriptional regulation of V2b INs are elucidated by the combinatory expression of several transcription factors; *GATA binding protein 2a (gata2a)*, *GATA binding protein 3 (gata3)*, *T-cell acute lymphocytic leukemia 1 (tal1)*, *and T-cell acute lymphocytic leukemia 2 (tal2)* with glutamate decarboxylase 1b (gad1b) in the p2 domain (Batista et al., 2008; Bello-Rojas and Bagnall, 2022; Del Barrio et al., 2007; Kimura et al., 2008, 2006). These transcription factors regulate their transcriptional activity, and the same gene regulatory network also found in the midbrain region. For example, *tal1* plays an important role to form GABAergic V2b identity which resembles the role of *tal2* in the formation of GABAergic neurons in midbrain of zebrafish (Wang et al., 2023; Zhang et al.,

2020). Nevertheless, *tal1* labels more mature GABAergic neurons and possibly in cooperation with *tal2* to acquire GABAergic identity in midbrain of mice (Achim et al., 2013). In tal1 mutants, the expression of *tal2* is not detectable in the p2 domain, suggesting *tal1* regulates the expression of *tal2*, however it is not clear whether *tal1* binds directly to *tal2* promoter or its regulatory elements to repress its expression in the maintenance of V2b INs pool (Andrzejczuk et al., 2018). Another transcription factors that are important to acquire GABAergic identity of V2b cells are both *gata2a* and *gata3*. Double knock-down analysis indicates that these transcription factors are essential to maintain GABAergic identity of V2b INs (Andrzejczuk et al., 2018; Gerber et al., 2019). Intriguingly, one of the p2 progenitor markers, foxn4, are involved in the determination of the fate of V2b INs by inducing the expression of *Mash1* (an orthologous gene of the zebrafish *achaete-scute family transcription factor bHLH 1a-ascl1*) and *delta-like 4 (Dll4)* to specify *gata2*-expressing V2b INs (Danilova et al., 2004; Del Barrio et al., 2007; Gouge et al., 2001; Li et al., 2004). Mutant and knockdown experiments indicate that *ascl1* is not the main regulatory transcription factor, but it engages in the development of Kolmer- Agduhr (KA) cells (Di Bella et al. 2019). V2b INs are the part of flexor-extensor alternation in limbed animals (Britz et al., 2015; McCrea and Rybak, 2008; Zhang et al., 2014). V2b INs directly act as an inhibitory role on axial motor neurons in speed-specific circuit (Callahan et al., 2019) (Figure 2).

1.3.3 V2s Interneurons

Emergence of another interneuron population named V2c is firstly proposed in the mice with the expression of *Sox1* in p2 domain of ventral spinal cord (Harris et al., 2019; Panayi et al., 2010). This interneuron population expresses *Sox1* gene, and do not express any identified V2a, and V2b interneuron markers, but they are lineally associated with V2b INs, since the origin of V2c INs are *Gata3*$^{+}$ cells (Panayi et al., 2010). The fate choice between V2b and V2c interneurons are relies on the presence of *Sox1* gene. In the absence of *Sox1* gene, V2b interneurons are generated in high numbers with less V2c INs, so the expression of *Sox1* gene is required for the maintenance of V2c interneuron pool in mice. The characteristics of V2c IN are not well studied in terms of its neurotransmitter identity, and synaptic connections with axonal projection in mice. Recently, a novel interneuron population named V2s has been characterized in zebrafish. V2s INs are generated from the late progenitor, V2b/V2s sister pairs, which express *gata2a*, *gata3*, *tal1*, *tal2*, *sox1a*, and *sox1b* transcription factors between

16 hpf and 30 hpf (Gerber et al., 2019) (Figure 3). One of the lately formed progenitors loses the expression of *gata2a*, *gata3*, *tal1*, and *tal2*, but maintains the expression of *sox1a* with *sox1b* and destined to commit V2s INs (Gerber et al., 2019) . In the absence of both *sox1a*, and *sox1b* transcription factors, lately produced V2b/V2s sister pairs generate more *gata3*$^{+}$, *tal1*$^{+}$, and *tal2*$^{+}$ V2b INs demonstrating that origin of V2c INs in mammalian and V2s in zebrafish are originated from *gata3*$^{+}$ interneurons (Gerber et al., 2019; Panayi et al., 2010) . V2s INs mainly develop and differentiate into glycinergic inhibitory interneurons with the distinct expression of *slc6a5* gene between 24 hpf to 30 hpf. The characteristics of V2s INs are recognizably distinct from other V2 INs, possessing oval-shaped soma with ipsilaterally extending long axon that bifurcates ventrally (Gerber et al., 2019). (Figure 5).

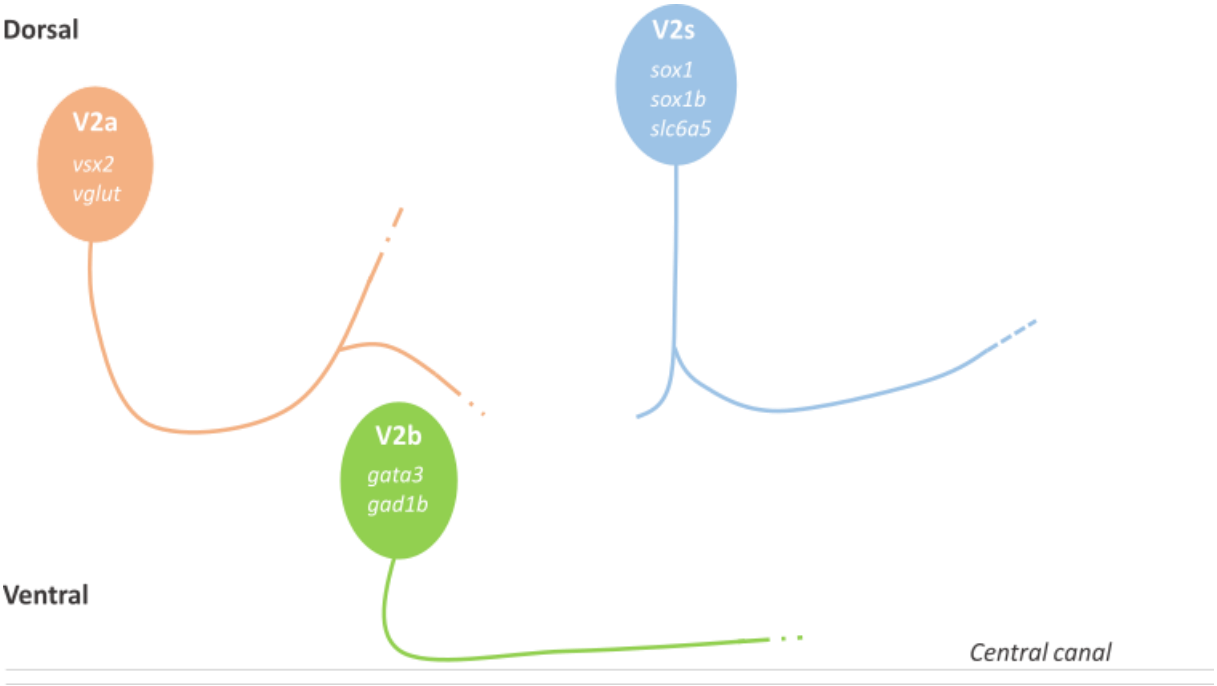

Figure 5: V2 subtypes with their expression marker genes. P2 domain generates three distinct cell populations in developing zebrafish spinal cord. V2a cells are circumferential descending interneurons and express *vsx2* transcription factor with *vglut2* glutamatergic neuron marker. V2b cells are ventral lateral descending interneurons expressing *gata3* transcription factor with *gad1b* gabaergic neuron marker. V2s cells are located more dorsal compared to other V2 cells, and possess long ipsilateral descending axon. V2s cells express *sox1a*, *sox1b* and glycinergic marker *slc6a5*.

1.4 Gene regulation

Gene regulation is a complex and fine-tuned process, which consists of a variety of regulatory elements. As already pointed out above, a broad range of signaling pathways induce neurogenic transcription factors (TFs) in neurons. Combinatorial expression of these transcription factors determines the identity of neurons. Transcription factors are essential elements that possess DNA-binding domain to regulate the transcription of target genes. Target genes contain specific DNA sequences to be recognized by DNA-binding domain of TFs. Promoter is a cis-regulatory element where transcription process is initiated (Dvir et al., 2001; Hochheimer and Tjian, 2003) . Transcription of eukaryotic genes entails binding of RNA-polymerase to the promoter region of the gene. The core promoter region is sufficient for initiation of transcription. Core promoter regions of the gene contain thymine (T) and, adenine (A) nucleotide repeats named TATA box, and general RNA polymerase II Transcription factor TFIID binds directly to TATA box region with TATA-binding proteins in the promoter to initiate the transcription process (Starr and Hawley, 1991). TATA box region is only initiator of transcription process also it is an essential determinant for the direction of transcription (Xu et al., 1991). Enhancers are also considered as cis-regulatory elements which are non-coding DNA region. The genomic position of enhancers varies, they can be situated in the up-and down-stream region, and in the intron region of the target gene (Figure 6).

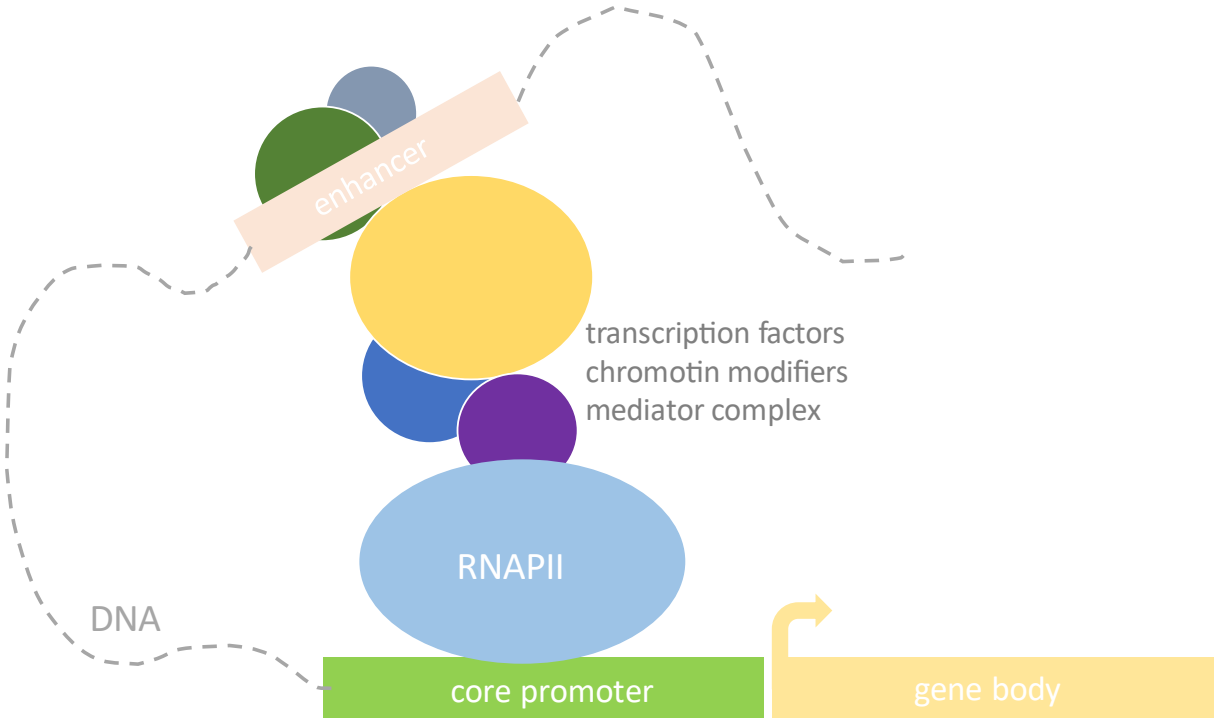

Figure 6: Transcriptional regulation of gene expression. Depiction of cis-regulatory modules in the regulation of the gene expression. Distally located enhancer (cis-regulatory modules) physically interact with transcription factors, chromatin modifiers and mediator complex to stabilize the position of RNA polymerase II (RNAPII) to enhance the expression of the target gene. Adapted from (Carullo et al., 2020)

Identification of enhancers is crucial to understanding which regulatory pathway is involved in the regulation of target gene. Enhancers harbor transcription factor binding sites to activate and enhance the transcription process spatiotemporally. For this reason, chromatin remodeling is an essential step for the binding of TFs to enhancers. This process requires open chromatin region, and is primarily regulated by chromatin remodeling, which rearchitects chromatin by histone modifications such as histone acetylation, histone methylation, and histone phosphorylation (Du et al., 2015; Greer and Shi, 2012; Kouzarides, 2002; Shahbazian and Grunstein, 2007; Timmermann et al., 2001; Turner, 2000). Histone acetylation is modulated by two families of enzymes; histone acetyltransferases (HATs), and histone deacetylases (HDACs) (Hai et al., 2021; Melesina et al., 2021; Moreno-Yruela et al., 2022; Roth et al., 2001; Y. Yang et al., 2020). HATs add an acetyl group in the tail of the N-terminal of histone proteins allowing access to TFs. In active promoter, histone acetylation is a common epigenetic modification (Ding et al., 2020; Li et al., 2020; Martin et al., 2021) . On the contrary, HDACs neutralize the functions of HATs by deacetylating histone proteins, and act as a transcriptional repressor to condense chromatin structure. Histone methylation is another epigenetic regulatory mechanism to determine the activity of enhancers. Histone methylation takes place mainly on lysine and arginine residues, and is mediated by lysine methyl transferases, arginine methyl transferases, respectively. Lysine methylation can be mono-, di- or tri-methylated, whereas arginine methylation can be mono-, di-methylated (Kim and Park, 2020; Kim et al., 2022; Li et al., 2021) . Different histone methylation with distinct positions is involved in gene activation. For instance, histone H3 trimethylated on lysine 4 (H3K4me3) modification occurs in 5’ region of active promoters, while histone H3 trimethylated on lysine 36 (H3K36me3) occurs 3’ region of the gene (Blomen and Boonstra, 2011; Huang et al., 2018). Histone methylation is not only regarded as a mark for gene activation, but also plays a crucial role in gene silencing. For instance, histone H3 monomethylated on lysine 9 (H3K9me) is considered as a repressive modification in different genes. Intriguingly, some epigenetic

modifications such as histone H3 trimethylated on lysine 9 (H3K9me3) are seen in both silenced genes/promoter or active genes. Recently, it has been documented that some enhancer regions have the potential to be transcribed. eRNAs are part of the regulatory mechanism of genes named as enhancer RNAs (eRNAs). Transcription of eRNAs depends on RNA polymerase II, and this process can be uni or bi-directional. In the beginning, they were assumed that they are noisy byproduct of gene transcription with no function, but it has been found that eRNAs are indicated as important components of the transcriptional regulation of some genes (Santa et al., 2010). eRNAs may interfere with the transcriptional control of the gene in several ways; (I) eRNAs are able to directly interact with factors to form a chromatin loop by acting as a scaffold, (II) eRNAs bind to transcription factors and mediators to stabilize RNA polymerase II to enhance the expression of the target gene, (III) eRNAs can entrap inhibitory cofactors to regulate target gene expression (Lewis et al., 2019).

2. Aim of the thesis

Understanding the transcriptional control of neurogenesis necessitates a simple platform to uncover underlying molecular mechanisms of neurogenesis. Compared to the brain, the spinal cord retains relatively simple cellular architecture and anatomy where neurogenesis occurs. V2s cells are a recently identified novel interneuron population which expresses *sox1a* and *sox1b* transcription factors in the p2 domain in the spinal cord. Previous studies suggest that *nkx1.2lb* gene is also expressed in V2s interneurons. However, the expression of *nkx1.2lb* gene in the spinal cord with its transcriptional regulation has not been investigated until now.

In this thesis, I aim to investigate the molecular mechanisms of the generation of V2s interneuron populations and its differentiation to shed light on its developmental complexity with the assistance of newly identified novel marker genes, and combination with ATAC-Seq approach, the regulatory mechanisms of *nkx1.2lb* are probed through its cis-regulatory modules.

3. Material and Methods

3.1 Material

3.1.1 Bacterial Strains

In this work, all cloning experiments are performed in chemically competent *Escherichia coli* strains (TOP10 from ThermoFischer and XL-1 Blue from ProMega).

3.1.2 Chemicals, enzymes, kits and equipments

Chemicals, enzymes and kits were listed in Table 1, 2, 3, 4.

Table 1: List of chemicals used in this work

Name	Manufecturer
Tricaine methanesulfonate (MS-222)	Sigma-Aldrich, Taufkirchen, Germany
4',6-diamidino-2-phenylindole (DAPI)	Sigma-Aldrich, Taufkirchen, Germany
Chloroform	VWR International GmbH, Darmstadt, Germany
Bovine Serum Albumin (BSA)	Sigma-Aldrich, Taufkirchen, Germany
Agarose	Peqlab, Erlangen, Germany
Citric Acid	Carl Roth GmbH + Co. KG; Karlsruhe, Germany
Dimethylformamide	Carl Roth GmbH + Co. KG; Karlsruhe, Germany
Ethanol (EtOH)	Carl Roth GmbH + Co. KG; Karlsruhe, Germany
Ethylene diaminetetra acetic acid (EDTA)	Carl Roth GmbH + Co. KG; Karlsruhe, Germany
Ethidiumbromide	Carl Roth GmbH + Co. KG; Karlsruhe, Germany
Formamide	VWR International GmbH, Darmstadt, Germany
Isopropanol	Carl Roth GmbH + Co. KG; Karlsruhe, Germany
Kanamycin	Sigma-Aldrich, Taufkirchen, Germany
Potassium chloride (KCl)	Sigma-Aldrich, Taufkirchen, Germany
Potassium hydroxide (KOH)	Carl Roth GmbH + Co. KG; Karlsruhe, Germany
Magnesium chloride (MgCl2)	Carl Roth GmbH + Co. KG; Karlsruhe, Germany
Magnesium sulphate (MgSO4)	Sigma-Aldrich, Taufkirchen, Germany
Methanol (MeOH)	Carl Roth GmbH + Co. KG; Karlsruhe, Germany
HEPES	Carl Roth GmbH + Co. KG; Karlsruhe, Germany
DNA- Ladder GeneRuler (mix)	ThermoFisher Scientific, Schwerte, Germany
dnTPs	Promega, Mannheim, Germany
Dimethylsulfoxide (DMSO)	Carl Roth GmbH + Co. KG; Karlsruhe, Germany
Magnesium chloride (MgCl2)	Carl Roth GmbH + Co. KG; Karlsruhe, Germany
Magnesium sulphate (MgSO4)	Sigma-Aldrich, Taufkirchen, Germany
Methanol (MeOH)	Carl Roth GmbH + Co. KG; Karlsruhe, Germany
NBT	Perkin Elmer, Waltham, USA
Paraformaldehyde	Merck, Darmstadt, Germany
Phosphate buffered saline (PBS)	Life Technologies GmbH, Darmstadt, Germany

Phenol red	Carl Roth GmbH + Co. KG; Karlsruhe, Germany
Sheep Serum	Merck, Darmstadt, Germany
Sodium Chloride (NaCl)	Carl Roth GmbH + Co. KG; Karlsruhe, Germany
Spectinomycin	Sigma-Aldrich, Taufkirchen, Germany
Sucrose	VWR International GmbH, Darmstadt, Germany
Tris-base	Carl Roth GmbH + Co. KG; Karlsruhe, Germany
Tris-HCl	Carl Roth GmbH + Co. KG; Karlsruhe, Germany
Trizol	ThermoFisher Scientific, Schwerte, Germany
Tween-20	Carl Roth GmbH + Co. KG; Karlsruhe, Germany

Table 2: Enzymes

Name	Manufecturer
XhoI	New England Biolabs Frankfurt am Main, Germany
EcoRI-HF	New England Biolabs Frankfurt am Main, Germany
HindIII	Thermo Fischer Scientific
GoTaq™ DANN Polymerase	Promega, Mannheim, Germany
Proteinase K	Carl Roth GmbH + Co. KG; Karlsruhe, Germany
Ribonuclease RNasin® RNase Inhibitor	Promega, Mannheim, Germany
SP6 RNA Polymerase	Promega, Mannheim, Germany
T7 RNA Polymerase	Promega, Mannheim, Germany
RNase free DNase	Promega, Mannheim, Germany
LR Clonase II	Gateway™ LR Clonase™ II Enzyme mix

Table 3: List of kits used in this work

Name	Manufecturer
pGEM®-T Easy Vector System	Promega, Mannheim, Germany
Qiagen Plasmid Midi Kit	QIAGEN Hilden, Germany
pCR®8/GW/TOPO® TA Cloning® Kit	ThermoFisher Scientific, Schwerte, Germany
Illustra ProbeQuant G-50 Micro Columns	GE Healthcare, Buckinghamshire, UK
NucleoBond Xtra BAC Kit	Macherey-Nagel, Germany
Plasmid purification Mini Kit	Macherey-Nagel, Germany

Table 4: List of equipments and tools used in this work

Name	Manufecturer
Bacteria Incubator	Heraeus, Hanau, Germany
Centrifuge	Eppendorf, Hamburg, Germany
Cool centrifuge J2-HS	Beckman, Stuttgart, Germany

Coverslips	Paul Marienfeld GmbH & Co KG, Lauda-Königshofen, Germany ThermoFisher Scientific, Schwerte, Germany
Dissection forceps	Fine Tip No. 5, Dumont
Eppendorf microcentrifuge tubes	Eppendorf, Hamburg, Germany
Falkon tubes	Greiner, Nürtingen, Germany
FemtoJet microinjector	Eppendorf, Hamburg, Germany
Flaming-Brown Needle puller	Sutter Instruments, USA
Gas microinjector	Tritech research inc., L.A., USA
Gel Chamber	ThermoFisher Scientific, Schwerte, Germany
Heating Block	Stuart, Chelmsford, UK
Incubator for fish embryos	Heraeus, Hanau, Germany
Microloader tips	Eppendorf, Hamburg, Germany
Mounting Medium	Polysciences, Pennsylvania, USA
Microscopes	Leica SP8 confocal microscope Leica DMI6000 SD Nikon SMZ18
NanoDrop	Erlangen, Germany
Needle puller	Sutter Instruments, USA
Parafilm	Sigma-Aldrich, Taufkirchen, Germany
PCR Thermocycler	Eppendorf, Hamburg, Germany
Petri dishes	Greiner, Nürtingen, Germany
Pipette tips	Corning, Corning, UK
Thermomixer	Eppendorf, Hamburg, Germany
Vortex Shaker	ThermoFisher Scientific, Schwerte, Germany

3.1.3 Softwares

Table 5: List of softwares

Name	**Source**
ApE	Wayne Davis from the University of Utah
Primer3 version 4.1.0	https://primer3.ut.ee/
Microsoft Excel	Microsoft office

3.1.4 Solutions

Table 6: List of solutions

Solutions	
60X E3 Medium	5 mM NaCl, 0.17 mM KCl, 10 mM HEPES, 0.33 mM $MgSO_4$, 0.33 mM $CaCl_2$
20X SSC	3 M NaCl, 0.3 M sodium citrate
4% Paraformaldehyte	40 g in 1000 liter
PBST	1X PBS, 0,1% Tween-20
PBT	1X PBS, 0.8% Triton X-100
Blocking Buffer for IHC	5%DMSO, 1%BSA in PBT
Hybridization Buffer	25 ml Formamide, 12.5 ml 20X SSC, 2.5 ml yeast tRNA (10 mg/ml), 50 µl heparin (50 mg/ml), 500 µl 10% Tween-20, 450 µl 1M Citric Acid, fill up with water to 50 ml
Pronase solution	0,5 g Pronase, 50 ml water
Proteinase K solution	10 µg/ml proteinase K in PTW
PTW	1X PBS, 1 ml Tween-20 (0,1% v/v final)
Staining Buffer	5 ml 1M Tris pH: 9.5, 2.5 ml, 1M MgCl2, 1 ml 5M NaCl, 500 µl 10% Tween-20, 41 ml water
Wash Buffer 1	250 ml Formamide, 25 ml 20X SSC, 250 µl 100% Tween-20 fill up with water to 500 ml
Wash Buffer 2	50 ml 20X SSC, 500 µl 100% Tween-20, fill up with water to 500 ml
Wash Buffer 3	5 ml 20X SSC, 500 µl 100% Tween-20, fill up with water up to 500 ml
Wash Buffer 4	2.5 ml 20X SSC, 250 µl 100% Tween-20, 250 ml PTW, fill up with water up to 500 ml
LB Medium	50 ml from 10x LB stock, 450 ml water
TE Buffer	10 mM Tris-HCl pH 8.0, 1 mM EDTA

Tricaine	2 g Tricaine powder, 490 ml water, 10 ml 1M Tris pH: 9.5
PTU Solution	0.0003% w/v phenylthiourea in 1x E3 medium
10XPBS	Dulbecco's Phosphate Buffered Saline
Blocking Buffer for in situ hybridization	5 ml 10X PBS, 500 µl 10% Tween-20, 1 ml BSA (100 mg/ml), 500 µl 100% DMSO, 43 ml water
1% H2O2 PTW	500 µl 30% H2O2, 15 ml PTW
Neutralization Buffer	315,2 g Tris-HCl, 1 liter water

3.1.5 Zebrafish lines

Oligonucleotides are listed in Table 7.

Table 7: Zebrafish lines used in this study

Transgenic line	**Reference**
Tg(dbx1b:EGFP)	European Zebrafish Resource Center (EZRC)
Tg(olig2:EGFP)	European Zebrafish Resource Center (EZRC)
Tg(-3.5nkx2.2a:GFP)	European Zebrafish Resource Center (EZRC)
Tg(glyt2:GFP)	European Zebrafish Resource Center (EZRC)
Tg(sox1a:GFP)	(Gerber et al., 2019)
Tg(vsx1:GFP)	European Zebrafish Resource Center (EZRC)

3.1.6 Oligonucleotides

Oligonucleotides are listed in Table 8.

Table 8: Oligonucleotides

Name	Sequence	Note
nkx1.2lb_CRM_1 Forward	TGTTTTCATGAGTTGCTGAGTTT	Primers encompassing the putative enhancer region CRM1, PCR product: 517 bp
nkx1.2lb_CRM_1 Reverse	GGATACTGACCCCTGTGTTAAA	
nkx1.2lb_CRM_2 Forward	TCCAAGTAAATTTGCTGCGAGA	Primers encompassing the putative enhancer region CRM2, PCR product: 699 bp
nkx1.2lb_CRM_2 Reverse	CCAAGCGTGAATTATATACCTGC	
nkx1.2lb_CRM_3 Forward	TGTTGTTGTTGTGTTTTCCTCA	Primers encompassing the putative enhancer region CRM3, PCR product: 1092 bp
nkx1.2lb_CRM_3 Reverse	GCTGTACAAGAGCCATTCATTG	
nkx1.2lb_CRM_4 Forward	CCACTTGAGGGATCGCACTA	Primers encompassing the putative enhancer region CRM4, PCR product: 730 bp
nkx1.2lb_CRM_4 Reverse	TCACCCCTCTCCATCTTATTCA	
nkx1.2lb_CRM_5 Forward	GCGCAGTCTTCTCCAAAGTC	Primers encompassing the putative enhancer region CRM5, PCR product: 983 bp
nkx1.2lb_CRM_5 Reverse	ACCATACTGCGATGCTTTGC	
nkx1.2lb_CRM_6 (eRNA)	GTTGAAGAAGGAGAGTTTGCAAG	Primers encompassing the putative enhancer region CRM6, PCR product: 852 bp
nkx1.2lb_CRM_6 (eRNA)	AATGAAAAGGGAAAAGGGGAAAA	
-1.5 kb nkx.1.2lb Forward	gagagaCTCGAGAGGGCTATGCTGGGAGGATT	Primers to amplify -1.5 kb upstream region of transcription starting site
-1.5 kb nkx.1.2lb Reverse	gagagaGGATCCCTTCTCCCGGTTCATAGCTCTC	
-2.5 kb nkx.1.2lb Forward	gagagaCTCGAGGGATGAGGGTATTGAAATAGTGC	Primer to amplify -2.5 kb upstream region of transcription starting site
cacna2d3 Forward	tgtgacacagaatacccagcc	Primer to amplify cacna2d3 gene for in situ prob
cacna2d3	aagactccaaacgaaacgcc	
cplx2l Forward	ggagaagaagataaagacccagagg	Primer to amplify cplx2l gene for in situ prob
cplx2l	tggacacatgcaagaccaga	
nefmb Forward	gaagaggaggagactgttgctg	Primer to amplify nefmb gene for in situ prob
nefmb	gcgctttaattctgtttcagacgc	

guide_1	GGGACGGTTCAAACCCAAAA	Primer to generate guide for CRISPR-Cas9 mutageesis
guide_2	GGCCGCTCATAGGAGGAGAA	Primer to generate guide for CRISPR-Cas9 mutageesis
guide_3	CAAGTTGAGACGTTCGCACA	Primer to generate guide for CRISPR-Cas9 mutageesis
guide_4	TATGAACCGGGAGAAGGTGC	Primer to generate guide for CRISPR-Cas9 mutageesis
guide_5	CAGAGGATGGGTTCGTGTTC	Primer to generate guide for CRISPR-Cas9 mutageesis
guide_6	TGCCGAGTTCGGACAACACG	Primer to generate guide for CRISPR-Cas9 mutageesis

3.1.7 Probes

Probes are listed in table 9.

Table 9: In situ probes

Name	Reference
nkx1.2lb	(Armant et al., 2013)
Insm1a	(Armant et al., 2013)
lhx5	(Armant et al., 2013)
onecut1	(Armant et al., 2013)
foxn4	(Armant et al., 2013)
lhx1a	(Armant et al., 2013)
Islr2	(Armant et al., 2013)

3.2 Methods

3.2.1 Zebrafish Maintenance

All zebrafish *danio rerio* stock lines in this study were maintained in the European Zebrafish Resource Center (EZRC) in Campus Nord, Karlsruhe Institute of Technology, Karlsruhe, Germany. Wild type zebrafish embryos are obtained from ABO line or AB2O2 Leo lines according to regular procedure. Following transgenic lines are used in this study; Tg(sox1a:eGFP) (Gerber et al., 2019), Tg(mnx1:Gal4;UAS:RFP;cry:CFP), Tg(-3.5nkx2.2a:GFP), TgBAC(vsx1:GFP), Tg(glyt2:GFP). After obtaining reporter zebrafish embryos, they were sorted manually under the fluorescent microscope.

3.2.2 Genomic DNA isolation from zebrafish embryos

Genomic DNA was obtained from 1 dpf zebrafish embryos. After collection of embryos, they are transferred into 1.5 ml eppendorf tube containing 100 µl KOH solution and incubated for 20 minutes at 95°C. After that, 100 µl Neutralization buffer was added and mixed ad stored at 4°C (Meeker et al., 2007).

3.2.3 Microinjection

The microinjection experiments were carried out with gas-driven MicroInjector system (Tritech) and SMZ645 (Nikon) stereomicroscopes. For each injection solution, 0.1% phenol red was added into the Injection solutions mix. The needles are filled with the injection solution containing 50 ng/µl plasmid for Tol2 based cloning. The concentration of morpholino is 0.15 µM. After obtaining fertilized eggs, they are placed into petri dish, and nearly 2 or 3 nl solution mix was injected into yolk. After that injected embryos were kept at 28°C in the incubator until they reached desired stages according to (Kimmel et al., 1995). Injection is performed in one-cell stage embryos according to Kimmel et al 1995.

3.2.4 CRISPR-Cas9 mutagenesis

The oligonucleotides 20 bp in length encompassing the target region were chosen in the CHOPCHOP (Labun et al., 2019). The target specific primers were attached with T7 promoter sequence (5’-TAATACGACTCACTATA-3’) and TracrRNA sequence

(GTTTTAGAGCTAGAAATAGCAAG) according to (Gagnon et al., 2014). Guide RNAs were generated according to (Shah et al., 2015). After running PCR, template was purified using DNA Clean & Concentrator, Zymo Research kit according to manufacturer's instructions. Guide RNAs were generated using T7 Turbo Mega, Promega according to manufacturer's instructions. As a final step, guide RNAs were purified using RNA Clean & Concentrator, Zymo Research. Guide RNAs were injected directly into the cell according to (Kimmel et al., 1995).

Table 10: Template synthesis for the generation of guide RNA

Nuclease free water	2.5 µl
2X Q5 Master mix	12.5 µL
10 µM scaffold oligo	5 µL
10 µM target-specific oligo	5 µL

Table 11: PCR protocol for the template synthesis for guide RNA

95°C for 30 sec	1 cycle
95°C for 10 sec	40 cycles
60°C for 10 sec	
72°C for 10 sec	
72°C for 10 sec	1 cycle

3.2.5 Fixation of zebrafish embryo

Collected embryos are dechorinated with pronase solution, after that they were incubated with BT-Fix for 2 hours at room temperature or 4°C for overnight and stored -20°C.

3.2.6 Agarose Gel Electrophoresis

1% to 2% agarose gels are prepared in 1X TAE to check the size of plasmids or PCR products. To visualize DNA 1-3 µl Ethidium Bromide was added into 100 ml agarose-TAE solution and electrophoresis was performed with 120 Volt.

3.2.7 Isolation of plasmid DNA

Plasmid DNA was isolated with Qigen Pasmid Mini or Midi Kits following the manufacturer`s instruction from overnight incubated bacteria with appropriate selective antibiotics in LB medium.

3.2.8 Bacterial Artificial Chromose (BAC) Isolation

BAC was isolated using NucleoBond Xtra BAC kit according to manufacturer`s instruction from overnight incubated bacteria culture.

3.2.9 Isolation of DNA from agarose gel

After running the agarose gel, DNA-containing region of agarose gel was taken and DNA was isolated using Macherey-Nagel Nucleospin Gel and PCR Clean-up kit in accordance with provider`s instruction.

3.2.10 Polymerase Chain Reaction (PCR)

Table 12: PCR protocol

Oligomix containing 5 µm and 5 µm Forward and Reverse primers	1 µl	**Initial denaturation:** 95°C for 2 min **Amplification:** 95° C for 45 sec x° (depending on primers) for 45 sec 72°C for 45 sec **Final Elongation:** 72°C for 10 min
Template (100 ng/µl)	0,5 µl	
DMSO	1,25 µl	
dNTP (25 mM)	0,5 µl	
5xGoTaq Buffer	5 µl	
$MgSO_4$ 25 (mM)	1 µl	
Go Taq Polymerase	0,5 µl	
Water	15,25 µl	
Total Volume	25 µl	

3.2.11 Synthesis of RNA DIG-DNP Probe

The plasmids were digested with appropriate restriction enzymes at 37°C (depending on enzymes) for 1 hour. In order to check the digested plasmid, it was controlled on agarose gel. Next, in vitro transcription was performed with one of the following polymerases T7, SP6 or T3 depending on the plasmid contructs in the presence of DIG or DNP labeling mix at 37°C for 3 hours. After that, probes are cleaned with Cytive Illustra Probe Quant G-50 micro column kit and all probes were diluted in hybridization buffer and stored at -20°C.

3.2.12 Chromogenic In situ Hybridization

Fixed embryos were dehydrated with 75% Methanol-PBS, 50% Methanol-PBS, 25% Methanol-PBS, for 5 minutes orderly for 5 minutes for each. Next, the embryos are washed with PTW three times for 5 minutes. Proteinase K treatment is performed for 5 minutes in 24 hpf embryos. The embryos are fixed with 4% PFA for 20 minutes at 4°C. To remove excess proteinase K, the embryos are washed with PTW three times for 5 minutes and washed with hybridization buffer. The embryos are incubated with hybridization buffer for 2 hours at 70°C. The embryos are incubated overnight with diluted probes depending on the probes (1:100-1:300). Next day, the embryos are washed two-times with wash buffer 1 for 30 minutes, 15 minutes once with wash buffer 2, two-times 30 minutes with wash buffer 3, and once with wash buffer 4 for 5 minutes at 70°C. After that, the embryos are washed with PTW three times for 5 minutes and incubated overnight with Anti-DIG antibody in the blocking buffer. Next day, the embryos are washed with PTW buffer 5 times for 5 minutes to get rid of unattached antibody and stained with staining buffer containing NBT-BCIP. The staining procedure is stopped by washing embyos with PTW.

3.2.13 Fluorescent In situ Hybridization

Fixed embryos were dehydrated with 75% Methanol-PBST, 50% Methanol-PBST, 25% Methanol-PBST for 5 minutes orderly for 5 minutes for each step. Next, the embryos were washed with 100% PBST five times for 5 minutes. Proteinase K treatment was performed for 45 minutes in 24 hpf embryos. The embryos were quickly washed with PBST two times without incubation: The embryos were fixed with 4% PFA for 20 minutes at room temperature. Then, embryos were washed with PBST five times for 5 minutes. Probe hybridization buffer, probe sets, probe wash buffer and amplification buffers were provided from Molecular Instruments, Inc. The embryos were incubated in pre-hybridization buffer for 30 minutes at 37°C. After that, the embryos were incubated with probe solution containing probe sets according to manufacturer's instruction. Then, the embryos were incubated with probe solution overnight at 37°C. Next day, the embryos were washed with probe wash buffer four times 15 minutes at 37°C. Then, the embryos were washed with 5X SSCT for two times at room temperature. Then, the embryos were incubated with amplification buffers containing amplifiers overnight at room temperature. In last day, the embryos were washed five times with 5X SSCT.

3.2.14 Immunohistochemistry

Fixed embryos are rehydrated with 75% Methanol-PBST; 50% Methanol-PBST, and 25% Methanol-PBST for 5 minutes each step respectively. Embryos are washed with PBST 3 times for 5 minutes and incubated with 150 mM Tris-HCl (pH:9) for 5 minutes after that they are incubated with 150 mM Tris-HCl (pH:9) again, but this time in pre-warmed 150 mM Tris-HCl (pH:9) for 15 minutes at 70°C. Embryos were washed with PBST for two times for 5 minutes. To increase penetration of antibody, the embryos were incubated with cold acetone for 20 minutes at -20°C. Next, acetone was removed and the embryos are rinsed with water 3 times. The embryos are incubated with blocking buffer for 3 hours at room temperature, then they are incubated with primary antibody in blocking buffer. Next day, the embryos are washed with PBT four times for 30 minutes. Then, they are incubated with the secondary antibody in blocking buffer for 2 hours in the dark at room temperature. Finally, they are washed with PBST five times for 5 minutes in the dark.

3.2.15 Gateway cloning

The cis-regulatory modules were cloned with Gateway cloning system according to (Kwan et al., 2007). Upstream regions of transcription starting site of nkx1.2lb were amplified with primers encompassing proper restriction enzyme recognition sites to generate 5' entry clone for subsequent cloning together with middle entry clone containing eGFP and 3' entry clone containing polyadenylation signal.

3.2.16 Identification of putative cis-regulatory modules of *nkx1.2lb* and enhancer screening assay

Putative cis-regulary modules of *nkx1.2lb* are retrieved from UCSC browser (*https://genome.ucsc.edu/*). Firstly, zebrafish assembly reference genome was selected. To find possible CRMs with ATAC-Seq, ChIP-Seq, and CAGE-Seq tracks are selected in DANIO-CODE Trach Hub. After that, possible CRMs near the gene are screened by their epigenetic activation of three methylation to the lysine 4 on the histone 3 protein (H3K4me3). Next, possible candidates were amplified by polymerase chain reaction as already explained in table 10. The CRMs-encoding regions were cloned into pCR8/GW/TOPO plasmid to obtain entry plasmid for further cloning into pT2KHGpzGATA2C1 destination vector (Navratilova et al.,

2009) (Figure 7, Figure 8). All plasmids were partially sequenced to validate inserted sequence in the plasmids.

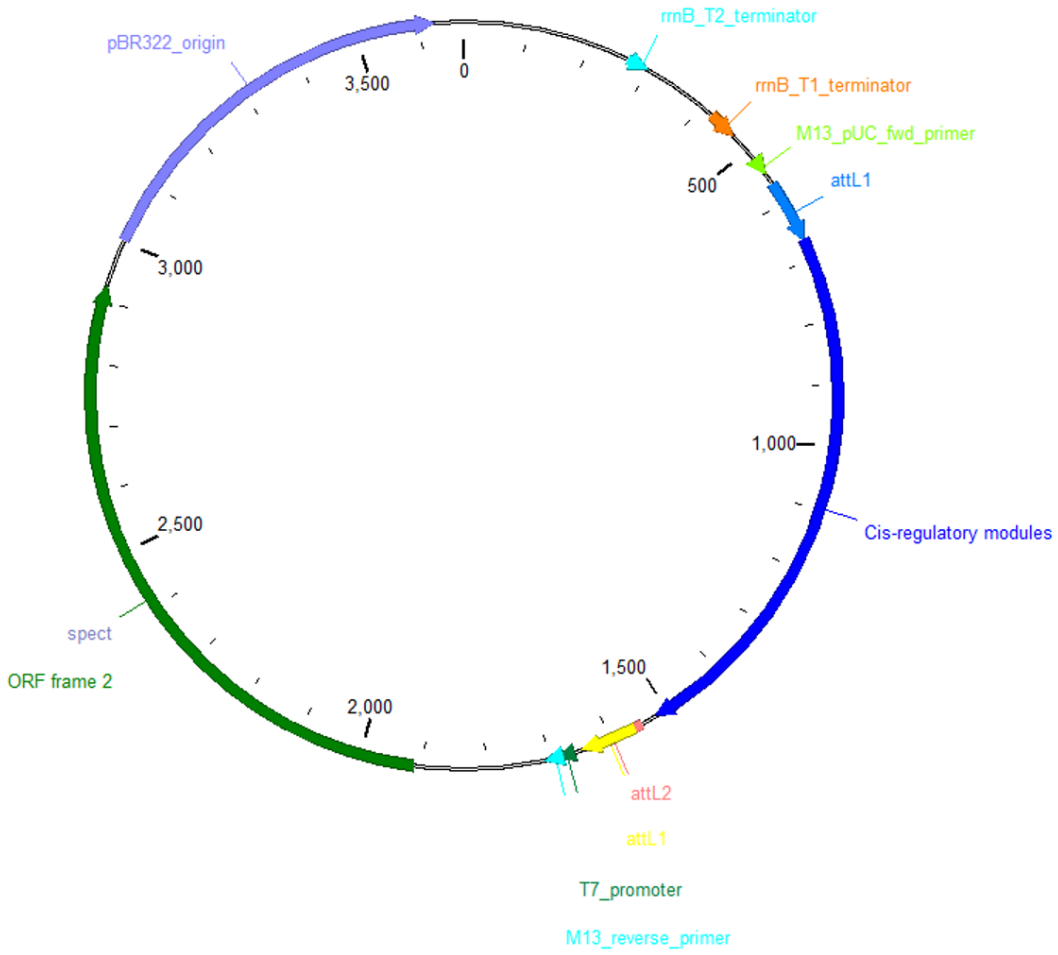

Figure 7: The plasmid map of pCR8/GW/TOPO containing the sequence of cis-regulatory modules.

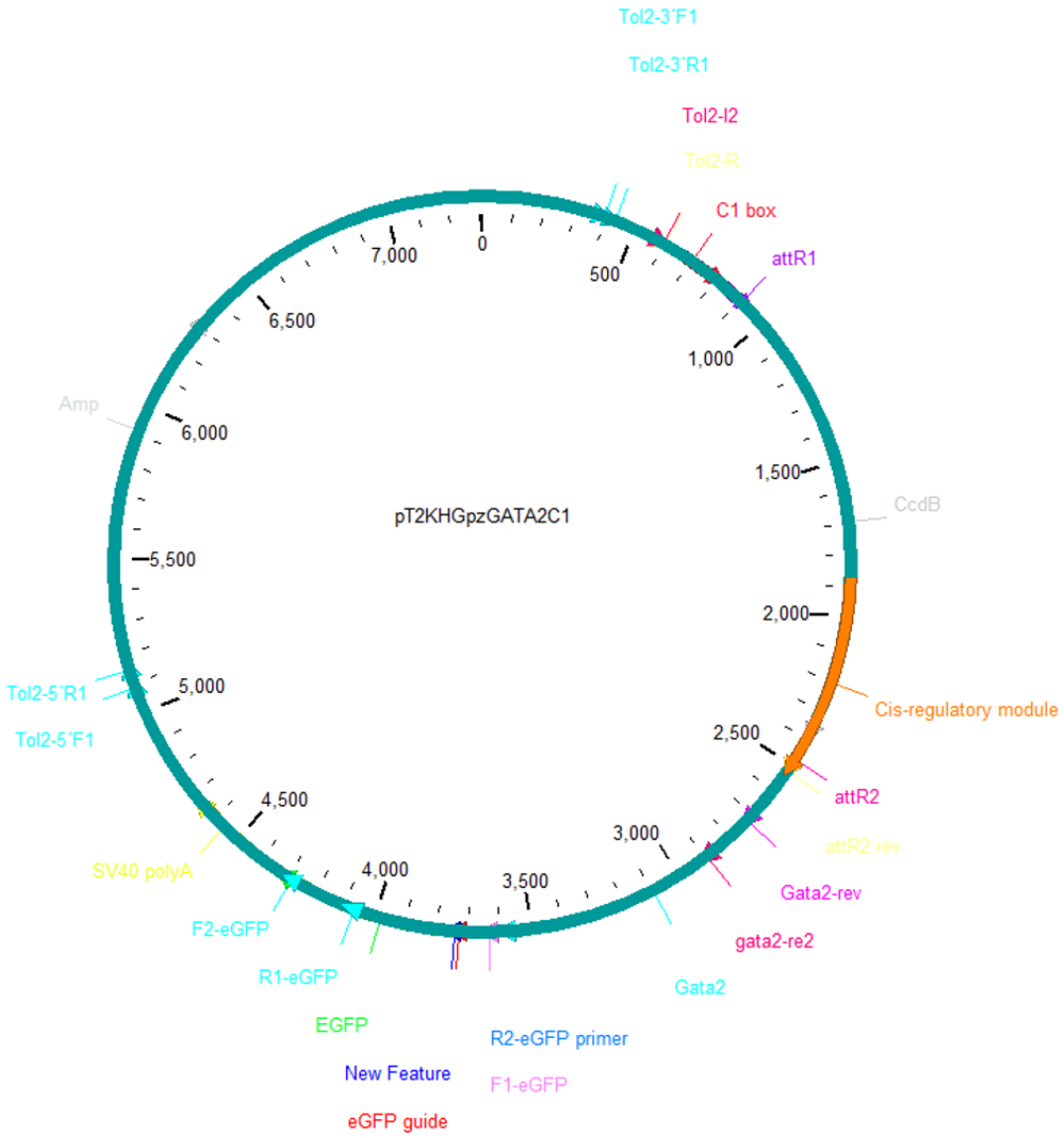

Figure 8: The plasmid map of pT2KHGpzGATA2C1 containing the sequence of cis-regulatory modules.

3.2.17 Quantification and statistical analysis

For the quantification analysis, the cells were counted over the span of five somites above the yolk extension at indicated time points. Data are presented as mean ± SEM unless otherwise stated. The unpaired two-tailed Student´s t-test was used for comparison of two samples calculated with Microsoft office Excel. The significance level is graded with the number of asterisks: * for $p < 0.05$, ** for $p < 0.01$, *** for $p < 0.001$ and **** for $p < 0.0001$.

3.2.18 Sample preparation and Image acquisition

After staining, the embryos were mounted laterally on glass slides using Aqua-Poly/Mount. Mounted embryos were stored at 4°C. Nikon SMZ18 and Confocal microscope TCS SP8 STED microscopes were used for chromogenic and fluorescent in situ hybridization.

4.RESULTS

4.1. In-depth characterization of the transcriptional network of V2 interneurons

Designation of gene regulatory networks in neurons is pivotal to apprehending the transcriptional regulation and better defining of the neuronal populations. It has been already documented that recently characterized V2s interneurons possess glycinergic identity with the expression of *sox1a*, and *sox1b* transcription factors (Gerber et al., 2019). These two transcription factors are crucial for the development of V2s interneurons. In the mammalian spinal cord, four distinct V2 cell populations have been identified, but only three V2 sub-populations have been characterized in zebrafish. Also, the transcriptional network of V2s cells still needs to be deeply characterized. In light of this information, several questions may arise; (I) Which transcription factors are involved in the development of V2s cells? (II) How heterogeneous V2s cells? (III) What is the regulatory mechanism of these transcription factors in the generation of V2s cells? Clarification of these questions necessitates in-depth investigation of *sox1a-expressing* V2s interneurons by using advanced technologies. For this purpose, I utilized a transgenic reporter line possessing endogeneous expression of *sox1a* tagged with eGFP named *Tg(sox1a:eGFP)* (Chen et al., 2023; Gerber et al., 2019). Recently, single-cell RNA sequencing is an emerging and robust technology to reveal the transcriptional control of each cell along with the detection of scarcely expressed mRNAs in certain cell populations. Spinal cords were collected and sequenced at four different developmental stages; 1dpf, 2 dpf, 3 dpf, and 5 dpf to deeply investigate the molecular program of V2s cluster. A colleague in our lab analyzed the single-cell RNA sequencing data, two distinct cell populations which are related to p2 domain-derived V2 interneurons were obtained. One of these clusters expresses V2 progenitor markers; forkhead box N4 *(foxn4)*, and visual system homeobox 1 homolog, chx10-like (*vsx1)* genes, so this cell cluster was annotated as V2-precursor. However, this cluster was detectable at only 1 dpf stage since V2 interneurons are mainly generated between 16 hpf-24 hpf (Batista et al., 2008; Gerber et al., 2019; Kimura et al., 2008). Enriched markers in V2-precursor cluster are *foxn4, vsx1, cholinergic receptor, nicotinic, alpha 2a (chrna2a), KN motif and ankyrin repeat domains 1a (kank1a), EBF transcription factor 3a (ebf3a), lin-28 homolog A (LIN28A),* basic helix-loop-helix family, member e22 *(bhlhe22), ectodermal-neural cortex 3 (enc3), and* cytochrome P450, family 4, subfamily T, polypeptide 8 *(cyp4t8)* (Figure 9)

gene	p_val	avg_log2FC	cluster
foxn4	0	1,96155	V2_pre
vsx1	3E-245	1,2154	V2_pre
chrna2a	1E-192	1,23247	V2_pre
kank1a	6E-177	1,43521	V2_pre
ebf3a	1E-166	1,74062	V2_pre
LIN28A	3E-166	1,93806	V2_pre
bhlhe22	1E-161	1,52526	V2_pre
enc3	4E-127	1,2947	V2_pre
cyp4t8	5E-116	0,73884	V2_pre

Figure 9: Enriched gene name list in V2 precursor interneuron cluster. P_val: p_value, avg_log2FC: average log2 fold change.

Another cell cluster expressing *sox1a*, *sox1b*, and *slc6a5* are annotated as V2s cluster which exists in all stages of the spinal cord. Single-cell RNA sequencing results revealed that a variety of transcription factors as well as receptor-encoding genes are enriched in the V2s cluster. In the gene list, *nkx1.2lb* is identified as the most enriched transcription factor followed by *immunoglobulin superfamily containing leucine-rich repeat 2 (islr2)* gene. Furthermore, *trafficking regulator of GLUT4 (SLC2A4) 1a* (*trarg1a)*, *calcium channel, voltage-dependent, alpha2/delta subunit 3* (*cacna2d3)*, *LIM homeobox 1a* (*lhx1a), one cut homeobox 1 (onecut1)*, *LIM homeobox 5* (*lhx5)*, (*nefmb) neurofilament medium chain b*, and, *complexin 2* (*cplx2)* genes are also enriched in V2s interneuron cluster in our single-cell RNA sequencing datasets (Figure 10).

gene	p_val	avg_log2FC	cluster
nkx1.2lb	0	3,37875815	V2s
islr2	0	3,10380969	V2s
trarg1a	0	2,53690483	V2s
cacna2d3	0	2,29777368	V2s
lhx1a	0	2,53733277	V2s
onecut1	5,8E-204	1,57298381	V2s
lhx5	1,7E-199	1,52428197	V2s
nefmb	2,2E-170	3,32022122	V2s
cplx2	3,36E-57	1,45289299	V2s

Figure 10: Enriched gene name list in V2s interneuron cluster. Single-cell RNA sequencing P_val: p-value, avg_log2FC: average log-2fold change.

The expression patterns of the candidates were screened to validate their specificity by performing whole-mount chromogenic in situ hybridization (Figure 11). According to chromogenic in situ hybridization experiments, their expressions were mainly restricted in the central nervous system. *Nkx1.2lb* expression is detected in the predominantly anterior part of the spinal cord, eye, and tegmentum region of the brain. The expression of *islr2* was observed mainly in the anterior part of the spinal cord resembling the expression pattern of *nkx1.2lb*, telencephalon, and eye. *Cplx2l* were expressed strongly in the spinal cord, telencephalon, and midbrain-hindbrain boundary. The expression of *cacna2d3* was observed in the middle region of the spinal cord, and the habenula region in the brain. The expression of *lhx5* was detected in the spinal cord, telencephalon, and hindbrain. Indeed, the identified markers were specifically expressed in spinal cord. Chromogenic in situ hybridization showed that identified markers were expressed mainly in the ventral spinal cord.

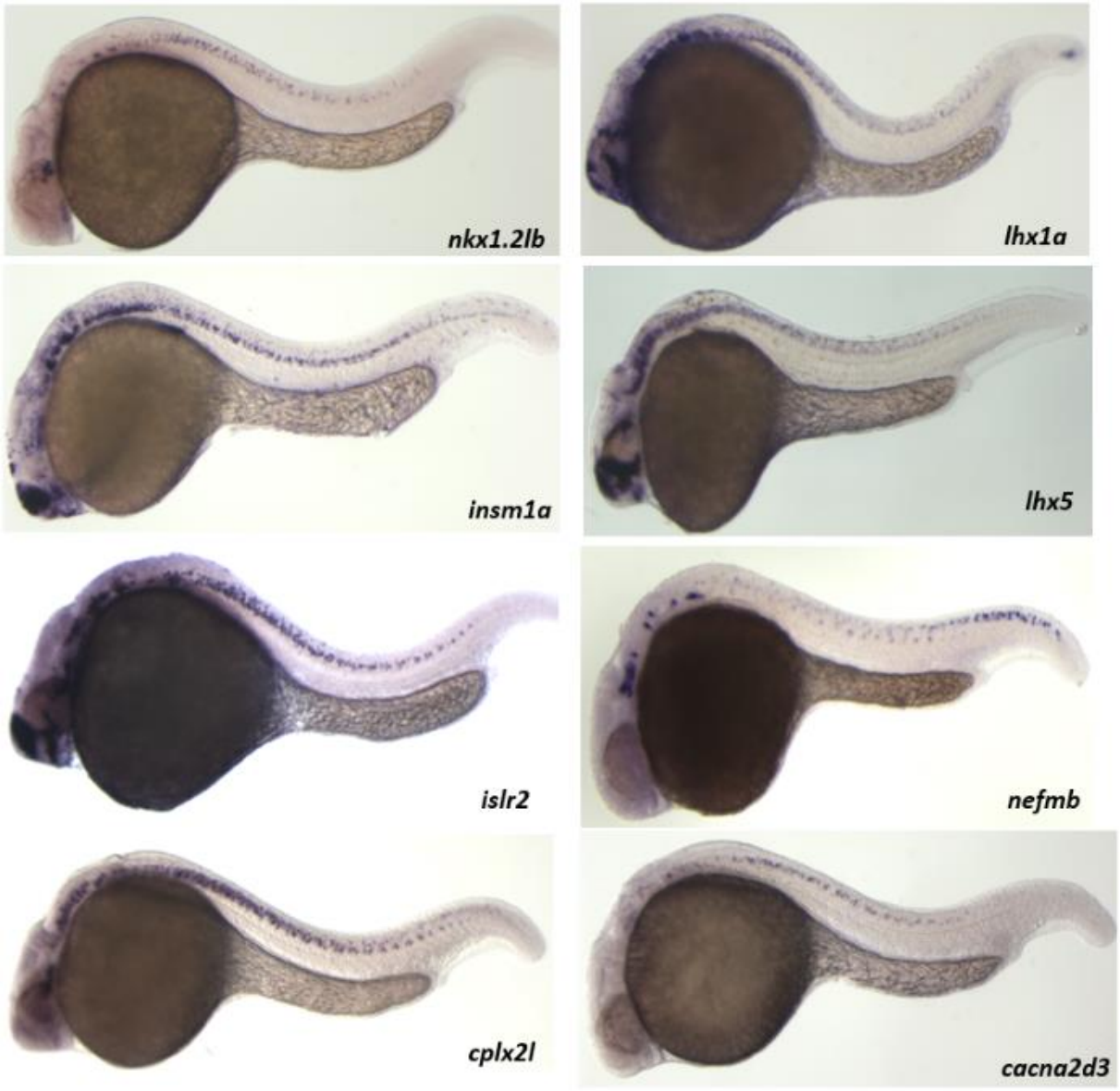

Figure 11: The expression of identified marker genes in V2s cluster in single-cell RNA sequencing at 24 hpf. The expression patterns of nkx1.*2lb*, *islr2*, *lhx5*, *cacna2d3*, *cplx2l*, *onecut*, *trarg1a*, and *insm1a* genes in the embryonic spinal cord at 24 hpf**.** Whole mount chromogenic in situ hybridization against *nkx1.2lb*, *islr2*, *lhx5*, *cacna2d3*, *cplx2l*, *lhx1a, nefmb* and *insm1a* mRNAs.

For mapping the expression patterns of *nkx1.2lb*, *islr2*, *lhx5*, *cacna2d3*, *cplx2l*, *onecut*, *trarg1a*, and *insm1a* genes in each domain in detail, I benefit from already published paper (Andrzejczuk et al., 2018) to demarcate the expressions of aforementioned candidate genes (Figure 12A,B). According to Andrzejczuk et al., 2018, the row just above the notochord was denoted as row 1, and other dorsal rows were named in ascending order. KA" cells were

located in row 1, and KA' cells were located in row 2 and row 3, while V2 cell markers were situated in row 4, and row 5 (Andrzejczuk et al., 2018) (Figure 12B). *Onecut 1* was expressed continuously from row 1 to row 7. *Insm1a* expression was observed in relatively ventral rows; row 1, row 2, row 3, row, 4, and row 5. The expression of *nkx1.2lb* was detected in row 2, row 3, row 4, and row 5, where V2 cells were located according to (Andrzejczuk et al., 2018). The expression of *trarg1a* was detected only in dorsal row 11, and row 12. The expression of *cplx2l* was observed in row 2, row 3, row 4, row 5, and row 6, while *cacna2d3* expression was detected in the middle region of spinal cord; row 4, row 5, row 6, and row 7. *lhx5*-positive cells were located in row 5, row 6, and row 7. *Islr2*-expressing cells were situated in row 2, row 3, row 4, and row 5 resembling the expression pattern of *nkx1.2lb.* Intriguingly, *trarg1a* expression was predominantly detected dorsally in row 11 and row 12. (Figure 12C). According to chromogenic in situ hybridization experiments, it is clear to state that *trarg1a* expression is not observed in the region of spinal cord where V2s interneurons located, so compared to single-cell RNA sequencing data, chromogenic in situ hybridization technique is less sensitive to detect scarcely expressed mRNAs.

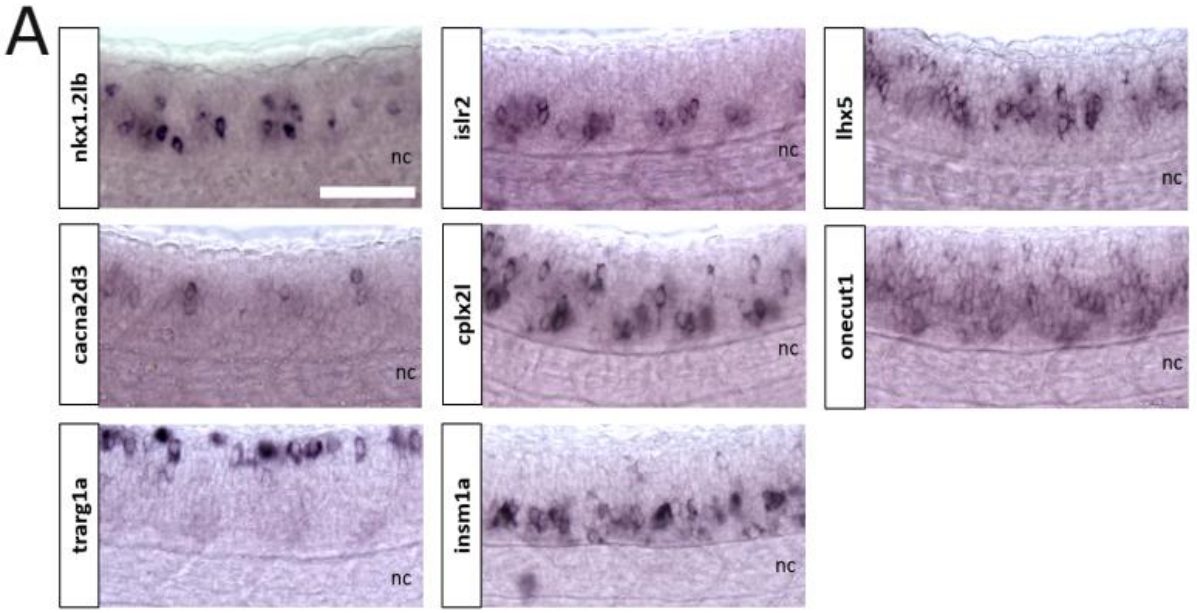

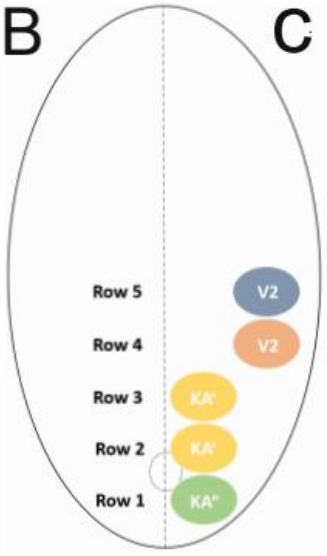

C

	onecut1	*insm1a*	*nkx1.2lb*	*trarg1a*	*cplx2l*	*cacna2d3*	*lhx5*	*islr2*
Row 1	X	X						
Row 2	X	X	X		X			X
Row 3	X	X	X		X			X
Row 4	X	X	X		X	X		X
Row 5	X	X	X		X	X	X	X
Row 6	X				X	X	X	
Row 7	X					X	X	
Row 8								
Row 9								
Row 10								
Row 11				X				
Row 12				X				

Figure 12: Mapping of the expression patterns of the genes enriched in V2s cluster in the single-cell RNA sequencing data. (A) Chromogenic in situ hybridization of *nkx1.2lb*, *islr2*, *lhx5*, *cacna2d3*, *cplx2l*, *onecut1*, *trarg1a*, and *insm1a* mRNAs in the embryonic spinal cord at 24 hpf. **(B)** An Illustration showing the positions of the ventral interneuron in indicated rows. **(C)** A table showing the presence of *nkx1.2lb*, *islr2*, *lhx5*, *cacna2d3*, *cplx2l*, *onecut*, *trarg1a*, and *insm1a*-expressing cells in the spinal cord. *Onecut1* gene expression was detected in row 1, row 2, row 3, row 4, row 5, row 6, row 7. Insm1a gene expression was detected in row 1, row 2, row 3, row 4, row, 5. *Nkx1.2lb* gene expression was detected in row 2, row 3, row 4 and row 5. Trarg1a expression was detected in row 11 and row 12. Cplx2l gene expression was detected in row 2, row 3, row 4, row, 5 and row 6. Cacna2d3 gene expression was detected in row 4, row 5, row 6 and row 7. lhx5 expression was detected in row 5, row 6 and row 7. Islr2 gene

expression was detected in row 2, row 3, row 4, row 5 Notocord was used as reference point to determine rows. Dorsal up, anterior left. Nc: notochord. Scale bar: 50 µm.

4.2. Characterization of nkx1.2lb gene in the developing zebrafish

In combination with single-cell RNA sequencing with expression pattern mapping demonstrated that *nkx1.2lb* emerged as a highly enriched, and specific candidate gene in the V2s interneuron cluster. It is important to determine the expression of a gene to further characterize its possible function and regulation. The expression pattern of *nkx1.2lb* was already shown, but not in detail (Bae et al., 2004). For this reason, the expression of *nkx1.2lb* gene was investigated deeply at different stages starting with the 14-19 somite stage (16 hpf) of zebrafish development by performing chromogenic in situ hybridization against *nkx1.2lb* mRNA. *Nkx1.2lb* expression was not detected at 16 hpf, however, it was slightly detected at 18 hpf in the spinal cord in a few numbers of the cells in the spinal cord (Figure 13B, B´). In the brain region, its expression was detected in the forebrain, however, it is predominantly seen in the midbrain region which is in line with previous expression pattern analysis of nkx1.2lb in the developing brain at 2 dpf (Bae et al., 2004; Wang et al., 2023) (Figure 9A-9A´). Also, strong *nkx1.2lb* expression in the heart region was observed, but it is not possible to exactly demarcate the region of *nkx1.2lb* expression in the heart. The slight expression of *nkx1.2lb* was also detected in the notochord while strong expression was obvious in the spinal cord (Figure 13).

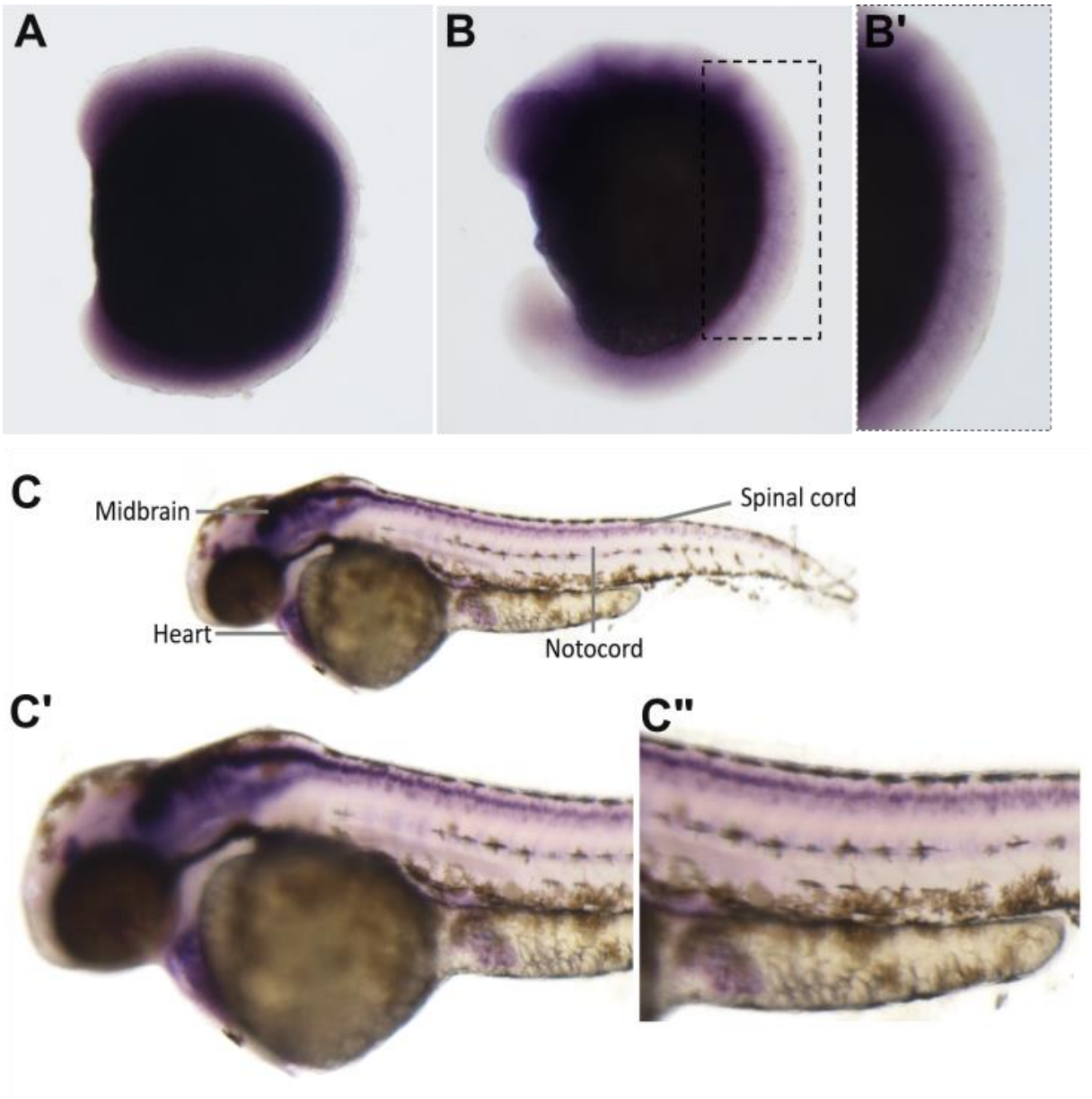

Figure 13: The expression pattern of *nkx1.2lb* gene at different developmental stages. (A) Whole mount chromogenic in situ hybridization against *nkx1.2lb* mRNA at 16 hpf. *Nkx1.2lb* expression was not detected in whole embryos at 16 hpf. **(B)** Whole mount chromogenic in situ hybridization against *nkx1.2lb* mRNA at 18 hpf. The expression of *nkx1.2lb* was detected in a few numbers of cells in the spinal cord region. **(B')** The dashed box indicates magnified region. **(C)** Whole-mount in situ hybridization against *nkx1.2lb* mRNA at 2 dpf stage. *nkx1.2lb* expression pattern in whole zebrafish embryos showing the expression pattern in the midbrain, heart, spinal cord, and notochord at 2 dpf embryo. **(C´)** The magnified region of the head part of the embryo showing strong *nkx1.2lb* expression in midbrain and heart. **(C´´)** The magnified region of the spinal cord showing strong *nkx1.2lb* expression in spinal cord, and its weak expression was in the notochord. Dorsal up, anterior left.

4.2.1 The expression profile of *nkx1.2lb* in the developing spinal cord

The position of *nkx1.2lb*-expressing cells in the spinal cord was shown between Rohon-beard neurons and primary motoneurons at 36 hpf of developmental stages (Bae et al., 2004), however, this expression analysis is not sufficient to assess the exact position of the cells. For this reason, I aim to characterize the expression pattern of *nkx1.2lb* with other domain markers to demarcate the position of the *nkx1.2lb*-expressing cells in the spinal cord (Figure 10). Oligodendrocyte lineage transcription factor 2 (*olig2)* marker was used to label the pMN domain in the developing spinal cord to describe the expression pattern of *nkx1.2lb*. In this co-labeling experiment, the stage of 30 hpf was intentionally selected to better visualize the subsets of the pMN domain with *nkx1.2lb* expression pattern (Myers et al., 1986; Ravanelli and Appel, 2015; Scott et al., 2021). *Nkx1.2lb*-positive cells are not co-localized with *olig2* marker suggesting *nkx1.2lb* expression is situated more dorsally compared to pMN domain (Figure 14A). Besides, the cellular shapes of these cells are dissimilar since *nkx1.2lb*-positive cells possess teardrop shapes extending dorsoventral position, while olig2-positive cells are spherical (Figure 14A). To demonstrate the *nkx1.2lb* expression also dorsal domain marker, developing brain homeobox 1b (*dbx1b*) to label V0 domain marker, was selected (Gribble et al., 2007). *Dbx1b*-positive neurons are easily distinguishable by their position in the spinal cord with their extending shapes compared to *nkx1.2lb*-positive cells, indicating the *nkx1.2lb*-positive cells are positioned more ventrally (Figure 14B). Another domain marker, *nkx2.2a* is widely expressed in both Kolmer-Agduhr ´´ (KA´´) cell population and lateral floor plate cells, so I used this marker to look into the localization of *nkx1.2lb*$^{+}$ cells at 1 dpf stage. *nkx1.2lb*-positive cells are located mainly more dorsally compared to *nkx2.2a*-positive cells supporting the single-cell RNA sequencing data that *nkx1.2lb* may be expressed primarily in p2 domain. However, I also detected a few numbers of cells that express both *nkx1.2lb* and *nkx2.2a* markers at 1 dpf (Figure 14C). Altogether, the co-labeling experiments with different domain-specific markers suggest that *nkx1.2lb*-expressing cells are located between the motor neuron domain and V0 domain which supports the idea of the position of *nkx1.2lb*-expressing cells in the ventral spinal cord.

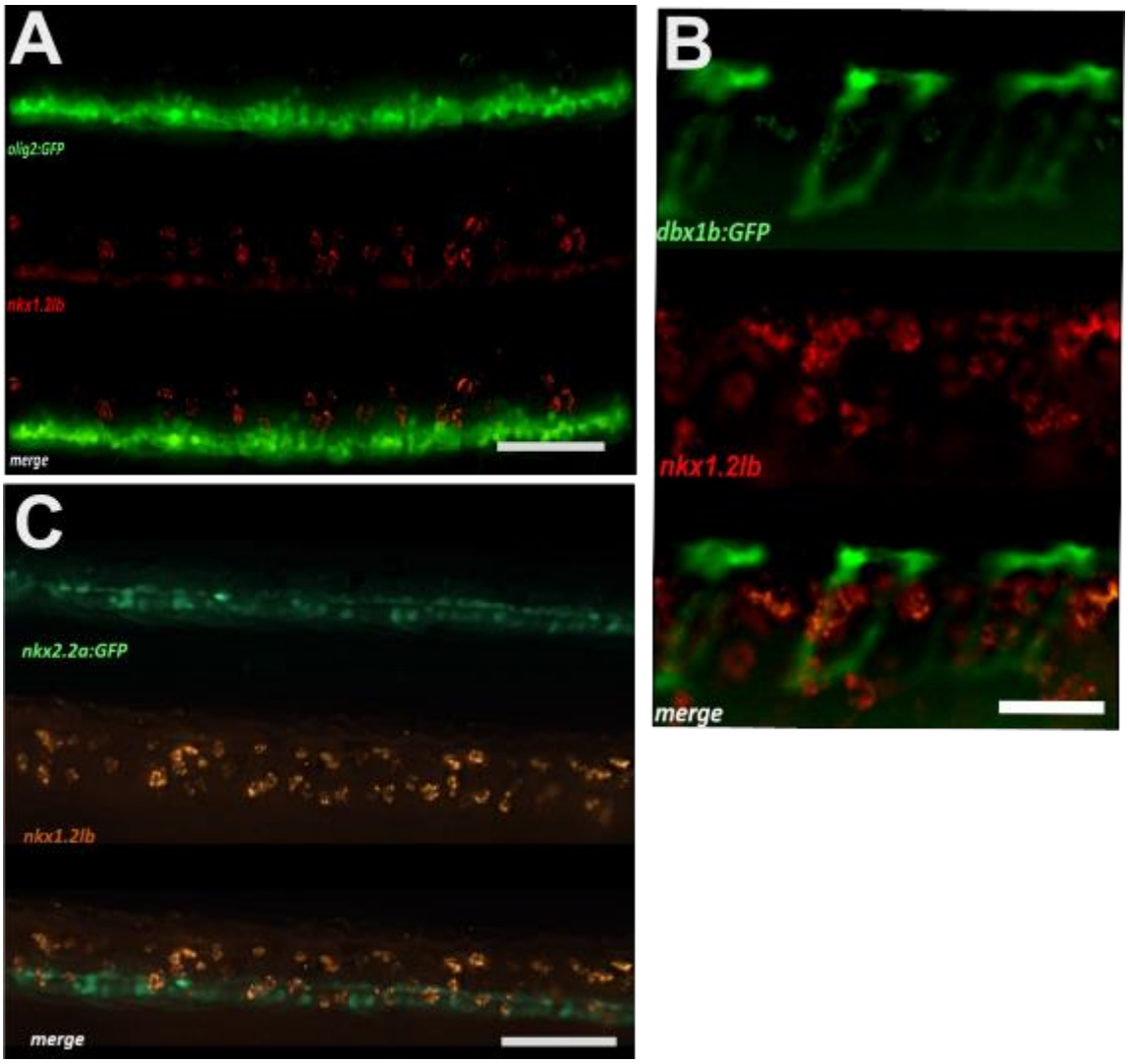

Figure 14: The expression pattern of *nkx1.2lb* with *olig2*, *nkx2.2a* and *dbx1b* markers in the embryonic spinal cord. (A) Immunofluorescent staining against GFP in *Tg(olig2:GFP)* reporter line with fluorescence in situ hybridization against *nkx1.2lb* mRNA showing the expression pattern of *nkx1.2lb* with *olig2* in embryonic spinal cord. The expression of *nkx1.2lb* was located dorsally compared to *olig2*-expressing cells. No co-localization was observed. **(B)** Immunofluorescent staining against GFP in *Tg(dbx1b:GFP)* reporter line with fluorescence in situ hybridization against *nkx1.2lb* mRNA showing the expression pattern of *nkx1.2lb* with *dbx1b* in embryonic spinal cord. No co-localization was observed. **(C)** Immunofluorescent staining against GFP in *Tg(nkx2.2a:GFP)* reporter line with fluorescence in situ hybridization against *nkx1.2lb* mRNA showing the expression pattern of *nkx1.2lb* with *nkx2.2a* in embryonic spinal cord. The expression of *nkx1.2lb* was co-localized in few ventrally located cells, the majority of *nkx1.2lb*-expressing cells were located dorsally. Dorsal up, anterior left. Scale bar: 50 µm.

The expression of *vsx1* labels the p2 cell progenitors which are the origin of all groups of the V2 cell population (Bello-Rojas and Bagnall, 2022). Transcriptional networks of *vsx1*$^{+}$ progenitor cells have not been investigated in detail, however, it has been documented that some *vsx1*$^{+}$ progenitors are co-localized with *foxn4* transcription factor (Kimura et al., 2008) . According to our single-cell sequencing results, some groups of cells in the V2 precursor cell population also express *nkx1.2lb* at 1 dpf stage. To investigate that I performed co-labeling approach targeting both *vsx1* and *nkx1.2lb* mRNAs to demonstrate the *nkx1.2lb* expression in *vsx1*$^{+}$ V2 progenitor cells at 1 dpf stage (Figure 15A). *Vsx1*$^{+}$ progenitor cells are located more ventrally, while *nkx1.2lb*$^{+}$ cells are located dorsally, proposing that *nkx1.2lb*$^{+}$ cells are already differentiated and located where mature V2 subpopulations are positioned. However, I observed that 12% of *vsx1*$^{+}$ progenitor cells which are located more ventrally also express *nkx1.2lb*, but the majority of *vsx1*$^{+}$ progenitor cells are not co-localized with *nkx1.2lb*. Besides, only 22% of *nkx1.2lb*$^{+}$ cells are co-labeled with *vsx1* (Figure 15A, B). Altogether, it can be proposed that some of *vsx1*$^{+}$ progenitor cells express *nkx1.2lb* during V2 cell development, implying the transcriptional heterogeneity of *vsx1*$^{+}$ progenitor cells (Figure 16).

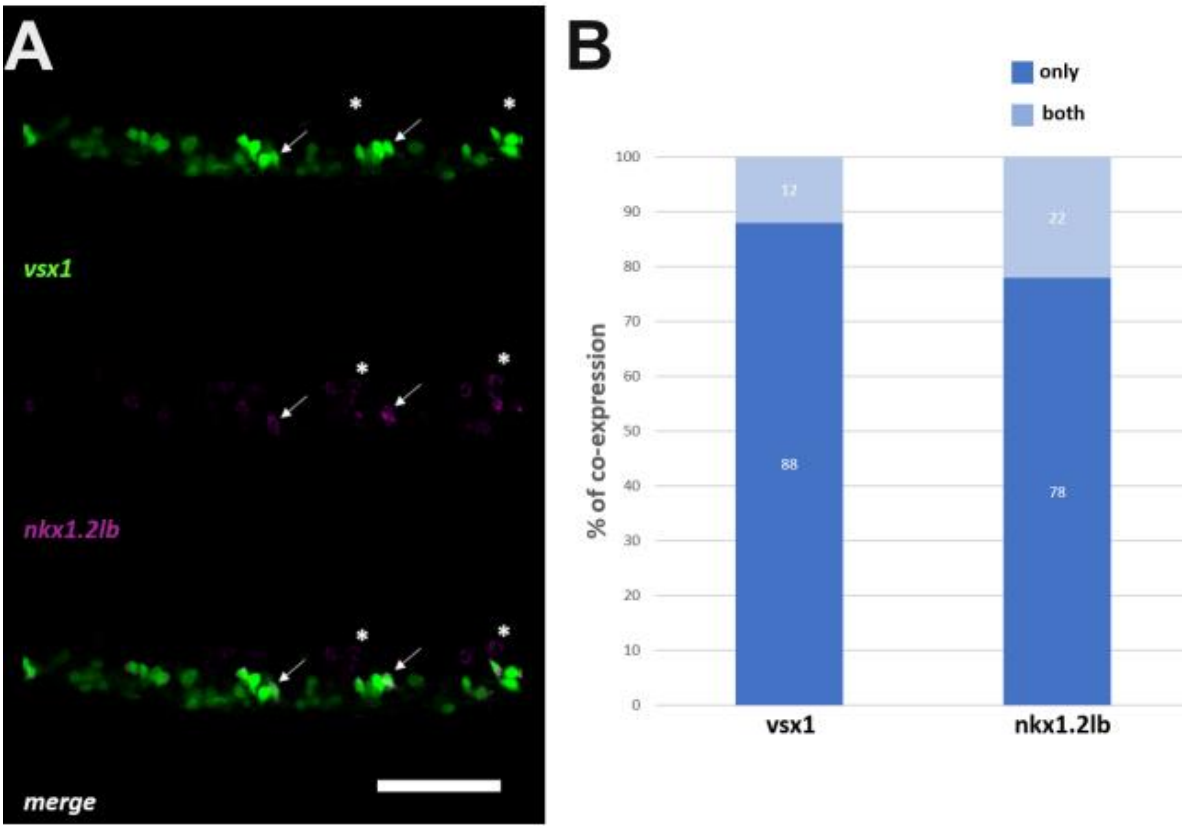

Figure 15: The expression of *nkx1.2lb* with *vsx1* gene in the embryonic spinal cord at 24 hpf. **(A)** Fluorescent in situ hybridization experiment against *nkx1.2lb* mRNA with immunofluorescence staining against GFP antibody in *Tg(vsx1:GFP)* reporter line at 24 hpf. Arrows indicate both *nkx1.2lb*$^{+}$ and *vsx1*$^{+}$ cells, and asterisks indicate only *nkx1.2lb*$^{+}$ cells. **(B)** Quantification of *nkx1.2lb*$^{+}$ and *vsx1*$^{+}$ cells. Data obtained from 3 fish for both quantifications. Dorsal up, anterior left. Scale bar: 50 µm.

.

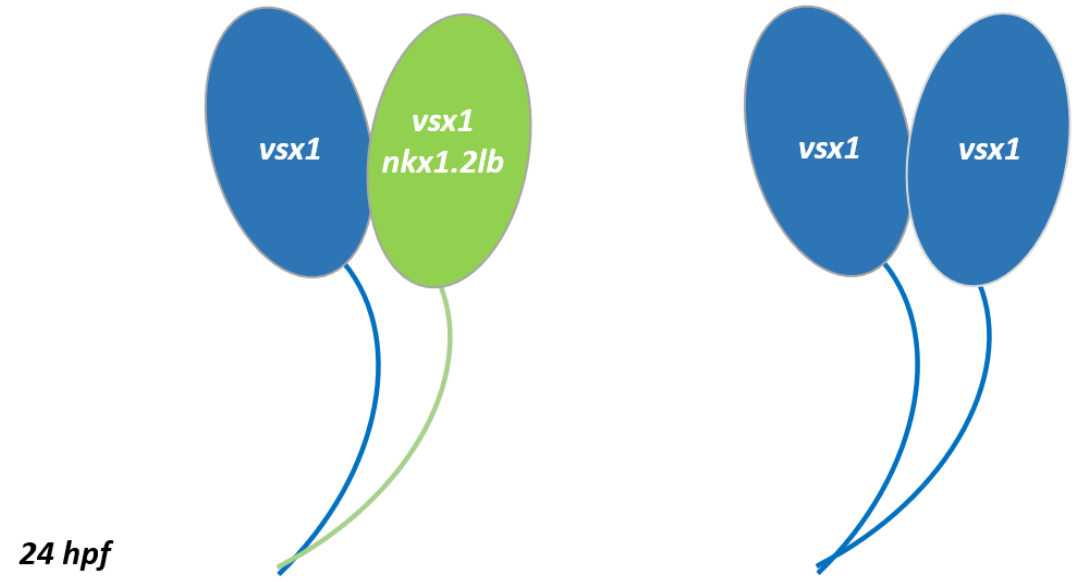

Figure 16: Proposed model of the transcriptional heterogeneity of *vsx1*-expressing progenitors in p2 domain.

4.2.2 *nkx1.2lb* is expressed in p2 domain

In the p2 domain, both V2b and V2 interneurons originated from lately formed sister pairs named V2b/V2s intermediate progenitors. *gata3* is one of the transcription factors that is widely used as a V2b interneuron marker (Andrzejczuk et al., 2018; Bello-Rojas and Bagnall, 2022; Callahan et al., 2019; Gerber et al., 2019). I performed fluorescent in situ hybridization against both *gata3* and *nkx1.2lb* mRNAs to specify whether *nkx1.2lb* is expressed in *gata3*-expressing cells. It is found that 60% of total *nkx1.2lb-expressing* cells are not co-localized with *gata3* (Figure 17, asterisks), while 40% of *nkx1.2lb*$^{+}$ cells are overlapped with *gata3* (Figure 17, arrows). Besides, only a small portion of total *gata3*$^{+}$ cells (30%) are solely positive for *gata3*, however, the majority of *gata3+* cells (60%) are co-localized with *nkx1.2lb* gene (Figure 17B).

It is clear to state that *gata3*$^{+}$ cells are mainly localized ventrally in the spinal cord and *nkx1.2lb*$^{+}$ cells are positioned more dorsal part of the developing spinal cord. Of note, gata3 is also expressed in both KA' and KA'' cells, and more ventrally located gata3-expressing cells shows KA cells. However dorsally located gata3-expressing cells mark V2b interneurons. Altogether, the co-labeling approach suggests that *nkx1.2lb* is partly co-localized with *gata3*-expressing V2b interneurons, however only *nkx1.2lb*$^{+}$ cells mainly localized more dorsal compared to *gata3*-expressing V2b interneurons which is in line with the idea that *nkx1.2lb*-expresing cells might be V2s interneurons.

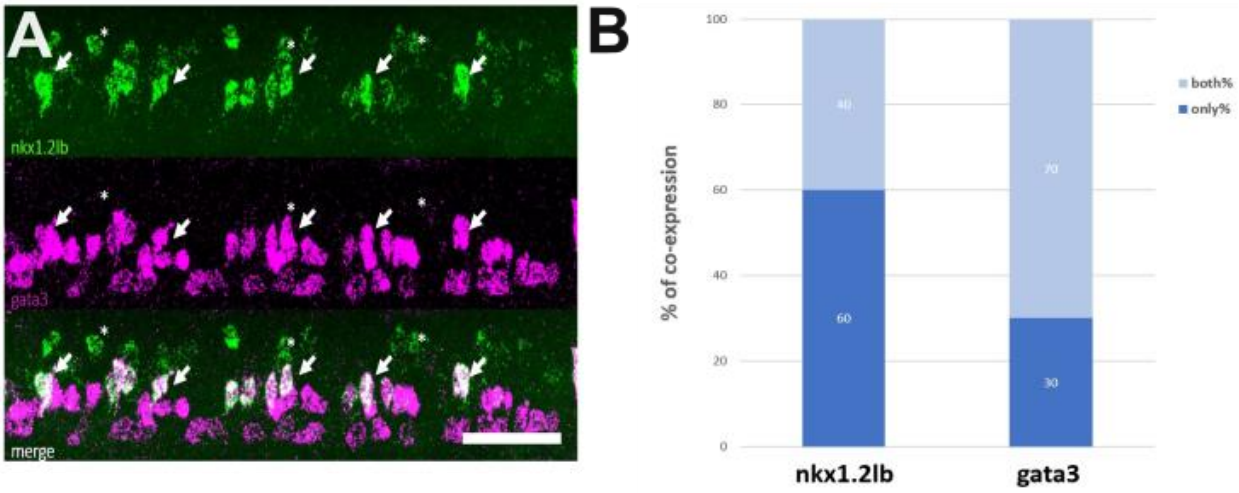

Figure 17: The expression of *nkx1.2lb* with *gata3* gene in the embryonic spinal cord at 24 hpf. (A) Fluorescent in situ hybridization against *nkx1.2lb* and *gata3* mRNAs at 24 hpf. Arrows indicate *nkx1.2lb*$^{+}$ and *gata3*$^{+}$ cells, and asterisks indicate only *nkx1.2lb*$^{+}$ cells. **(B)** Quantification of *nkx1.2lb*$^{+}$ and *gata3*$^{+}$ cells. Data obtained from 4 fish for both quantifications. Dorsal up, anterior left. Scale bar: 50 µm.

According to the single-cell analysis, *nkx1.2lb* gene co-expressed with *sox1a+* V2s interneurons. For this reason, I aim to map the expression of *nkx1.2lb* gene in V2s cells, so fluorescent in situ hybridization was conducted against *nkx1.2lb* mRNA with *sox1a*$^{+}$ V2s cells in *Tg(sox1a:eGFP)* reporter line at 24 hpf (Figure 18). This reporter line was already generated, and commonly used to label V2s cells (Bello-Rojas and Bagnall, 2022; Gerber et al., 2019). Of note, only *sox1a*$^{+}$ V2s cells were included for quantification analysis by taking into account several anatomical and positional characteristics of V2s and KA cells, since *sox1a* expression is

shared by both cell types; (I) *sox1a*$^{+}$ V2s cells possess teardrop shape extending dorso-ventral axis, and are localized more dorsally, (II) Both KA cells localized more ventrally compare to V2s cells, (III) KA cells have hair-like projections (cillia). I observed that 38% of total *nkx1.2lb*$^{+}$ cells are co-localized with *sox1a*$^{+}$ V2s cells, and these cells (*sox1a*$^{+}$*, nkx1.2lb*$^{+}$) are mainly observed in dorsal part of the spinal cord (Figure 14 Arrows), while 62% of total *nkx1.2lb*$^{+}$ cells are not co-localized with *sox1a*$^{+}$ V2s cells (Figure 14 asterisks). Besides, majority of *sox1a*$^{+}$ V2s cells express *nkx1.2lb* (%72 of total *sox1a*$^{+}$ V2s cells), and 28% of total *sox1a*$^{+}$ V2s cells do not express *nkx1.2lb* gene, suggesting the existence of transcriptionally distinct V2s cell population, which is in line with our single-cell RNA sequencing result (*sox1a*$^{+}$*, nkx1.2lb*$^{+}$ *cells*). To sum up, I detected together with single-cell RNA sequencing data that at least 3 transcriptionally distinct cells exist in V2 cell population; (i) *sox1a*$^{+}$*, nkx1.2lb*$^{+}$ cells, (ii) *sox1a*$^{+}$*, nkx1.2lb*$^{-}$ cells, (iii) *sox1*$^{-}$*, nkx1.2lb*$^{+}$ cells in p2 domain.

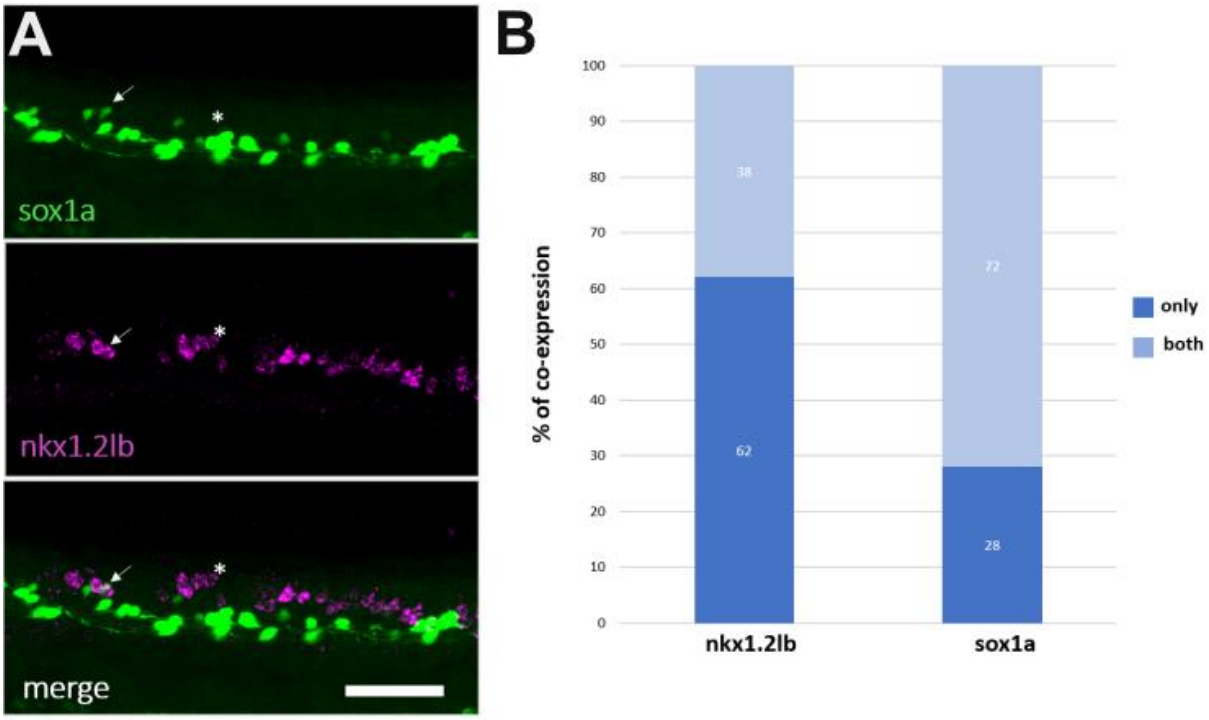

Figure 18: The expression of *nkx1.2lb* with *sox1a* gene in the embryonic spinal cord at 24 hpf. (A) Fluorescent in situ hybridization against *nkx1.2lb* with immunofluorescence staining against GFP antibody in *Tg(sox1a:eGFP)* reporter line at 24 hpf. Arrows indicate *nkx1.2lb*$^{+}$ and *sox1a*$^{+}$ cells, and asterisks indicate only *nkx1.2lb*$^{+}$ cells. **(B)** Quantification of *nkx1.2lb*$^{+}$ and *sox1a*$^{+}$ cells. Data obtained from 4 fish for both quantifications. Dorsal up , anterior left. Scale bar: 50 µm.

Sox1b gene is also essential for the development of V2s cells in the developing spinal cord in zebrafish (Gerber et al., 2019). In addition to *sox1a* expression in the p2 domain, also *sox1b* is a reliable marker to detect V2s interneurons. For co-expression analysis, I performed fluorescent in situ hybridization against both *sox1b* and *nkx1.2lb* mRNAs at 24 hpf stage (Figure 19A). I considered some anatomical features and positions of *sox1b*-expressing cells, since *sox1b* is also expressed in both KA cells (Gerber et al., 2019; L. Yang et al., 2020). I excluded both KA' and KA" cells for the quantification of co-expression analysis according to a couple of features of both KA' and KA" cells; (I) Both KA cells are located more ventrally compared to V2s cells, (II) Both KA cells possess cilia, (III) V2s cells in teardrop shape. I found that 33% of *nkx1.2lb*-expressing cells are co-localized with sox1b and the vast majority of them are not co-localized with *sox1b*. Besides, 32% of total *sox1b*-expressing cells are co-localized with *nkx1.2lb,* while 68% of *sox1b*-expressing cells are not co-localized with *nkx1.2lb*. *nkx1.2lb*$^{+}$ cells are predominantly localized more ventral compared to *sox1b*-expressing cells (Figure 19B). In summary, the ratio of *nkx1.2lb* expression with both V2s markers (*sox1a* and *sox1b*) are relatively same and proposes that *nkx1.2lb* is a reliable V2s marker and might be expressed in other cell populations in p2 domain.

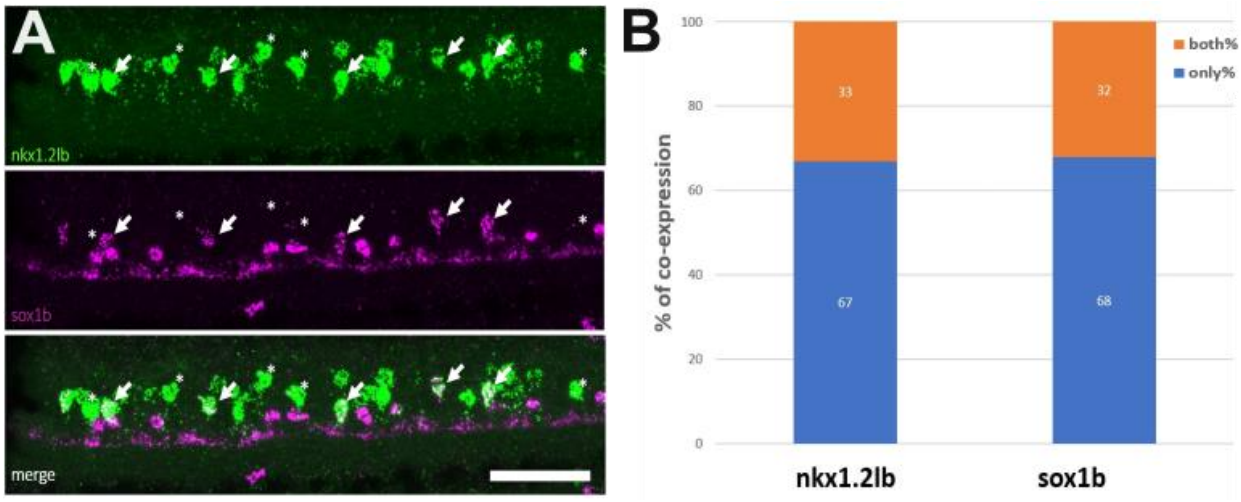

Figure 19: The expression of *nkx1.2lb* with *sox1b* gene in the embryonic spinal cord at 24 hpf. (A) Fluorescent in situ hybridization against *nkx1.2lb* and *sox1b* mRNAs at 24 hpf. Arrows indicate *nkx1.2lb*$^{+}$ and *sox1b*$^{+}$ cells, and asterisks indicate only *nkx1.2lb*$^{+}$ cells. **(B)** Quantification of *nkx1.2lb*$^{+}$ and *sox1b*$^{+}$ cells. Data obtained from 6 fish for both quantifications. Dorsal up, anterior left. Scale bar: 50 µm.

It has been documented that V2s interneurons are purely glycinergic cells and express glyt2 (slc6a5) marker (Gerber et al., 2019). To investigate the expression of *nkx1.2lb* gene in glycinergic interneurons, fluorescent in situ hybridization and immunostaining were performed in *Tg(glyt2:GFP)* line at 48 dpf (Figure 20). For this measurement, 48-hour post-fertilized embryos were chosen on purpose since V2s interneurons acquire their glycinergic characteristic at this stage of development (Gerber et al., 2019). Besides, in the transgenic line glycinergic neurons can be detected straightforwardly at this stage. I found that 53% of total *nkx1.2lb*$^{+}$ cells are co-localized with *glyt2*$^{+}$cells, (Figure 20A. arrows), while 47% of total *nkx1.2lb*$^{+}$ cells are not co-localized with *glyt2*$^{+}$ cells (Figure 20B). Furthermore, the majority of *glyt2*$^{+}$ cells do not express *nkx1.2lb* (%67 of total *glyt2*$^{+}$ cells), and a small portion of (33% of total *glyt2*$^{+}$ cells) *glyt2*$^{+}$ cells are co-localized with *nkx1.2lb* (Figure 20B). Co-labeling approach suggests that *nkx1.2lb* is expressed partly in glycinergic neurons.

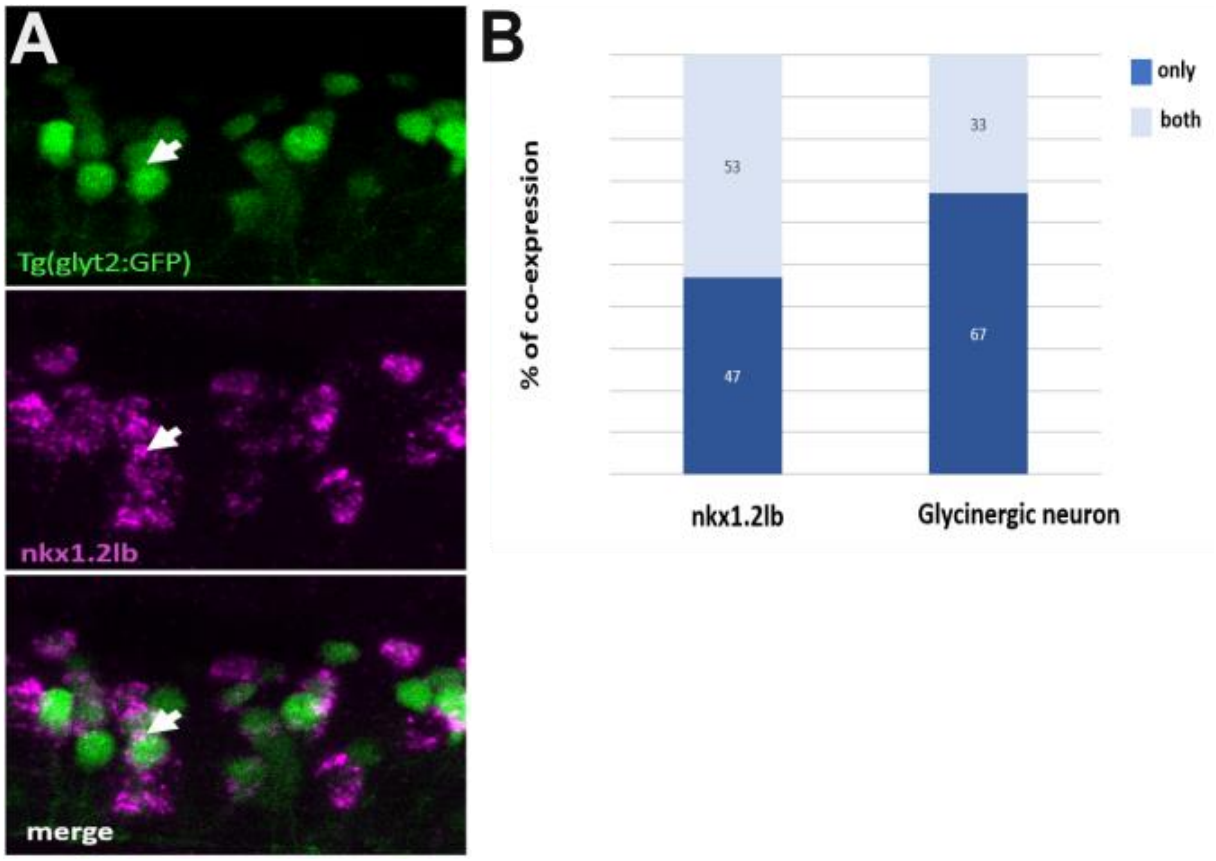

Figure 20: The expression of *nkx1.2lb* with *glyt2* gene in the embryonic spinal cord at 48 hpf. **(A)** Fluorescent in situ hybridization against *nkx1.2lb* mRNA with immunofluorescence staining against GFP antibody in *Tg(glyt2:GFP)* reporter line at 48 hpf. Arrow indicates *nkx1.2lb*$^{+}$ and *glyt2*$^{+}$ cells **(B)** Quantification of *nkx1.2lb*$^{+}$ and *glyt2*$^{+}$ cells. Data obtained from 5 fish for both quantifications. Dorsal up, anterior left.

Another highly specific gene is *islr2*, and its expression is restricted in V2 cell population. In our single-cell RNA sequencing data, *islr2* gene expression was detected in *nkx1.*2lb-expressing cells. To map its expression pattern with the expression of *nkx1.2lb* gene, I conducted fluorescent in situ hybridization against *islr2* and *nkx1.2lb* mRNAs at 24 hpf (Figure 21). I detected that 50% of *nkx1.2lb*$^{+}$ cells are co-localized with *islr2* (Figure 21A, asterisk), also half of *nkx1.2lb*$^{+}$cells (50% of *nkx1.2lb*$^{+}$ cells) do not express *islr2* gene (Figure 21, arrows). Furthermore, only 21% of *islr2*$^{+}$ cells are co-localized with nkx1.2lb gene, while a great number of *islr2*$^{+}$ cells do not express *nkx1.2lb*. In general, the expression of *islr2* is seen ventrally compared to the expression of *nkx1.2lb* gene.

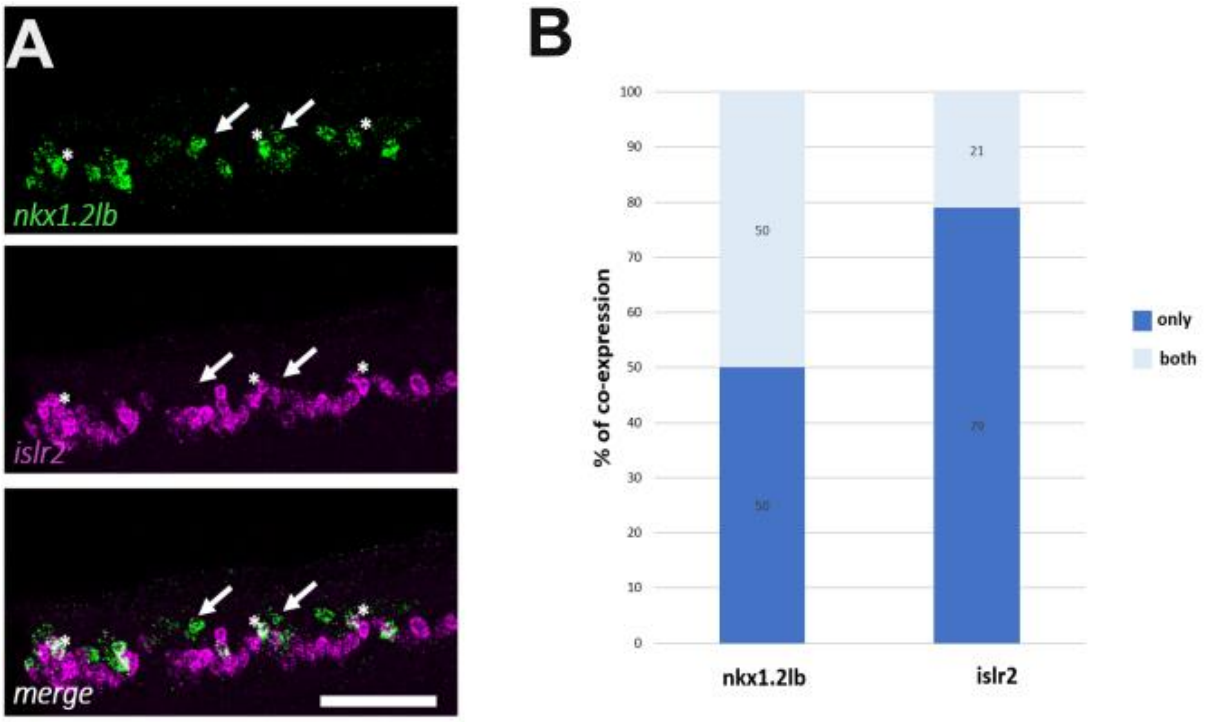

Figure 21: The expression of *nkx1.2lb* with *islr2* gene in the embryonic spinal cord at 24 hpf. (A) Fluorescent in situ hybridization against *nkx1.2lb* and *islr2* mRNAs at 24 hpf. Arrows indicate *nkx1.2lb*$^{+}$ and *islr2*$^{+}$ cells, and asterisks indicate only *nkx1.2lb*$^{+}$ cells. **(B)** Quantification of *nkx1.2lb*$^{+}$ and *islr2*$^{+}$ cells. Data obtained from 5 fish for both quantifications. Dorsal up, anterior left. Scale bar: 50 µm.

4.3 Heterogeneity of V2s interneurons

V2s interneurons are purely glycinergic cells expressing *sox1a, sox1b and slc6a5 (glyt2)* marker genes. According to our co-labeling experiments with single-cell RNA sequencing data,

nkx1.2lb is expressed in V2s cluster at different developmental stages and partly co-localized with these V2s markers (Figure 18,19,20). Interestingly, I also observed that *nkx1.2lb* marker expression is broader than *sox1a* expression in the V2s cluster at different developmental stages in our dataset and it is not always co-expressed with known V2s markers which raises the possibility of the presence of transcriptionally distinct V2s interneurons during development. I scrutinize the V2s interneuron cluster in terms of the expression of already known markers with new markers including *nkx1.2lb* and *islr2* in addition to gabaergic (gad1b) and glycinergic (slc6a5) neurotransmitter markers. I examined these distinct cell populations and divided the V2s cluster into transcriptionally distinct subpopulations at 2 dpf and 3 dpf stages, since V2s cells are rather homogenous cell populations at 1 dpf sample. I identified six distinct subpopulations at 2 dpf (Table 13). Subpopulation-1 was identified as *nkx1.2lb^{+}, sox1a^{+}, sox1b^{+}, islr2^{+}, gad1b^{+} and slc6a5^{+}*. Subpopulation-2 was defined as *nkx1.2lb^{+}, sox1^{-}, sox1b^{+}, islr2^{+}, gad1b^{+} and slc6a5^{+}*. Subpopulation-3 was defined as *nkx1.2lb^{+}, sox1a^{+}, sox1b^{+}, islr2^{-}, gad1b^{+} and slc6a5^{+}*. Intriguingly, subpopulation-1,2,3 express both (gabaergic and glycinergic) neurotransmitter markers. Purely glycinergic subpopulation-4 is defined as *nkx1.2lb^{+}, sox1a^{+}, sox1b^{+}, islr2^{+}, gad1b^{-} and slc6a5^{+}*. On the contrary, subpopulation-5 is solely gabaergic cells and defined as *nkx1.2lb^{+}, sox1a^{+}, sox1b^{-}, islr2^{-}, gad1b^{+} and slc6a5^{-}*. Only glycinergic and *nkx1.2lb* expression was detected in subpopulation-6 which is defined as *nkx1.2lb^{+}, sox1a^{-}, sox1b^{-}, islr2^{-}, gad1b^{-} and slc6a5^{+}*.

	nkx1.2lb	***sox1a***	***sox1b***	***islr2***	***gad1b***	***slc6a5***
Subpopulation-1	X	X	X	X	X	X
Subpopulation-2	X	-	X	X	X	X
Subpopulation-3	X	X	X	-	X	X
Subpopulation-4	X	X	X	X	-	X
Subpopulation-5	X	X	-	-	X	-
Subpopulation-6	X	-	-	-	-	X

Table 13: Detected subpopulations of V2s interneuron by single-cell RNA sequencing at 2 dpf.

I also examined the V2s cluster at the stage of 3 dpf. I found seven transcriptionally distinct subpopulations of V2s interneuron at 3 dpf (Table 14). Subpopulation-1 was a purely glycinergic population and identified as *nkx1.2lb*$^{+}$*, sox1a*$^{+}$*, sox1b*$^{+}$*, islr2*$^{+}$*, gad1*$^{-}$ *and slc6a5*$^{+}$. Subpopulation-2 was glycinergic cells and defined as *nkx1.2lb*$^{+}$*, sox1a*$^{+}$*, sox1b*$^{-}$*, islr2*$^{+}$*, gad1b*$^{-}$ *and slc6a5*$^{+}$. Subpopulation-3 was also glycinergic and defined as *nkx1.2lb*$^{+}$*, sox1a*$^{-}$*, sox1b*$^{+}$*, islr2*$^{-}$*, gad1b*$^{-}$ *and slc6a5*$^{+}$. Subpopulation-4 was the only subpopulation expressing both neurotransmitter markers and was defined as *nkx1.2lb*$^{+}$*, sox1a*$^{-}$*, sox1b*$^{-}$*, islr2*$^{-}$*, gad1b*$^{+}$ *and slc6a5*$^{+}$. Subpopulation-5 and Subpopulation-6 did not express any neurotransmitter marker and defined as *nkx1.2lb*$^{+}$*, sox1a*$^{+}$*, sox1b*$^{-}$*, islr2*$^{-}$*, gad1b*$^{-}$*, slc6a5*$^{-}$ and *nkx1.2lb*$^{+}$*, sox1a*$^{-}$*, sox1b*$^{-}$*, islr2*$^{-}$*, gad1b*$^{+}$ *and slc6a5*$^{-}$, respectively. Altogether, V2s subpopulations are transcriptionally more heterogeneous and consist of different subpopulations. Moreover, V2s subpopulations at 3 dpf are more differentiated subpopulations exhibiting *slc6a5* expression compared to the subpopulation at 2 dpf.

	nkx1.2lb	***sox1a***	***sox1b***	***islr2***	***gad1b***	***slc6a5***
Subpopulation-1	X	X	X	X	-	X
Subpopulation-2	X	X	-	X	-	X
Subpopulation-3	X	-	X	-	-	X
Subpopulation-4	X	-	-	-	X	X
Subpopulation-5	X	X	-	-	-	-
Subpopulation-6	X	-	-	-	-	-
Subpopulation-7	X	-	-	-	X	-

Table 14: Detected subpopulations of V2s interneuron by single-cell RNA sequencing at 3 dpf.

4.4 Characterization of the functions of nkx1.2lb in V2s cell development

After the characterization of *nkx1.2lb* expression in the spinal cord, the other aim is to investigate the possible role of *nkx1.2lb* in the development of V2s interneuron, for this reason, knock-down approach was used against *nkx1.2lb* gene.

4.4.1 The role of nkx1.2lb in V2 progenitor cells

V2 precursor cells are the source of V2 interneurons in the spinal cord. V2 precursor cells express *vsx1*, and *foxn4* transcription factors in zebrafish spinal cord (Kimura et al., 2008). As shown in figure (15,18,19), *nkx1.2lb* is expressed in V2 precursor cluster and V2s interneuron cluster in our single-cell RNA sequencing data, and it is clear that some *nkx1.*2lb-expressing cells are co-localized with *vsx1*-expressing, raising the possibility that *nkx1.*2lb may be responsible for the maintenance of *vsx1*$^{+}$ *or foxn4*$^{+}$ progenitor pools. To interrogate this possibility, immunostaining and chromogenic in situ hybridization were performed and the number of *vsx1*$^{+}$ *and foxp3*$^{+}$ progenitor cells in *nkx1.2lb* knock-down embryos were quantified at 24 hpf (Figure 22). First, I utilized *Tg(vsx1:GFP)* reporter line, which is already used to assess p2 progenitors in the spinal cord (Kimura et al., 2008). Morpholino was injected into 1-cell stage embryos according to (Kimmel et al., 1995). No anatomical differences were detected in *vsx1*$^{+}$ V2 precursors in the group of *nkx1.2lb* knock-down embryos (Figure 22A). Additionally, the quantification analysis of *vsx1*$^{+}$ V2 precursor cells showed no significant change between control and *nkx1.2lb* knock-down embryos, suggesting *nkx1.2lb* may not be essential for the development of *vsx1*$^{+}$ V2 precursor at 24 hpf (Figure 22A'). In addition, I used another V2 precursor marker to assess the possible function of *nkx1.2lb* gene in the development of *foxn4*$^{+}$ progenitor cells (Figure 22B). Neither the position of the *foxn4*$^{+}$ V2 precursor cells (*foxn4*$^{+}$ cells were detected in row 3 and row 4 in both cases) nor their numbers in knock-down of *nkx1.2lb* compared to control embryos were detected (Figure 22B,B'). Altogether, the knock-down of *nkx1.2lb* did not affect the generation of *vsx1*$^{+}$ *or foxn4*$^{+}$ V2 progenitor cells in the developing spinal cord.

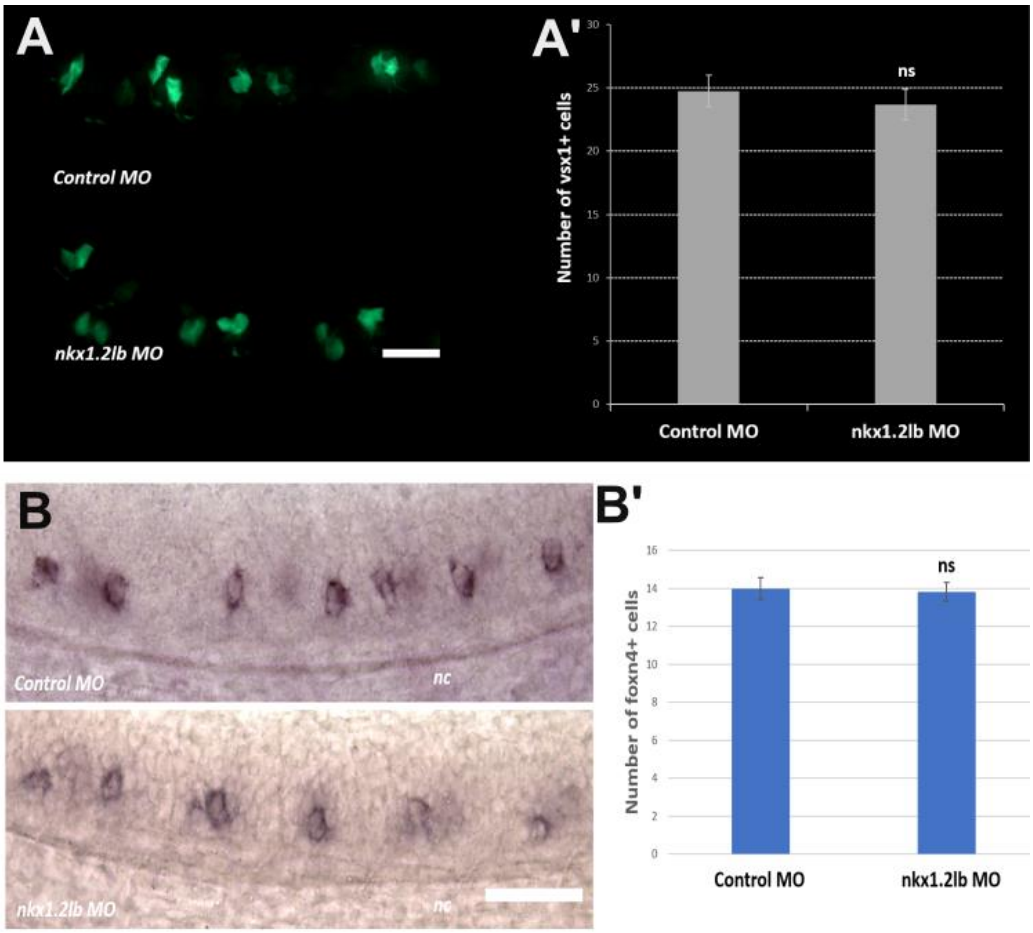

Figure 22: The effect of *nkx1.2lb* knock-down on *vsx1⁺ or foxn4⁺* V2 progenitor marker genes at 24 hpf. (A) Immunofluorescence staining against GFP antibody in *Tg(vsx1:GFP)* reporter line as a marker of V2 progenitor in control morpholino injected embryos and *nkx1.2lb* morpholino injected embryos at 24 hpf stage. **(A')** Quantification of *vsx1*⁺ cells (data are shown as mean ± SEM). Data obtained from 12 fish for control morpholino-injected embryos and 12 fish from *nkx1.2lb* morpholino injected fish. **(B)** Whole mount chromogenic in situ hybridization against *foxn4* mRNA in control morpholino injected and *nkx1.2lb* morpholino injected fish at 24 hpf. **(B')** Quantification of *foxn4*⁺ cells in both control morpholino-injected embryos and *nkx1.2lb* morpholino injected embryos at 24 hpf stage (data are shown as mean ± SEM). Data obtained from 6 fish from control morpholino-injected embryos and 6 fish from *nkx1.2lb* morpholino injected fish. Significance is indicated by asterisks. nc: notochord. P>0.05 ns. Dorsal up, anterior left. Scale bar: 50 µm.

4.4.2 The role of *nkx1.2lb* in V2s cells

Nkx1.2lb is expressed in both V2 precursor cells and V2s interneurons as shown in figure 11 and figure 14. *Nkx1.2lb* knock-down did not cause any change in the number of *vsx1+* and *foxn4+* progenitor cells as shown in figure 22. The expression of nkx1.2lb occurs in relatively

late stage of the development in the spinal cord as shown in figure 13, so the possible function of *nkx1.2lb* was assessed in the development of V2s interneurons. For this aim, I used *Tg(sox1a:EGFP)* reporter line to label V2s interneurons (Figure 23A). In this analysis, only dorsally positioned sox1a^{+} cells are considered since KA´ and KA´´ cells also express *sox1a* gene. (I) s*ox1a*$^{+}$ V2s cells possess teardrop shape extending dorso-ventral axis, and are localized more dorsally, (II) Both KA cells localized more ventrally compare to V2s cells, (III) KA cells have hair-like projections (cillia) (Figure 23B). I observed that the number of V2s interneurons was significantly decreased in *nkx1.2lb* morphants (Figure 23C). In addition, I analysed both KA´ and KA´´ cells in nkx1.2lb morphants, but I did not observe any significant change in the total number of both KA´ and KA´´ cells (Figure 23D). These observations suggest two ideas; firstly, *nkx1.2lb* knock-down results in less production of V2s interneurons, while the number of both KA cell was not affected. Secondly, morpholino injection did not cause toxic effects on the embryos.

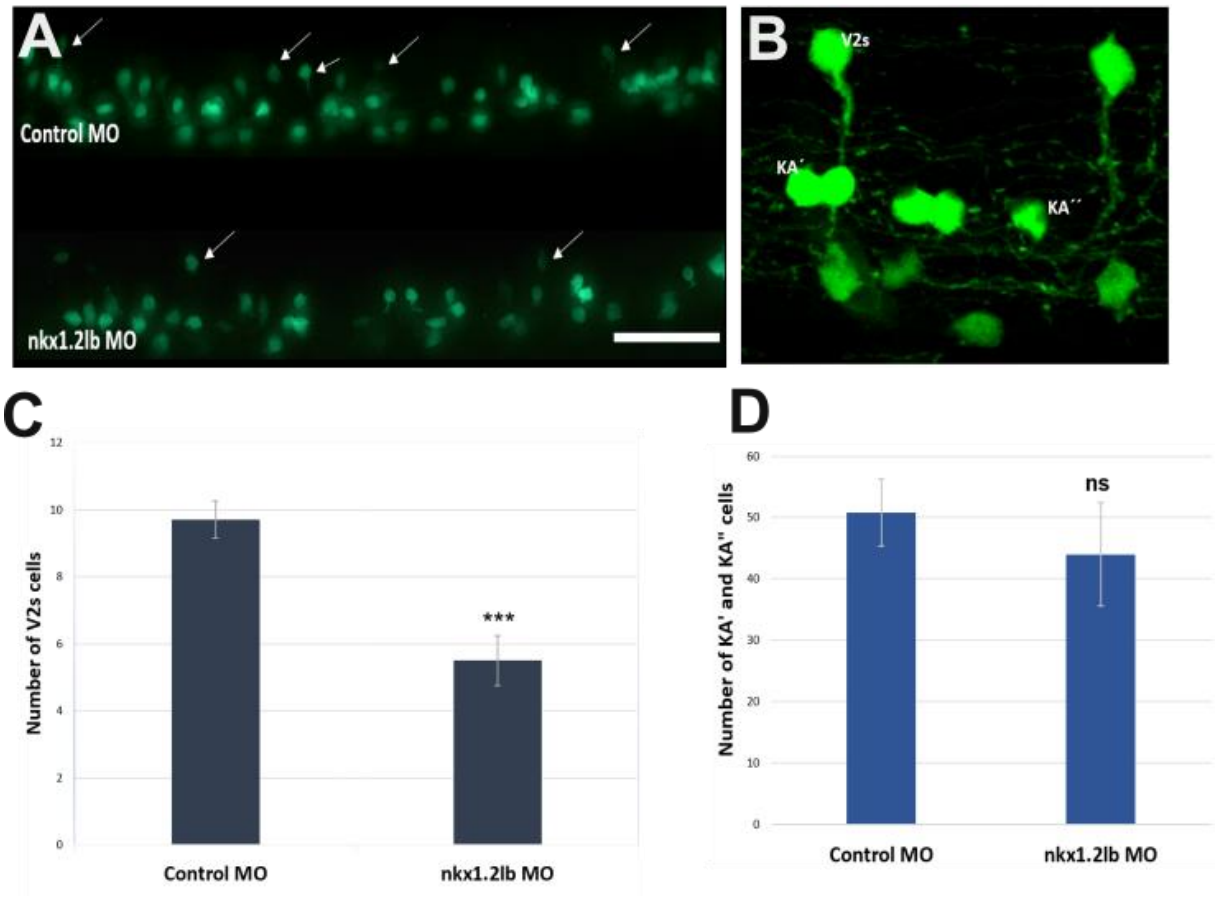

Figure 23: Knock-down of *nkx1.2lb* leads to the generation of a small number of V2s interneurons at 24 hpf stage. (A) Immunofluorescence staining against GFP antibody in *Tg(sox1a:EGFP)* reporter line as a marker of V2s interneurons and KA' and KA'' cells in control morpholino injected embryos and *nkx1.2lb* morpholino injected embryos at 24 hpf stage. **(B)** *Tg(sox1a:EGFP)* reporter line showing dorsally located V2s interneuron and ventrally located KA' and KA'' cells at 24 hpf stage. **(C)** Quantification of V2s cells in both groups (data are shown as mean ± SEM). Data obtained from 13 fish for control morpholino-injected embryos and 13 fish from *nkx1.2lb* morpholino injected fish. **(D)** Quantification of KA´ and KA´´ cells in both groups (data are shown as mean ± SEM). Data obtained from 11 fish for control morpholino-injected embryos and 11 fish from *nkx1.2lb* morpholino injected embryos. Significance is indicated by asterisks. P ≤ 0.001 ***, P>0.05 ns. Dorsal up, anterior left. Scale bar: 50 µm.

Glycinergic identity of V2s cells are characterized by the expression of *slc6a5* gene (Gerber et al., 2019). To determine whether glycinergic cells are affected by the knock-down of nkx1.2lb I quantified the total number of *slc6a5*-expressing cells at 30 hpf. I intentionally chose this stage since V2s interneurons begins to differentiate into glycinergic characteristics (Gerber et al., 2019). *Nkx1.2lb* morphants display significant decrease in the number of glycinergic neurons, proposing knock-down of *nkx1.2lb* causes less glycinergic cell developments in the spinal cord (Figure 24). However, this data is preliminary to propose the possible functions of *nkx1.2lb* in the generation of V2s interneuron since glycinergic identity is not only restricted in V2s interneurons.

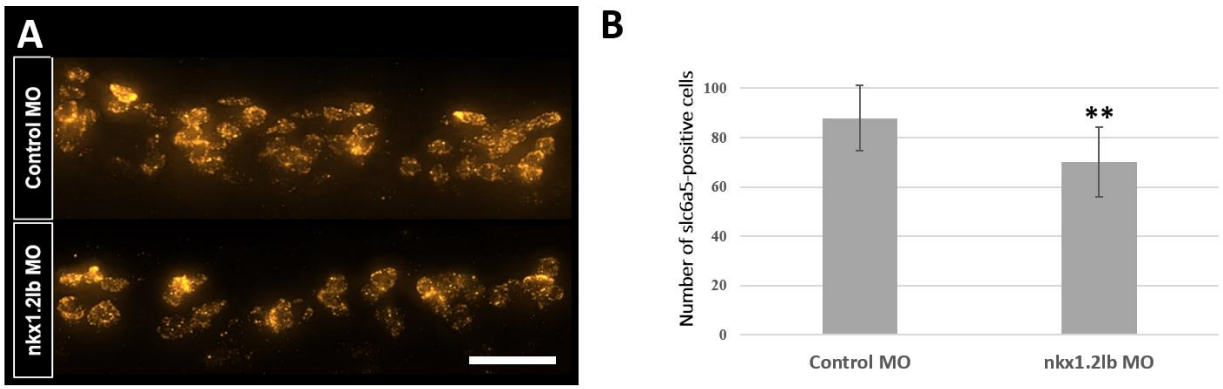

Figure 24: Knock-down of nkx1.2lb embryos develop a small number of glycinergic neurons at 30 hpf stage. (A) Fluorescent in situ hybridization experiments against glycinergic neurotransmitter marker, *slc6a5* mRNA in control morpholino injected embryos and *nkx1.2lb* morpholino injected embryos at 30 hpf spinal cord. **(B)** Quantification of slc6a5+ cells (data are shown as mean ± SEM). Data obtained from 12 fish for control morpholino-injected embryos and 12 fish from *nkx1.2lb* morpholino injected fish. Significance is indicated by

asterisks. P ≤ 0.01 **. Dorsal up, anterior left. Scale bar: 50 µm. of (data are shown as mean ± SEM). Data obtained from 12 fish for control morpholino-injected embryos and 12 fish from *nkx1.2lb* morpholino injected fish. Significance is indicated by asterisks. P ≤ 0.01 **. Dorsal up, anterior left. Scale bar: 50 µm.

Our single-cell RNA sequencing data revealed novel candidate genes enriched in V2s interneuron cluster, and novel candidates were validated by chromogenic in situ hybridization in detail as already shown in figure 12. The possible candidates were positioned where *sox1a*-expressing V2s interneurons located. Furthermore, positions of *nkx1.*2lb-expressing cells (between row 2 to row 5) are co-exist with the *cacna2d3, cplx2l and islr2* candidates, so in order to understand whether these candidates are down-stream targes of *nkx1.2lb* gene, chromogenic in situ hybridization was performed in *nkx1.2lb* knock-down embryos and their positions were determined (Figure 25). The expression of *cacna2d3* was detected in row 4, row 5, row 6 and row 7 in control and *nkx1.2lb* knock-down embryos, also the number of *cacna2d3*$^{+}$ cells did not change (Figure 25A, A´). *cplx2l-expressing* cells were observed in row 2, row 3, row 4, row 5, row 6 and row 7 in both control and *nkx1.2lb* knock-down embryos, no difference in the number of *cplx2l-expressing* cells observed in *nkx1.2lb* knock-down embryos (Figure 22B, B'). The expression of *islr2* was observed in row 2, row 3, row 4 and row 5, also *nkx1.2lb* knock-down did not affect the number of *islr2-expressing* cells (Figure 25C, C'). Altogether knock-down approach suggests that these markers were not affected by the knock-down of *nkx1.2lb*.

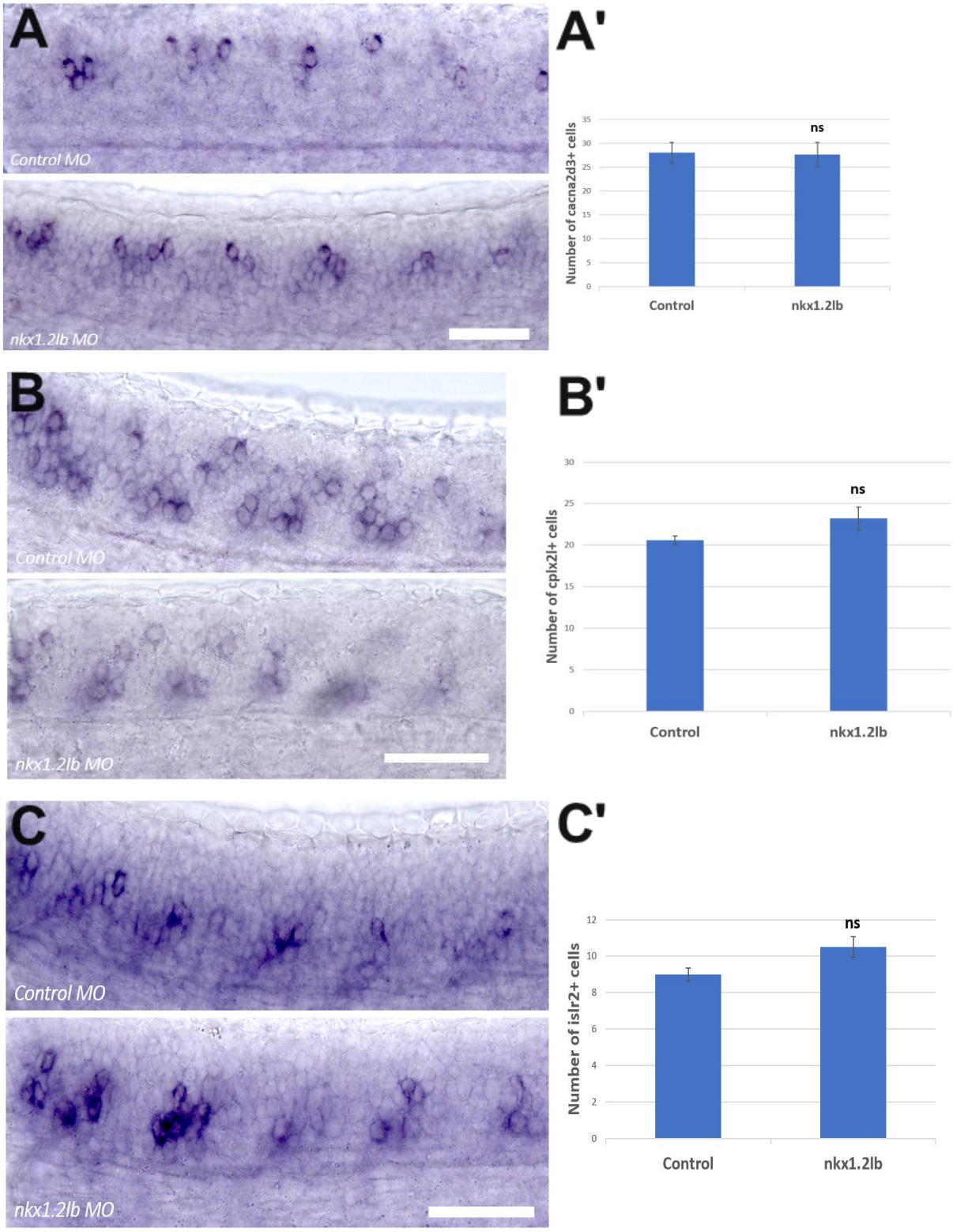

Figure 25: Chromogenic in situ hybridization against *cacna2d3*, *cplx2l* and *islr2* mRNAs in *nkx1.2lb* knock-down with control morpholino injected embryos at 24 hpf stage. (A) Chromogenic in situ hybridization against *cacna2d3* mRNA in nkx1.2lb morphant and control morpholino injected embryos at 24 hpf. **(A')** Quantification of cacna2d3^{+} cells (data are shown as mean ± SEM). Data obtained from 5 fish for control morpholino-injected embryos and 5 fish

from *nkx1.2lb* morpholino injected embryos at 24 hpf. **(B)** Chromogenic in situ hybridization against *cplx2l* mRNA in *nkx1.2lb* morphant and control morpholino injected embryos at 24 hpf. **(B')** Quantification of cplx2l^{+} cells (data are shown as mean ± SEM). Data obtained from 5 fish for control morpholino-injected embryos and 5 fish from *nkx1.2lb* morpholino injected fish **(C)** Chromogenic in situ hybridization against *islr2* mRNA in *nkx1.2lb* morphant and control morpholino injected embryos at 24 hpf. **(C')** Quantification of islr2^{+} (data are shown as mean ± SEM). Data obtained from 4 fish for control morpholino-injected embryos and 4 fish from *nkx1.2lb* morpholino injected fish. Significance is indicated by asterisks. P>0.05 ns. Dorsal up, anterior left. Scale bar: 50 µm.

4.4.3 Generation of CRISPR mutant for *nkx1.2lb*

Knock-down of *nkx1.2lb* resulted in the production of a smaller number of V2s interneurons without influencing the number of KA cells as shown in figure 23. Next approach to further support this data is the generation of *nkx1.2lb* mutant zebrafish. For this purpose, I screened three pairs of guide RNAs targeting *nkx1.2lb* gene and they were injected into 1- cell stage zebrafish embryos according to (Kimmel et al., 1995). Unfortunately, selected guide RNAs were not efficient enough to delete *nkx1.2lb* gene entirely, except guide #3 and guide #5. Nevertheless, this guide RNA was not used for further experiments (Figure 25, 26).

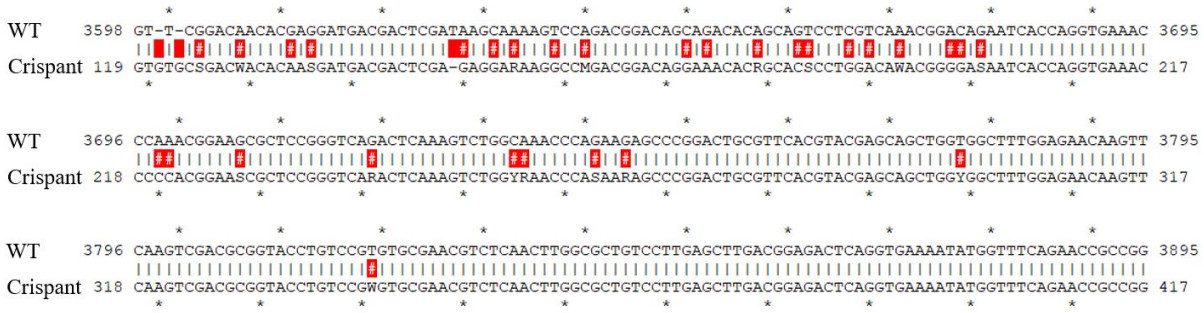

Figure 26: Sequence alignment of wild-type and guide-3 injected *nkx1.2lb* crispant. Guide RNA #3 genereted mismatches in exon 2 of *nkx1.2lb* gene. Number sign (#) indicates possible point mutations

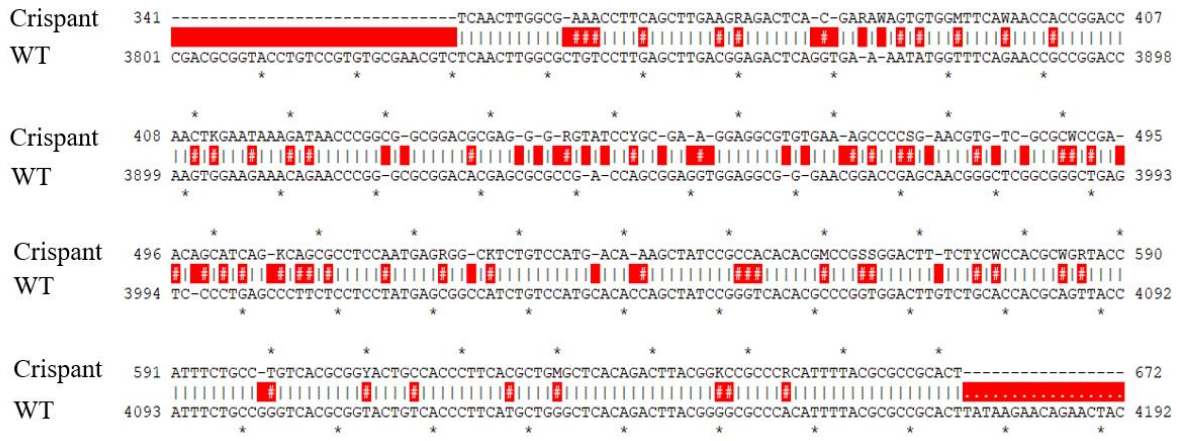

Figure 27: Sequence alignment of wild-type and guide-5 injected *nkx1.2lb* crispants. Guide RNA #5 generated mismatches in exon 2 of *nkx1.2lb* gene. Number sign (#) indicates possible point mutations

4.5 Characterization and validation of cis-regulator modules of *nkx1.2lb* gene

As yet, the expression pattern of *nkx1.2lb* gene at different stages of development was investigated. As shown in figure 13, the expression of *nkx1.2lb* is detected strongly in heart and spinal cord. Next, I aim to dissect putative cis-regulatory modules (CRMs) of *nkx1.2lb* gene to clarify how *nkx1.2lb* gene is transcriptionally regulated in these organs. For this aim, I benefited from promoter bashing technique to identify putative promoter region of *nkx1.2lb* gene. First, 2.5 kilobase (-2.5 kb) up-stream region of transcription starting site (TSS) of *nkx1.2lb* gene was cloned with Gateway strategy to assess the activity of the cloned region. The GFP activity was detected only in the heart (Figure 28) resembling the expression *nkx1.2lb* in the heart (Figure 13). After that 1.5 kb up-stream region (-1.5 kb) of transcription starting site of *nkx1.2lb* gene was also cloned with the same Gateway strategy. It is found that the activity of this region again partially resembled the *nkx1.2lb* gene expression in heart, but -1.5 kb region displayed weaker activity in the heart compared to the activity of -2.5 kb region, suggesting -1.5 kb region may be sufficient and contains minimal promoter region to induce promoter activity of *nkx1.2lb* and they are presumably active in the heart, since the located cells in the heart were contracting in both cases (Figure 28).

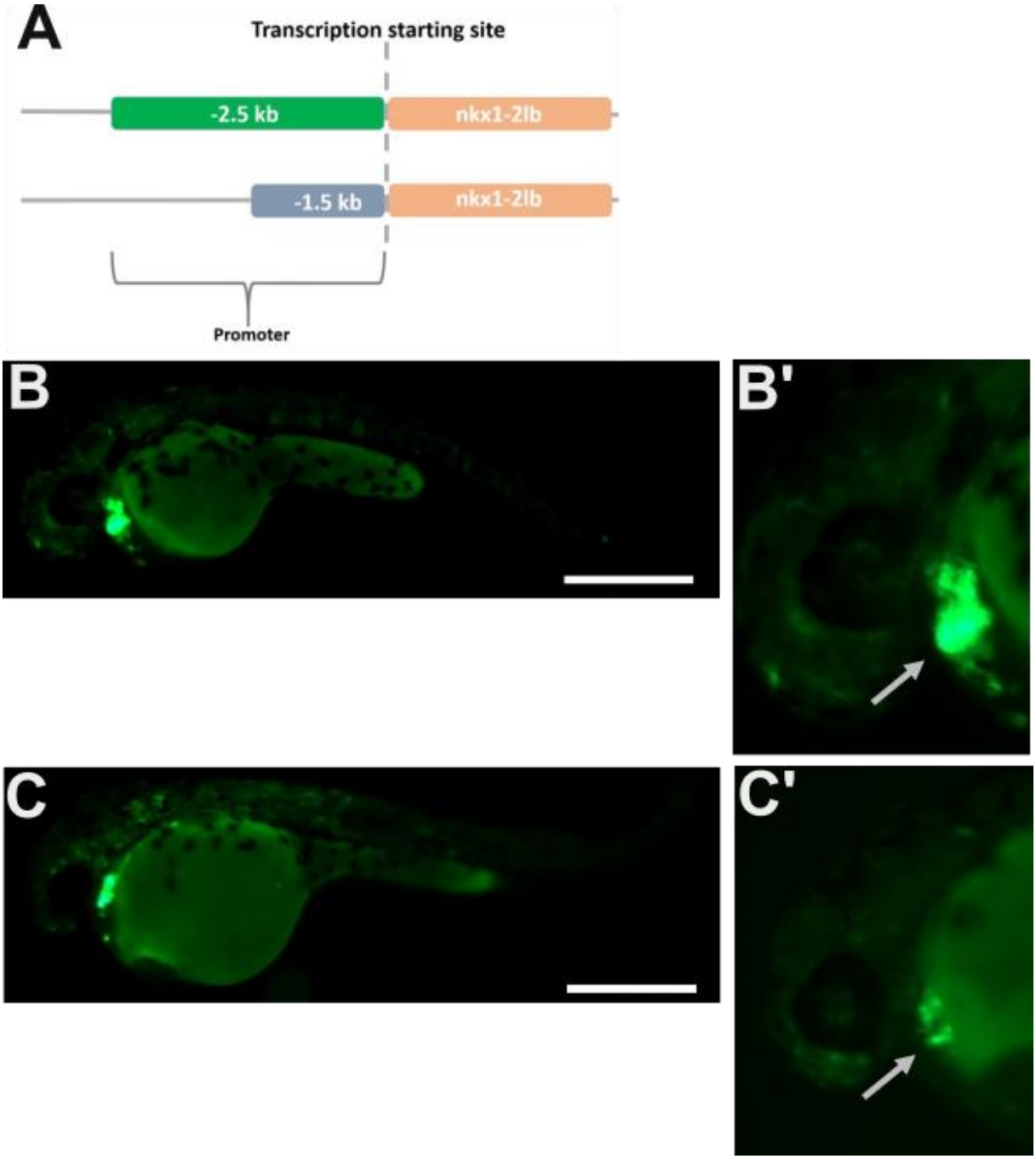

Figure 28: Promoter activity of *nkx1.2lb* gene in the heart. (A) Cloning strategy to identify putative promoter region of *nkx1.2lb.* Longer (-2.5 kb), and shorter (-1.5 kb) versions of 5´ region of *nkx1.2lb* are cloned to determine its promoter region. **(B)** The activity of 2.5 upstream region of *nkx1.2lb* gene was detected at 2 dpf stage of embryos. **(B')** Magnified region of the anterior part of the fish in figure (B), arrow indicates the activity in the heart (B). **(C)** The activity of 1.5 upstream region of *nkx1.2lb* gene was detected at 2 dpf stage of embryos. **(C')** Magnified region of the anterior part of the fish in figure (C), arrow indicates the activity in the heart. Dorsal up, anterior left. Scale bar: 50 µm.

The longer and shorter versions of the putative promoter activities partially reflect the expression pattern of *nkx1.2lb* gene as shown in Figure 3, by showing the activity solely in the heart. Transcriptional regulation of a gene requires cooperative activation of distinct cis-regulatory modules of the target gene. Hence, putative enhancer regions of *nkx1.2lb* were retrieved from existing Assay for transposase accessible chromatin-sequencing (ATAC-Seq) data in UCSC Genome Browser with DANIO-CODE Track hub (Baranasic et al., 2022). According to the browser, nkx1.2lb is located in chromosome 14, and ATAC-Seq peaks are predominantly detected in upstream region of *nkx1.2lb*, suggesting these regions may possess open chromatin regions where enhancers are enriched. In general, I found 6 possible different putative enhancers near the upstream region of *nkx1.2lb* (Figure 25A). To test the activity of each putative CRM in the regulation of *nkx1.2lb*, an expression vector was generated with the help of already established protocol (Navratilova et al., 2009). The expression vector contains promoter of *gata2a* driving the expression of enhanced GFP (eGFP), flanked by the tol2 transposase sites which render possible the integration of the construct into the zebrafish genome. Putative CRMs are cloned into the expression vector, and expression vectors were injected into one-cell stage embryos (Figure 29).

Figure 29: Putative cis-regulatory elements of *nkx1.2lb* gene. A depiction showing the positions of putative enhancers of nkx1.2lb gene. CRM1 is located 52.7 kb, CRM2 is located 43.7 kb, CRM3 is located 39.7 kb, CRM4 is located 35 kb, and CRM5 is located 29 kb up-stream region from TSS of the gene respectively. eRNA-encoding region (CRM-6) is located in the intron of *nkx1.2lb* gene.

After injection of each CRM, GFP activity was screened to assess possible activity of each CRM. After that expression vectors containing each CRM named as; *nkx1.2lb-CRM1-gata2:eGFP*, *nkx1.2lb-CRM2-gata2:eGFP*, *nkx1.2lb-CRM3-gata2:eGFP*, *nkx1.2lb-CRM4-gata2:eGFP*, *nkx1.2lb-CRM5-gata2:eGFP*, *nkx1.2lb-CRM6-gata2:eGFP.* According to danRer 10, the length

of CRM-1 is 420 bp, positioned in chr14:14705157-14705577, and annotated as weak enhancer in ATAC-Seq data. The activity of CRM-1 was not observed in the embryos. CRM-2 is located in chr14:14713631-14714251, 620 bp in length, and annotated as active enhancer. The activity of CRM-2 was not detected. CRM-3 is positioned in chr14:14717461-14718456, 995 bp in length, and annotated as active enhancer. The activity of CRM-3 was not detectable (Figure 30).

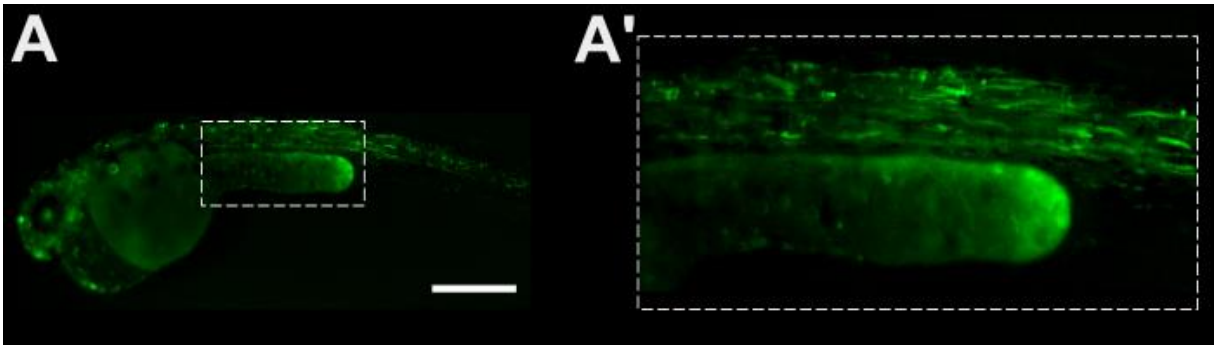

Figure 30: The activity of CRM-3 at 2 dpf embryos in the spinal cord (A) The activity showing the whole embryos at 2 dpf. **(A'')** Magnified region of dashed box in figure x (A) showing the artifact in the muscle fibers. Dorsal up, anterior left. Scale bar: 200 µm.

CRM-4 is located in chr14:14,722,628-14,723,237, 609 bp in length, and annotated as a flanking enhancer in ATAC-seq data. The activation of CRM-4 was detected only in the heart, not in the spinal cord (Figure 31). This activity resembles the activity observed in both longer and shorter versions of the promoter activity which is only detected in heart (Figure 31). The activity was detected probably in the cardiac muscles since the cells possessing GFP activity were contracting.

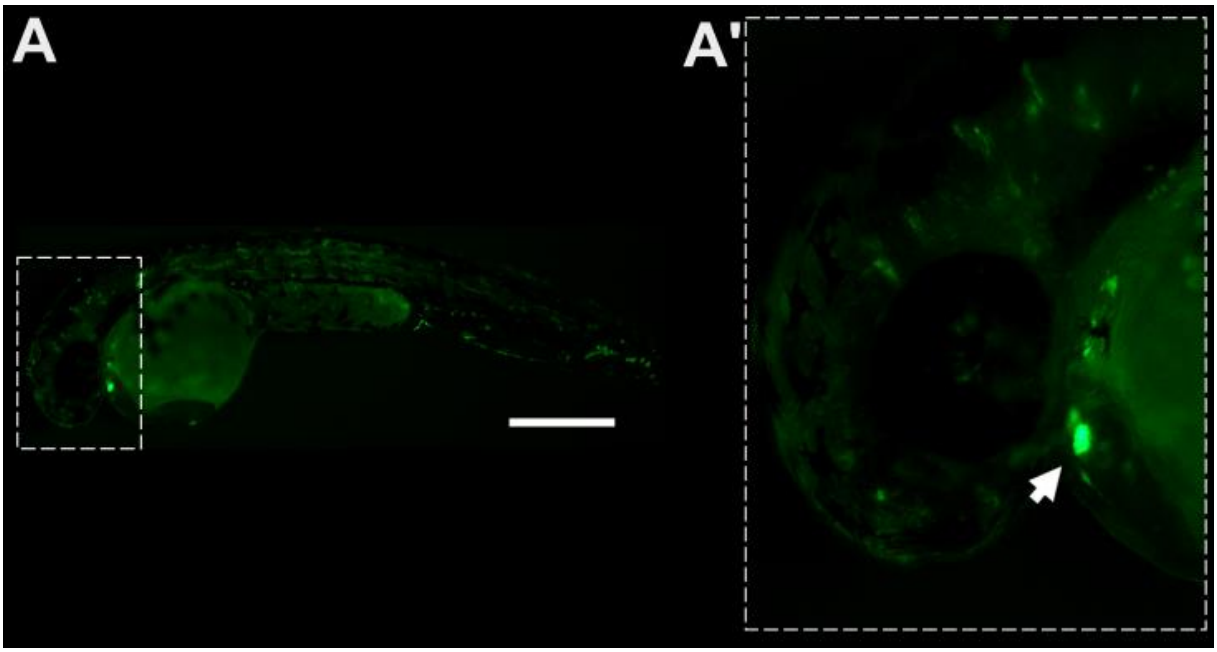

Figure 31: The activity of CRM-4 at 2 dpf embryos in the spinal cord (A) The activity in the heart region of the embryo at 2 dpf. **(A')** Magnified region of dashed box in Figure A in anterior part of the embryo at 2 dpf showing the activity in the cardiac muscle. Dorsal up, anterior left. Scale bar: 200 µm.

CRM-5 is situated in chr14:14,726,574-14,727,382, 809 bp in length, and annotated as a flanking enhancer. CRM-5 is the closest cis-regulatory module to the gene body of *nkx1.2lb* and its activity was only observed in the spinal cord (Figure 32). These cells are neurons since they possess descending axonal projections and are positioned relatively in the dorsal when compared to the position of the notochord. Altogether CRM-5 activity might mark several V2s interneurons since they positioned ventrally and possess descending projections that are only detected in V2s interneurons in comparison to other identified V2 interneurons (V2a, V2b), and other adjacent neuronal populations in the other domains, V1 interneurons, and motor neurons.

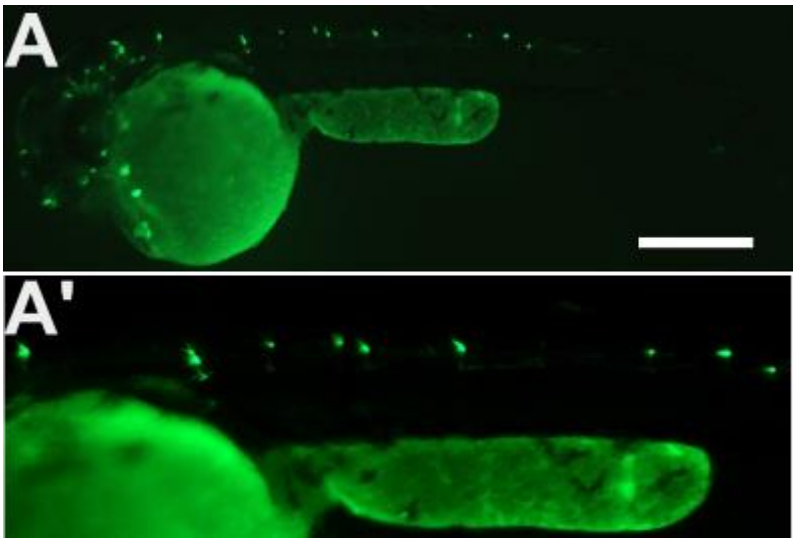

Figure 32: The activity of CRM-5 at 2 dpf embryos in the spinal cord (A) The activity in the spinal cord region of the embryo at 2 dpf. **(A')** Magnified region of the spinal cord in Figure A showing CRM-5 activity in the neurons in the spinal. Dorsal up, anterior left. 200 µm.

The regulatory function of eRNAs has already elucidated in neurons (Carullo et al., 2020). In the genome browser, also there is an eRNA-encoding region which is located in the introgenic region of *nkx1.2lb.* The position of the CRM-6 is chr14:14760994-14761421, and 428 bp in length. Also, this region was cloned into gata2a promoter-containing plasmid to assess its activity in the developing embryos. The construct is named *nkx1.2lb-CRM6-gata2*. The activity of eRNA-encoding region was detected specifically only in the spinal cord. To further characterize the neuron showing the activity of eRNA region, fluorescent in situ hybridization was performed against *nkx1.2lb* mRNA, with *sox1a* mRNA. The cell displaying CRM-6 activity, indeed expresses *nkx1.2lb,* but not *sox1a* gene (Figure 33). Its axonal projection with its bifurcated anatomy also partly resembles the anatomy of *sox1a*-expressing V2s interneuron, however *nkx1.2lb*$^{+}$ interneuron possess shorter branch compared to *sox1a*-expressing V2s interneuron (Figure 33G-H).

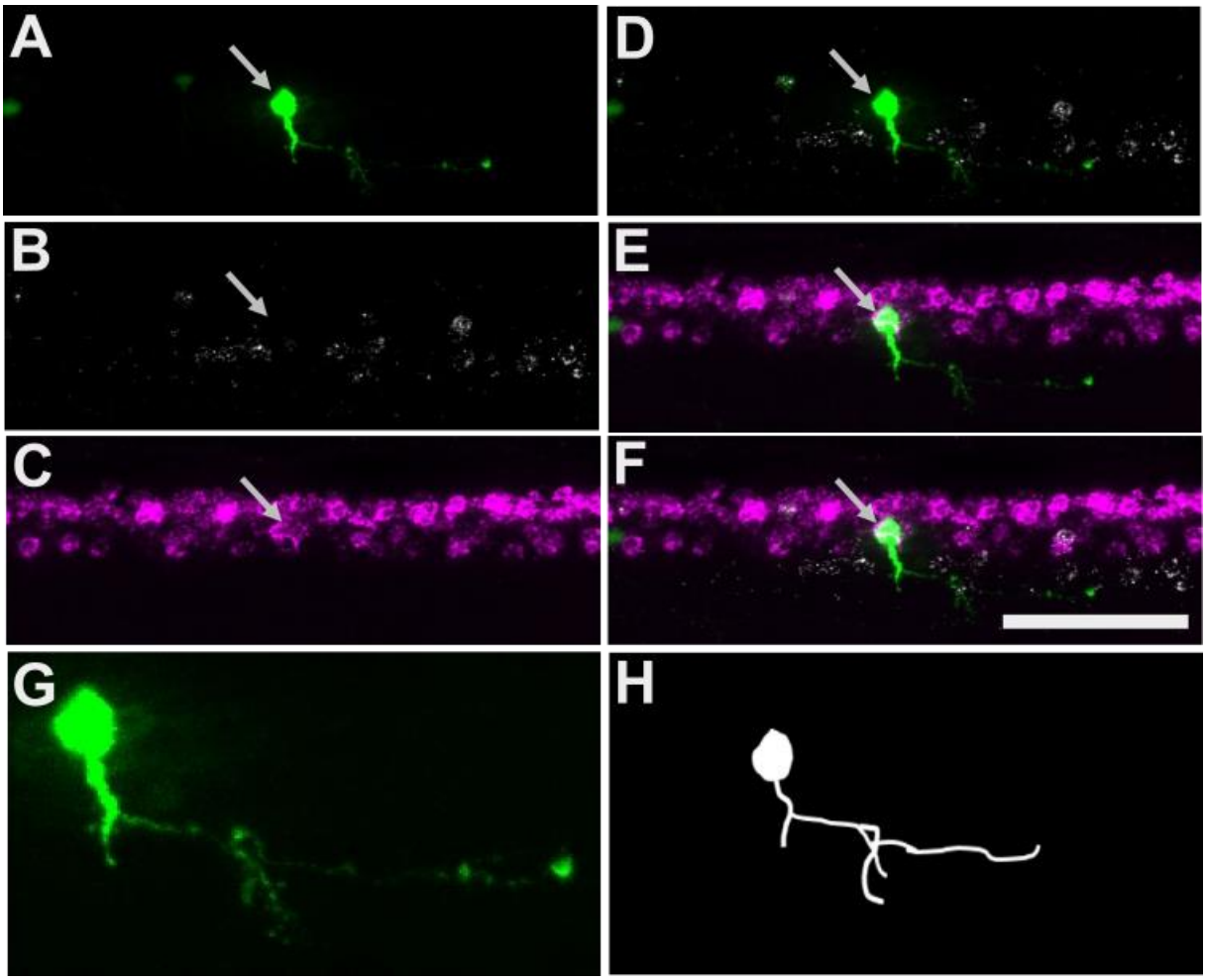

Figure 33: The activity of CRM-6 at 3 dpf embryos in the spinal cord. Fluorescent in situ hybridization against *nkx1.2lb* and *sox1a* mRNAs in combination with immunofluorescence staining against GFP at 3 dpf stage in the spinal cord. **(A)** Immunostaining against GFP showing the activity of CRM-6 in the interneuron at 3 dpf embryos in the spinal cord. **(B)** Fluorescent in situ hybridization against *sox1a* mRNA at 3 dpf embryos in the spinal cord. **(C)** Fluorescent in situ hybridization against *nkx1.2lb* mRNA at 3 dpf embryos in the spinal cord. **(D)** Merged images of (A) and (B) showing the activity of CRM6 with the localization of *sox1a* mRNA at 3 dpf embryos in the spinal cord. **(E)** Merged images of (B) and (C) showing the activity of CRM6 with the localization of *nkx1.2lb* mRNA at 3 dpf embryos in the spinal cord. **(F)** Merged images of (A), (B) and (C) at 3 dpf embryos in the spinal cord showing the activity of CRM-6 with the expressions of *nkx1.2lb* and *sox1a* mRNAs at 3 dpf embryos in the spinal cord. **(G)** Magnified image of the interneuron showing the activity of CRM-6 **(H)** The anatomy of *nkx1.2lb*$^{+}$ *sox1a*$^{-}$ interneuron possessing CRM-6 activity at 3 dpf embryos in the spinal cord. Dorsal up, anterior left. Scale bar: 200 µm.

Altogether, cis-regulatory modules of *nkx1.2lb* were identified with the help of epigenomic approaches using the UCSC genome browser with DANIO-CODE track hub, and I mapped their activities in developing zebrafish embryos. Longer and shorter versions of possible promoter-containing region of the *nkx1.2lb* gene showed the activity in the cardiac muscles. Distantly located CRM-1, CRM-2, and CRM-3 did not display any activity in the developing zebrafish embryos. CRM-4 is the only screened enhancer showing the activity in the heart while CRM-5 and CRM-6 (eRNA-encoding region) display the activity in the spinal cord (Figure 34).

	CRM-1	CRM-2	CRM-3	CRM-4	CRM-5	-2.5 kb	-1.5 kb	eRNA-encoding region (CRM-6)
Heart	-	-	-	+	-	+	+	-
Spinal cord	-	-	-	-	+	-	-	+

Figure 34: Summary of the activity of CRMs of *nkx1.2lb*

5. Discussion

5.1 Novel candidate markers for V2 precursor cells and V2s interneurons

Understanding the development of V2s interneuron requires a deep delination of the progenitor's transcriptional network. In our single-cell RNA sequencing data, novel markers for V2 precursor were identified (Figure 9). *Foxn4* and *vsx1* transcription factors are already been studied, and their expressions label V2 precursor cells which are the source of all V2 subpopulations (Kimura et al., 2008). Another marker, *chrna2a* gene was enriched in V2 precursor cluster (Figure 9). Its expression was already demonstrated the spinal cord (Rima et al., 2020). The mammalian ortholog of chrna2a is expressed in the interneuron populations where neural progenitors are situated including the hippocampus and neocortex (Lotfipour et al., 2013; Tan and Shi, 2013; Tokarska and Silberberg, 2022). *Chrna2* is required for the formation of synaptic plasticity and memory in hippocampus (Kleeman et al., 2016). However, in the zebrafish spinal cord, its function is not clarified. Development and regeneration processes share the same molecular program (Cochella and Chaker, 2023). *Lin28a* is expressed in Muller glia-derived progenitor cells in retina regeneration by inducing the expression of neurogenic transcription factor, *ascl1a* (Mitra et al., 2019). Interestingly, the expression of *Lin28a* is regulated in the retina by Notch signaling and the generation of V2 cells from V2 precursor cells is also responsive to Notch pathway, suggesting *Lin28* gene is sensitive to Notch pathway and regulates the progenitor activity regardless of the organs where it is expressed. (Mitra et al., 2019). *Sox1a* and *sox1b* genes are determining transcription factors for the generation of V2s interneurons, however, better characterization of the transcriptional modulation of V2s interneurons necessitates the investigation of genes that are expressed in V2s cells. By our single cell RNA sequencing together with the expression screening analyses proposed that *nkx1.2lb, islr2, cacna2d3 and cplx2* are identified as novel V2s markers (Figure 11, 12). Their expression patterns are enriched in the ventral spinal cord where V2s cells are located (Figure 12). However, among the candidates, the position of *trarg1a*-expressing cells in the dorsal part of the spinal cord was significantly distinguished. This observation can be explained by the possibility that the level of *trarg1* expression was low in V2s cells, whereas its expression is high in dorsally-located cells. Therefore, the chromogenic in situ hybridization technique is not sufficiently robust to display its expression in the p2 domain. The spinal cord is one of the centers of sensory information filtering and harbors interneurons (Borisoff et al.,

2006; Corbett et al., 2014; Sagner and Briscoe, 2019) . Loss of function analysis of *cacna2d3* leads to impairment of sensory information filtering and reduced habituation in zebrafish (Santistevan et al., 2022). Observation of *cacna2d3* in V2s interneuron cluster proposes that *cacna2d3* may function in the filtration of sensory information of V2s interneurons since V2s interneurons are in close contact with other neuronal populations including motor neurons (unpublished data). *Cplx2l* expression is relatively broader compared to other candidate markers (Figure 12). In a recent single-cell RNA sequencing study on locomotor circuitry, *cplx2l* was found to be expressed in ventral spinal cord neurons including KA cells, motor neurons and V2s interneurons by regulating transmitter release (Kelly et al., 2023). This statement further supports the idea that *cplx2l* expressed in V2s interneurons (Figure 12). *Islr2* is a highly expressed receptor encoding gene in single-cell RNA sequencing data and is necessary for retinal axon navigation in both zebrafish and mice (Chen et al., 2023; Panza et al., 2015). Additionally, *islr2* controls axonal projections by regulating cytoskeletal reorganization in hippocampal neurons (Abudureyimu et al., 2018) suggesting *islr2* may organize the axonal projections of V2s interneurons.

5.2 *Nkx1.2lb* as a V2s interneuron marker gene and its function in p2 domain

Nkx1.2lb is a member of the Nkx gene family and an evolutionally conserved transcription factor (Bae et al., 2004). The expression pattern of *nkx1.2lb* has not been well characterized in the developing zebrafish spinal cord. Here, the expression pattern was deeply investigated in the spinal cord of zebrafish and found that *nkx1.2lb* is mainly expressed in central nervous system including hindbrain, spinal cord and heart. (Figure 11, 12, 13). The ortholog of *nkx1.2lb* in mice, *sax2* is found to be expressed in the brain and ventral neural tube (Simon et al., 2007). In line with these observations, *nkx1.2lb* expression displays evolutionarily conserved activity across different species (Bae et al., 2004; Simon et al., 2007). The expression of *nkx1.2lb* is not overlapped with other domain markers in the spinal cord, this observation consolidates the idea that *nkx1.2lb*-expressing cells are located in p2 domain as suggested previously (Simon et al., 2007). *Nkx1.2lb*-expressing cells are co-localized with known V2s markers; *sox1a, sox1b* and glycinergic marker *(glyt2)* and it has been annotated in a recent study as a unique marker of V2s interneuron, supporting the idea that *nkx1.2lb* marks the V2s interneurons in the developing zebrafish spinal cord (Figure 18, 19, 20) (Kelly et al., 2023). Additionally, it has been proposed that *sax2* gene is also expressed in V2 domain in the spinal cord (Simon et al., 2007).

Neither in mice nor in zebrafish the functions of *nkx1.2lb* in the spinal cord has not been investigated. Attenuation of *nkx1.2lb* did not affect the expression patterns of two V2 precursor marker genes indicating *nkx1.2lb* has no effects on the pool of *vsx1*$^{+}$ and *foxn4*$^{+}$ V2 progenitors (Figure 22). Attenuation of *nkx1.2lb* expression severely affects the number of *sox1a*-expressing V2s interneurons (Figure 23). Besides, disorganization of axonal projections of V2s interneuron was not reported. Therefore, this observation does not support the speculation in the brain that the ortholog of *nkx1.2lb* in mice, *sax2*, is involved in axon guidance (Simon et al., 2007). The discrepancy can be explained by the idea that *nkx1.2lb* possesses a tissue-specific role in each tissue which is already proposed (Simon et al., 2007). Attenuation *nkx1.2lb* leads to the production of fewer glycinergic neurons in the spinal cord (Figure 24). However, this observation is not conclusive, it is important to note that the glycinergic characteristic is not exclusive to V2s interneurons in the spinal cord, also two commissural interneurons, dl6dmrt3 and V0d cells possess also glycinergic characteristics (Satou et al., 2020). The most expressed transcription factor-encoding gene in V2s cluster in single-cell RNA sequencing data is *nkx1.2lb* gene, which raises the possibility that *nkx1.2lb* may function as a master regulator for the identified candidates (Figure 10). Intriguingly, knock-down of *nkx1.2lb* has no impact on the generation of *cacna2d3*, *cplx2l,* and *islr2* gene markers (Figure 25). This observation leads to the speculation that the regulatory network of *nkx1.2lb* is distinct from these candidates, suggesting *cacna2d3*, *cplx2l,* and *islr2* genes are not the downstream targets of *nkx1.2lb* in V2s interneuron.

5.3 The transcriptional regulation of *nkx1.2lb* gene

It has been postulated that the regulation of sax2 gene (ortholog of *nkx1.2lb* in mice) shows autoregulation in both positive and negative feedback mechanism depending on the cell types (Simon et al., 2007). In the light of this observation, the transcriptional regulation of *nkx1.2lb* was investigated by characterizing its CRMs. The promoter activity of *nkx1.2lb* is not sufficient for *nkx1.2lb* expression in the spinal cord (Figure 28). Its partial promoter activity in the heart proposes that the transcriptional control of *nkx1.2lb* does not solely depend on the promoter activity raising a possibility that *nkx1.2lb* transcription may be regulated together with other cis-regulatory modules. According to DANIO-Code browser, six putative CRMs of nkx1.2lb have been presented (Figure 29). The CRM-4 is active only in the heart muscle mimicking the promoter activity of *nkx1.2lb* even it is localization 35 kb upstream from the promoter region

(Figure 31). CRM-5 is the nearest enhancer element showing the activity only in the spinal cord (Figure 29, 32). These cells are located ventral spinal cord possessing descending axonal projections suggesting that CRM-5 is active and driving the expression to some extent of *nkx1.2lb* gene in the spinal cord. In addition, CRM-6 is situated in the introgenic region of *nkx1.2lb* gene and annotated as an eRNA-encoding region which is active only in the spinal cord. The regulatory functions of eRNA in the transcription of neuronal genes have been elucidated (Carullo et al., 2020). The interneuron showing the activity of CRM-6 is located in the ventral spinal cord. Overall, it is clearly stated that the transcriptional control of *nkx1.2lb* requires a combination of different cis-regulatory modules of *nkx1.2lb* gene in each tissue where it is expressed.

The expression of *nkx1.2lb* gene and its knock-down observations increase the possibility that *nkx1.2lb*-expressing interneurons are somehow different compared with *sox1a*-expressing V2s interneurons. The interneuron exhibiting the activity of CRM-6 expresses *nkx1.2lb* gene (Figure 33). It can be clearly stated that the activation of CRM-6 drives the expression of *nkx1.2lb* in this ventrally located interneuron. This observation leads to a question whether the activity of CRM-6 is involved in the *nkx1.2lb* gene expression in *sox1a*-expressing V2s interneurons since its anatomy partly resembles the anatomy of V2s interneurons (Gerber et al., 2019). However, CRM-6 is active in the *nkx1.2lb*-expressing cell which does not express *sox1a* gene (Figure 33). This interneuron possesses descending axonal projection with bifurcation resembling the *sox1a*-expressing V2s cells (Gerber et al., 2019). However, according to the anatomy of both its axonal branching and length of its projection, it can be clearly stated that only *nkx1.2lb*-expressing interneuron displays anatomically distinct projection (Figure 33G-H). Also, this data is further supported and demonstrated by showing the recognizable differences between the anatomy of both *sox1a* and *nkx1.2lb*-expressing V2s interneuron and only *nkx1.2lb*-expressing V2s interneuron in the same developmental stages of V2s interneuron (Figure 33G, unpublished data). *Sox1a*-expressing V2s interneurons are in close contact with both medial longitudinal fasciculus (MLF) and *mnx1*-expressing primary and secondary motor neurons (unpublished data), however, further experiments need to be performed to characterize axonal projection of *nkx1.2lb*-expressing cells for better understanding.

5.4 V2s interneurons are transcriptionally distinct cell population

Transcriptional Heterogeneity of V2s interneurons have been already shown and the expression of *nkx1.2lb* diversify the V2s interneuron population (Table13, 14). *Nkx1.2lb* expression is detected strongly in the V2s cluster, strikingly its expression is broader than *sox1a* expression in the V2s cluster at 2 and 3 dpf (Chen et al., 2023) (Table13, 14). Therefore, *nkx1.2lb*-expressing cells were chosen to subdivide the V2s cluster into different subpopulations according to the expressions of known V2s marker genes at 2 dpf and 3 dpf stages (Table 13-14). Intriguingly, not all V2s subpopulations express *sox1a* and *sox1b* markers at 2 and 3 dpf. In addition, purely glycinergic subpopulations were hardly observed at 2 dpf, however glycinergic identity is regained at 3 dpf, proposing that V2s cells are still in the way of differentiation. The challenging part of this thesis is to detect these marker genes at the same time to provide the heterogeneity of these cell populations since, it is not technically possible to detect six marker genes to detect their co-localization which require six fluorophores at the same moment. V2s interneurons are composed of both transcriptionally and anatomically distinct cell populations as shown in (Table 13-14, Figure 33), although these cell populations are still need to be examined in detail to further investigate their functions in the spinal circuit.

6. Future perspective

Identified novel candidates can be used to pave the way for the characterization of V2s interneurons in the developing spinal cord, and these marker genes are valuable drug targets to enhance spinal cord-related neurodegenerative diseases to promote regeneration.

7. References

Abudureyimu, S., Asai, N., Enomoto, A., Weng, L., Kobayashi, H., Wang, X., Chen, C., Mii, S., Takahashi, M., 2018. Essential Role of Linx/Islr2 in the Development of the Forebrain Anterior Commissure. Sci Rep 8, 7292. https://doi.org/10.1038/s41598-018-24064-0

Achim, K., Peltopuro, P., Lahti, L., Tsai, H.-H., Zachariah, A., Åstrand, M., Salminen, M., Rowitch, D., Partanen, J., 2013. The role of Tal2 and Tal1 in the differentiation of midbrain GABAergic neuron precursors. Biol Open 2, 990–997. https://doi.org/10.1242/bio.20135041

Agnew, C., Ayaz, P., Kashima, R., Loving, H.S., Ghatpande, P., Kung, J.E., Underbakke, E.S., Shan, Y., Shaw, D.E., Hata, A., Jura, N., 2021. Structural basis for ALK2/BMPR2 receptor complex signaling through kinase domain oligomerization. Nat Commun 12, 4950. https://doi.org/10.1038/s41467-021-25248-5

Ampatzis, K., Song, J., Ausborn, J., El Manira, A., 2014. Separate Microcircuit Modules of Distinct V2a Interneurons and Motoneurons Control the Speed of Locomotion. Neuron 83, 934–943. https://doi.org/10.1016/j.neuron.2014.07.018

Andrews, M.G., Kong, J., Novitch, B.G., Butler, S.J., 2019. Chapter Twelve - New perspectives on the mechanisms establishing the dorsal-ventral axis of the spinal cord, in: Wellik, D.M. (Ed.), Current Topics in Developmental Biology, Organ Development. Academic Press, pp. 417–450. https://doi.org/10.1016/bs.ctdb.2018.12.010

Andrzejczuk, L.A., Banerjee, S., England, S.J., Voufo, C., Kamara, K., Lewis, K.E., 2018. Tal1, Gata2a, and Gata3 Have Distinct Functions in the Development of V2b and Cerebrospinal Fluid-Contacting KA Spinal Neurons. Front. Neurosci. 12. https://doi.org/10.3389/fnins.2018.00170

Appel, B., Korzh, V., Glasgow, E., Thor, S., Edlund, T., Dawid, I.B., Eisen, J.S., 1995. Motoneuron fate specification revealed by patterned LIM homeobox gene expression in embryonic zebrafish. Development 121, 4117–4125. https://doi.org/10.1242/dev.121.12.4117

Armant, O., März, M., Schmidt, R., Ferg, M., Diotel, N., Ertzer, R., Bryne, J.C., Yang, L., Baader, I., Reischl, M., Legradi, J., Mikut, R., Stemple, D., van IJcken, W., van der Sloot, A., Lenhard, B., Strähle, U., Rastegar, S., 2013. Genome-wide, whole mount *in situ*

analysis of transcriptional regulators in zebrafish embryos. Developmental Biology 380, 351–362. https://doi.org/10.1016/j.ydbio.2013.05.006

Attisano, L., Tuen Lee-Hoeflich, S., 2001. The Smads. Genome Biol 2, reviews3010.1. https://doi.org/10.1186/gb-2001-2-8-reviews3010

Bae, Y.-K., Shimizu, T., Muraoka, O., Yabe, T., Hirata, T., Nojima, H., Hirano, T., Hibi, M., 2004. Expression of *sax1*/*nkx1.2* and *sax2*/*nkx1.1* in zebrafish. Gene Expression Patterns 4, 481–486. https://doi.org/10.1016/j.modgep.2003.12.001

Baranasic, D., Hörtenhuber, M., Balwierz, P.J., Zehnder, T., Mukarram, A.K., Nepal, C., Várnai, C., Hadzhiev, Y., Jimenez-Gonzalez, A., Li, N., Wragg, J., D'Orazio, F.M., Relic, D., Pachkov, M., Díaz, N., Hernández-Rodríguez, B., Chen, Z., Stoiber, M., Dong, M., Stevens, I., Ross, S.E., Eagle, A., Martin, R., Obasaju, O., Rastegar, S., McGarvey, A.C., Kopp, W., Chambers, E., Wang, D., Kim, H.R., Acemel, R.D., Naranjo, S., Łapiński, M., Chong, V., Mathavan, S., Peers, B., Sauka-Spengler, T., Vingron, M., Carninci, P., Ohler, U., Lacadie, S.A., Burgess, S.M., Winata, C., van Eeden, F., Vaquerizas, J.M., Gómez-Skarmeta, J.L., Onichtchouk, D., Brown, B.J., Bogdanovic, O., van Nimwegen, E., Westerfield, M., Wardle, F.C., Daub, C.O., Lenhard, B., Müller, F., 2022. Multiomic atlas with functional stratification and developmental dynamics of zebrafish cis-regulatory elements. Nat Genet 54, 1037–1050. https://doi.org/10.1038/s41588-022-01089-w

Batista, M.F., Jacobstein, J., Lewis, K.E., 2008. Zebrafish V2 cells develop into excitatory CiD and Notch signalling dependent inhibitory VeLD interneurons. Dev Biol 322, 263–275. https://doi.org/10.1016/j.ydbio.2008.07.015

Beederman, M., Lamplot, J.D., Nan, G., Wang, J., Liu, X., Yin, L., Li, R., Shui, W., Zhang, H., Kim, S.H., Zhang, W., Zhang, J., Kong, Y., Denduluri, S., Rogers, M.R., Pratt, A., Haydon, R.C., Luu, H.H., Angeles, J., Shi, L.L., He, T.-C., 2013. BMP signaling in mesenchymal stem cell differentiation and bone formation. J Biomed Sci Eng 6, 32–52. https://doi.org/10.4236/jbise.2013.68A1004

Bello-Rojas, S., Bagnall, M.W., 2022. Clonally related, Notch-differentiated spinal neurons integrate into distinct circuits. eLife 11, e83680. https://doi.org/10.7554/eLife.83680

Berg, E.M., Björnfors, E.R., Pallucchi, I., Picton, L.D., El Manira, A., 2018. Principles Governing Locomotion in Vertebrates: Lessons From Zebrafish. Front. Neural Circuits 12. https://doi.org/10.3389/fncir.2018.00073

Bijlsma, M.F., Damhofer, H., Roelink, H., 2012. Hedgehog-Stimulated Chemotaxis Is Mediated by Smoothened Located Outside the Primary Cilium. Science Signaling 5, ra60–ra60. https://doi.org/10.1126/scisignal.2002798

Blomen, V.A., Boonstra, J., 2011. Stable transmission of reversible modifications: maintenance of epigenetic information through the cell cycle. Cell Mol Life Sci 68, 27–44. https://doi.org/10.1007/s00018-010-0505-5

Blotta, S., Jakubikova, J., Calimeri, T., Roccaro, A.M., Amodio, N., Azab, A.K., Foresta, U., Mitsiades, C.S., Rossi, M., Todoerti, K., Molica, S., Morabito, F., Neri, A., Tagliaferri, P., Tassone, P., Anderson, K.C., Munshi, N.C., 2012. Canonical and noncanonical Hedgehog pathway in the pathogenesis of multiple myeloma. Blood 120, 5002–5013. https://doi.org/10.1182/blood-2011-07-368142

Bond, C.W., Angeloni, N., Harrington, D., Stupp, S., Podlasek, C.A., 2013. Sonic Hedgehog Regulates Brain-Derived Neurotrophic Factor in Normal and Regenerating Cavernous Nerves. The Journal of Sexual Medicine 10, 730–737. https://doi.org/10.1111/jsm.12030

Bonner, J., Gribble, S.L., Veien, E.S., Nikolaus, O.B., Weidinger, G., Dorsky, R.I., 2008. Proliferation and patterning are mediated independently in the dorsal spinal cord downstream of canonical Wnt signaling. Developmental Biology 313, 398–407. https://doi.org/10.1016/j.ydbio.2007.10.041

Borisoff, J.F., McPhail, L.T., Saunders, J.T.W., Birch, G.E., Ramer, M.S., 2006. Detection and classification of sensory information from acute spinal cord recordings. IEEE Transactions on Biomedical Engineering 53, 1715–1719. https://doi.org/10.1109/TBME.2006.877800

Britz, O., Zhang, J., Grossmann, K.S., Dyck, J., Kim, J.C., Dymecki, S., Gosgnach, S., Goulding, M., 2015. A genetically defined asymmetry underlies the inhibitory control of flexor–extensor locomotor movements. eLife 4, e04718. https://doi.org/10.7554/eLife.04718

Buglino, J.A., Resh, M.D., 2008. Hhat Is a Palmitoylacyltransferase with Specificity for N-Palmitoylation of Sonic Hedgehog * ◆. Journal of Biological Chemistry 283, 22076–22088. https://doi.org/10.1074/jbc.M803901200

Bumcrot, D.A., Takada, R., Mcmahon, A.P., 1995. Proteolytic Processing Yields Two Secreted Forms of Sonic hedgehog. Molecular and Cellular Biology 15, 2294–2303. https://doi.org/10.1128/MCB.15.4.2294

Callahan, R.A., Roberts, R., Sengupta, M., Kimura, Y., Higashijima, S., Bagnall, M.W., 2019. Spinal V2b neurons reveal a role for ipsilateral inhibition in speed control. eLife 8, e47837. https://doi.org/10.7554/eLife.47837

Carullo, N.V.N., Phillips III, R.A., Simon, R.C., Soto, S.A.R., Hinds, J.E., Salisbury, A.J., Revanna, J.S., Bunner, K.D., Ianov, L., Sultan, F.A., Savell, K.E., Gersbach, C.A., Day, J.J., 2020. Enhancer RNAs predict enhancer–gene regulatory links and are critical for enhancer function in neuronal systems. Nucleic Acids Research 48, 9550–9570. https://doi.org/10.1093/nar/gkaa671

Caspary, T., Anderson, K.V., 2003. Patterning cell types in the dorsal spinal cord: what the mouse mutants say. Nat Rev Neurosci 4, 289–297. https://doi.org/10.1038/nrn1073

Chang, W., Pedroni, A., Bertuzzi, M., Kizil, C., Simon, A., Ampatzis, K., 2021. Locomotion dependent neuron-glia interactions control neurogenesis and regeneration in the adult zebrafish spinal cord. Nat Commun 12, 4857. https://doi.org/10.1038/s41467-021-25052-1

Chen, F., Köhler, M., Cucun, G., Takamiya, M., Kizil, C., Cosacak, M.I., Rastegar, S., 2023. sox1a:eGFP transgenic line and single-cell transcriptomics reveal the origin of zebrafish intraspinal serotonergic neurons. iScience 26, 107342. https://doi.org/10.1016/j.isci.2023.107342

Chen, M.-H., Li, Y.-J., Kawakami, T., Xu, S.-M., Chuang, P.-T., 2004. Palmitoylation is required for the production of a soluble multimeric Hedgehog protein complex and long-range signaling in vertebrates. Genes Dev. 18, 641–659. https://doi.org/10.1101/gad.1185804

Chizhikov, V.V., Millen, K.J., 2005. Roof plate-dependent patterning of the vertebrate dorsal central nervous system. Developmental Biology 277, 287–295. https://doi.org/10.1016/j.ydbio.2004.10.011

Chizhikov, V.V., Millen, K.J., 2004. Control of Roof Plate Development and Signaling by Lmx1b in the Caudal Vertebrate CNS. J. Neurosci. 24, 5694–5703. https://doi.org/10.1523/JNEUROSCI.0758-04.2004

Choudhry, Z., Rikani, A.A., Choudhry, A.M., Tariq, S., Zakaria, F., Asghar, M.W., Sarfraz, M.K., Haider, K., Shafiq, A.A., Mobassarah, N.J., 2014. Sonic hedgehog signalling pathway: a complex network. Ann Neurosci 21, 28–31. https://doi.org/10.5214/ans.0972.7531.210109

Clovis, Y., Seo, S.Y., Kwon, J., Rhee, J.C., Yeo, S., Lee, J.W., Lee, S., Lee, S.-K., 2016. Chx10 consolidates V2a interneuron identity through two distinct gene repression modes. Cell Rep 16, 1642–1652. https://doi.org/10.1016/j.celrep.2016.06.100

Cochella, L., Chaker, Z., 2023. Development, regeneration and aging: a bizarre love triangle. Development 150, dev202086. https://doi.org/10.1242/dev.202086

Corbett, E.A., Sachs, N.A., Körding, K.P., Perreault, E.J., 2014. Multimodal decoding and congruent sensory information enhance reaching performance in subjects with cervical spinal cord injury. Front. Neurosci. 8. https://doi.org/10.3389/fnins.2014.00123

Cordle, J., Johnson, S., Zi Yan Tay, J., Roversi, P., Wilkin, M.B., de Madrid, B.H., Shimizu, H., Jensen, S., Whiteman, P., Jin, B., Redfield, C., Baron, M., Lea, S.M., Handford, P.A., 2008. A conserved face of the Jagged/Serrate DSL domain is involved in Notch trans-activation and cis-inhibition. Nat Struct Mol Biol 15, 849–857. https://doi.org/10.1038/nsmb.1457

Cornell, R.A., Eisen, J.S., 2002. Delta/Notch signaling promotes formation of zebrafish neural crest by repressing Neurogenin 1 function. Development 129, 2639–2648. https://doi.org/10.1242/dev.129.11.2639

Cucun, G., Köhler, M., Pfitsch, S., Rastegar, S., 2024. Insights into the mechanisms of neuron generation and specification in the zebrafish ventral spinal cord. FEBS J 291, 646–662. https://doi.org/10.1111/febs.16913

Danesin, C., Darche-Gabinaud, R., Escalas, N., Bouguetoch, V., Cochard, P., Al Oustah, A., Ohayon, D., Glise, B., Soula, C., 2021. Sulf2a controls Shh-dependent neural fate specification in the developing spinal cord. Sci Rep 11, 118. https://doi.org/10.1038/s41598-020-80455-2

Danilova, N., Visel, A., Willett, C.E., Steiner, L.A., 2004. Expression of the winged helix/forkhead gene, *foxn4*, during zebrafish development. Developmental Brain Research 153, 115–119. https://doi.org/10.1016/j.devbrainres.2004.05.014

Del Barrio, M.G., Taveira-Marques, R., Muroyama, Y., Yuk, D.-I., Li, S., Wines-Samuelson, M., Shen, J., Smith, H.K., Xiang, M., Rowitch, D., Richardson, W.D., 2007. A regulatory network involving Foxn4, Mash1 and delta-like 4/Notch1 generates V2a and V2b spinal interneurons from a common progenitor pool. Development 134, 3427–3436. https://doi.org/10.1242/dev.005868

Dennler, S., Huet, S., Gauthier, J.-M., 1999. A short amino-acid sequence in MH1 domain is responsible for functional differences between Smad2 and Smad3. Oncogene 18, 1643–1648. https://doi.org/10.1038/sj.onc.1202729

Dessaud, E., McMahon, A.P., Briscoe, J., 2008. Pattern formation in the vertebrate neural tube: a sonic hedgehog morphogen-regulated transcriptional network. Development 135, 2489–2503. https://doi.org/10.1242/dev.009324

Ding, H., Wang, F., Shi, X., Ma, H., Du, Y., Hou, L., Xing, N., 2020. LncRNA MALAT1 induces the dysfunction of β cells via reducing the histone acetylation of the PDX-1 promoter in type 1 diabetes. Experimental and Molecular Pathology 114, 104432. https://doi.org/10.1016/j.yexmp.2020.104432

Diotel, N., Lübke, L., Strähle, U., Rastegar, S., 2020. Common and Distinct Features of Adult Neurogenesis and Regeneration in the Telencephalon of Zebrafish and Mammals. Front. Neurosci. 14. https://doi.org/10.3389/fnins.2020.568930

Du, J., Johnson, L.M., Jacobsen, S.E., Patel, D.J., 2015. DNA methylation pathways and their crosstalk with histone methylation. Nat Rev Mol Cell Biol 16, 519–532. https://doi.org/10.1038/nrm4043

Dvir, A., Conaway, J.W., Conaway, R.C., 2001. Mechanism of transcription initiation and promoter escape by RNA polymerase II. Current Opinion in Genetics & Development 11, 209–214. https://doi.org/10.1016/S0959-437X(00)00181-7

Eldar, A., Dorfman, R., Weiss, D., Ashe, H., Shilo, B.-Z., Barkai, N., 2002. Robustness of the BMP morphogen gradient in Drosophila embryonic patterning. Nature 419, 304–308. https://doi.org/10.1038/nature01061

England, S., Batista, M.F., Mich, J.K., Chen, J.K., Lewis, K.E., 2011. Roles of Hedgehog pathway components and retinoic acid signalling in specifying zebrafish ventral spinal cord neurons. Development 138, 5121–5134. https://doi.org/10.1242/dev.066159

Ericson, J., Rashbass, P., Schedl, A., Brenner-Morton, S., Kawakami, A., Heyningen, V. van, Jessell, T.M., Briscoe, J., 1997. Pax6 Controls Progenitor Cell Identity and Neuronal Fate in Response to Graded Shh Signaling. Cell 90, 169–180. https://doi.org/10.1016/S0092-8674(00)80323-2

Fainsod, A., Deißler, K., Yelin, R., Marom, K., Epstein, M., Pillemer, G., Steinbeisser, H., Blum, M., 1997. The dorsalizing and neural inducing gene *follistatin* is an antagonist of *BMP-4*. Mechanisms of Development 63, 39–50. https://doi.org/10.1016/S0925-4773(97)00673-4

Farreny, M.-A., Agius, E., Bel-Vialar, S., Escalas, N., Khouri-Farah, N., Soukkarieh, C., Danesin, C., Pituello, F., Cochard, P., Soula, C., 2018. FGF signaling controls Shh-dependent oligodendroglial fate specification in the ventral spinal cord. Neural Dev 13, 3. https://doi.org/10.1186/s13064-018-0100-2

Fassier, C., Hutt, J.A., Scholpp, S., Lumsden, A., Giros, B., Nothias, F., Schneider-Maunoury, S., Houart, C., Hazan, J., 2010. Zebrafish atlastin controls motility and spinal motor axon architecture via inhibition of the BMP pathway. Nat Neurosci 13, 1380–1387. https://doi.org/10.1038/nn.2662

Feng, X.-H., Derynck, R., 2005. SPECIFICITY AND VERSATILITY IN TGF-β SIGNALING THROUGH SMADS. Annual Review of Cell and Developmental Biology 21, 659–693. https://doi.org/10.1146/annurev.cellbio.21.022404.142018

Fleet, A.J., Hamel, P.A., 2018. The protein-specific activities of the transmembrane modules of Ptch1 and Ptch2 are determined by their adjacent protein domains. Journal of Biological Chemistry 293, 16583–16595. https://doi.org/10.1074/jbc.RA118.004478

Frank, E., Mendelson, B., 1990. Specification of synaptic connections between sensory and motor neurons in the developing spinal cord. J Neurobiol 21, 33–50. https://doi.org/10.1002/neu.480210104

Funayama, N., Fagotto, F., McCrea, P., Gumbiner, B.M., 1995. Embryonic axis induction by the armadillo repeat domain of beta-catenin: evidence for intracellular signaling. Journal of Cell Biology 128, 959–968. https://doi.org/10.1083/jcb.128.5.959

Gagnon, J.A., Valen, E., Thyme, S.B., Huang, P., Ahkmetova, L., Pauli, A., Montague, T.G., Zimmerman, S., Richter, C., Schier, A.F., 2014. Efficient Mutagenesis by Cas9 Protein-Mediated Oligonucleotide Insertion and Large-Scale Assessment of Single-Guide RNAs. PLOS ONE 9, e98186. https://doi.org/10.1371/journal.pone.0098186

Gazave, E., Lapébie, P., Richards, G.S., Brunet, F., Ereskovsky, A.V., Degnan, B.M., Borchiellini, C., Vervoort, M., Renard, E., 2009. Origin and evolution of the Notch signalling pathway: an overview from eukaryotic genomes. BMC Evol Biol 9, 249. https://doi.org/10.1186/1471-2148-9-249

Gerber, V., Yang, L., Takamiya, M., Ribes, V., Gourain, V., Peravali, R., Stegmaier, J., Mikut, R., Reischl, M., Ferg, M., Rastegar, S., Strähle, U., 2019. The HMG box transcription factors Sox1a and Sox1b specify a new class of glycinergic interneuron in the spinal cord of zebrafish embryos. Development 146, dev172510. https://doi.org/10.1242/dev.172510

Gouge, A., Holt, J., Hardy, A.P., Sowden, J.C., Smith, H.K., 2001. Foxn4--a new member of the forkhead gene family is expressed in the retina. Mech Dev 107, 203–206. https://doi.org/10.1016/s0925-4773(01)00465-8

Grainger, S., Willert, K., 2018. Mechanisms of Wnt signaling and control. WIREs Systems Biology and Medicine 10, e1422. https://doi.org/10.1002/wsbm.1422

Greer, E.L., Shi, Y., 2012. Histone methylation: a dynamic mark in health, disease and inheritance. Nat Rev Genet 13, 343–357. https://doi.org/10.1038/nrg3173

Gribble, S.L., Nikolaus, O.B., Dorsky, R.I., 2007. Regulation and Function of DbxGenes in the Zebrafish Spinal Cord. Dev Dyn 236, 3472–3483. https://doi.org/10.1002/dvdy.21367

Grishin, N.V., 2001. MH1 domain of Smad is a degraded homing endonuclease1. Journal of Molecular Biology 307, 31–37. https://doi.org/10.1006/jmbi.2000.4486

Hai, R., He, L., Shu, G., Yin, G., 2021. Characterization of Histone Deacetylase Mechanisms in Cancer Development. Front. Oncol. 11. https://doi.org/10.3389/fonc.2021.700947

Harris, A., Masgutova, G., Collin, A., Toch, M., Hidalgo-Figueroa, M., Jacob, B., Corcoran, L.M., Francius, C., Clotman, F., 2019. Onecut Factors and Pou2f2 Regulate the Distribution of V2 Interneurons in the Mouse Developing Spinal Cord. Front. Cell. Neurosci. 13. https://doi.org/10.3389/fncel.2019.00184

Henderson, K.W., Menelaou, E., Hale, M.E., 2019. Sensory neurons in the spinal cord of zebrafish and their local connectivity. Current Opinion in Physiology, Motor Control Systems 8, 136–140. https://doi.org/10.1016/j.cophys.2019.01.008

Hill, C.S., 2016. Transcriptional Control by the SMADs. Cold Spring Harb Perspect Biol 8, a022079. https://doi.org/10.1101/cshperspect.a022079

Hochheimer, A., Tjian, R., 2003. Diversified transcription initiation complexes expand promoter selectivity and tissue-specific gene expression. Genes Dev. 17, 1309–1320. https://doi.org/10.1101/gad.1099903

Huang, P., Xiong, F., Megason, S.G., Schier, A.F., 2012. Attenuation of Notch and Hedgehog Signaling Is Required for Fate Specification in the Spinal Cord. PLOS Genetics 8, e1002762. https://doi.org/10.1371/journal.pgen.1002762

Huang, Y., Gu, L., Li, G.-M., 2018. H3K36me3-mediated mismatch repair preferentially protects actively transcribed genes from mutation. J Biol Chem 293, 7811–7823. https://doi.org/10.1074/jbc.RA118.002839

Ille, F., Atanasoski, S., Falk, S., Ittner, L.M., Märki, D., Büchmann-Møller, S., Wurdak, H., Suter, U., Taketo, M.M., Sommer, L., 2007. Wnt/BMP signal integration regulates the balance between proliferation and differentiation of neuroepithelial cells in the dorsal spinal cord. Developmental Biology 304, 394–408. https://doi.org/10.1016/j.ydbio.2006.12.045

Imai, F., Yoshida, Y., 2018. Molecular mechanisms underlying monosynaptic sensory-motor circuit development in the spinal cord. Dev Dyn 247, 581–587. https://doi.org/10.1002/dvdy.24611

Jacobs, C.T., Kejriwal, A., Kocha, K.M., Jin, K.Y., Huang, P., 2022. Temporal cell fate determination in the spinal cord is mediated by the duration of Notch signalling. Dev Biol 489, 1–13. https://doi.org/10.1016/j.ydbio.2022.05.010

Jeong, Y., Epstein, D.J., 2003. Distinct regulators of Shh transcription in the floor plate and notochord indicate separate origins for these tissues in the mouse node. Development 130, 3891–3902. https://doi.org/10.1242/dev.00590

Jessell, T.M., 2000. Neuronal specification in the spinal cord: inductive signals and transcriptional codes. Nat Rev Genet 1, 20–29. https://doi.org/10.1038/35049541

Karunaratne, A., Hargrave, M., Poh, A., Yamada, T., 2002. GATA Proteins Identify a Novel Ventral Interneuron Subclass in the Developing Chick Spinal Cord. Developmental Biology 249, 30–43. https://doi.org/10.1006/dbio.2002.0754

Katz, H.R., Menelaou, E., Hale, M.E., 2021. Morphological and physiological properties of Rohon-Beard neurons along the zebrafish spinal cord. J Comp Neurol 529, 1499–1515. https://doi.org/10.1002/cne.25033

Kelly, J.J., Wen, H., Brehm, P., 2023. Single-cell RNAseq analysis of spinal locomotor circuitry in larval zebrafish. eLife 12, RP89338. https://doi.org/10.7554/eLife.89338

Kikuchi, A., Yamamoto, H., Sato, A., Matsumoto, S., 2011. Chapter 2 - New Insights into the Mechanism of Wnt Signaling Pathway Activation, in: Jeon, K.W. (Ed.), International Review of Cell and Molecular Biology. Academic Press, pp. 21–71. https://doi.org/10.1016/B978-0-12-386035-4.00002-1

Kim, I., Park, J.-W., 2020. Hypoxia-driven epigenetic regulation in cancer progression: A focus on histone methylation and its modifying enzymes. Cancer Letters 489, 41–49. https://doi.org/10.1016/j.canlet.2020.05.025

Kim, J., Lee, H., Yi, S.-J., Kim, K., 2022. Gene regulation by histone-modifying enzymes under hypoxic conditions: a focus on histone methylation and acetylation. Exp Mol Med 54, 878–889. https://doi.org/10.1038/s12276-022-00812-1

Kim, W., Kim, H., Katanaev, V.L., Joon Lee, S., Ishitani, T., Cha, B., Han, J., Jho, E., 2012. Dual functions of DP1 promote biphasic Wnt-on and Wnt-off states during anteroposterior neural patterning. The EMBO Journal 31, 3384–3397. https://doi.org/10.1038/emboj.2012.181

Kimble, J., Simpson, P., 1997. THE LIN-12/Notch SIGNALING PATHWAY AND ITS REGULATION. Annual Review of Cell and Developmental Biology 13, 333–361. https://doi.org/10.1146/annurev.cellbio.13.1.333

Kimmel, C.B., Ballard, W.W., Kimmel, S.R., Ullmann, B., Schilling, T.F., 1995. Stages of embryonic development of the zebrafish. Developmental Dynamics 203, 253–310. https://doi.org/10.1002/aja.1002030302

Kimura, Y., Higashijima, S., 2019. Regulation of locomotor speed and selection of active sets of neurons by V1 neurons. Nat Commun 10, 2268. https://doi.org/10.1038/s41467-019-09871-x

Kimura, Y., Okamura, Y., Higashijima, S., 2006. alx, a zebrafish homolog of Chx10, marks ipsilateral descending excitatory interneurons that participate in the regulation of spinal locomotor circuits. J Neurosci 26, 5684–5697. https://doi.org/10.1523/JNEUROSCI.4993-05.2006

Kimura, Y., Satou, C., Higashijima, S., 2008. V2a and V2b neurons are generated by the final divisions of pair-producing progenitors in the zebrafish spinal cord. Development 135, 3001–3005. https://doi.org/10.1242/dev.024802

Kléber, M., Lee, H.-Y., Wurdak, H., Buchstaller, J., Riccomagno, M.M., Ittner, L.M., Suter, U., Epstein, D.J., Sommer, L., 2005. Neural crest stem cell maintenance by combinatorial Wnt and BMP signaling. The Journal of Cell Biology 169, 309–320. https://doi.org/10.1083/jcb.200411095

Kleeman, E., Nakauchi, S., Su, H., Dang, R., Wood, M.A., Sumikawa, K., 2016. Impaired function of α2-containing nicotinic acetylcholine receptors on oriens-lacunosum moleculare cells causes hippocampus-dependent memory impairments. Neurobiology of Learning and Memory 136, 13–20. https://doi.org/10.1016/j.nlm.2016.09.010

Knafo, S., Fidelin, K., Prendergast, A., Tseng, P.-E.B., Parrin, A., Dickey, C., Böhm, U.L., Figueiredo, S.N., Thouvenin, O., Pascal-Moussellard, H., Wyart, C., 2017. Mechanosensory neurons control the timing of spinal microcircuit selection during locomotion. Elife 6, e25260. https://doi.org/10.7554/eLife.25260

Koinuma, D., Tsutsumi, S., Kamimura, N., Imamura, T., Aburatani, H., Miyazono, K., 2009. Promoter-wide analysis of Smad4 binding sites in human epithelial cells. Cancer Science 100, 2133–2142. https://doi.org/10.1111/j.1349-7006.2009.01299.x

Korzh, V., Edlund, T., Thor, S., 1993. Zebrafish primary neurons initiate expression of the LIM homeodomain protein Isl-1 at the end of gastrulation. Development 118, 417–425. https://doi.org/10.1242/dev.118.2.417

Kouzarides, T., 2002. Histone methylation in transcriptional control. Current Opinion in Genetics & Development 12, 198–209. https://doi.org/10.1016/S0959-437X(02)00287-3

Kretzschmar, M., Liu, F., Hata, A., Doody, J., Massagué, J., 1997. The TGF-beta family mediator Smad1 is phosphorylated directly and activated functionally by the BMP receptor kinase. Genes Dev. 11, 984–995. https://doi.org/10.1101/gad.11.8.984

Kugel, J.F., Goodrich, J.A., 2017. Finding the start site: redefining the human initiator element. Genes Dev 31, 1–2. https://doi.org/10.1101/gad.295980.117

Kwan, K.M., Fujimoto, E., Grabher, C., Mangum, B.D., Hardy, M.E., Campbell, D.S., Parant, J.M., Yost, H.J., Kanki, J.P., Chien, C.-B., 2007. The Tol2kit: A multisite gateway-based construction kit for Tol2 transposon transgenesis constructs. Developmental Dynamics 236, 3088–3099. https://doi.org/10.1002/dvdy.21343

Labun, K., Montague, T.G., Krause, M., Torres Cleuren, Y.N., Tjeldnes, H., Valen, E., 2019. CHOPCHOP v3: expanding the CRISPR web toolbox beyond genome editing. Nucleic Acids Res 47, W171–W174. https://doi.org/10.1093/nar/gkz365

Le Dréau, G., Martí, E., 2013. The multiple activities of BMPs during spinal cord development. Cell. Mol. Life Sci. 70, 4293–4305. https://doi.org/10.1007/s00018-013-1354-9

Le Dréau, G., Martí, E., 2012. Dorsal-ventral patterning of the neural tube: a tale of three signals. Dev Neurobiol 72, 1471–1481. https://doi.org/10.1002/dneu.22015

Lee, S.-K., Pfaff, S.L., 2001. Transcriptional networks regulating neuronal identity in the developing spinal cord. Nat Neurosci 4, 1183–1191. https://doi.org/10.1038/nn750

Lewis, M.W., Li, S., Franco, H.L., 2019. Transcriptional control by enhancers and enhancer RNAs. Transcription 10, 171–186. https://doi.org/10.1080/21541264.2019.1695492

Li, S., Mo, Z., Yang, X., Price, S.M., Shen, M.M., Xiang, M., 2004. Foxn4 controls the genesis of amacrine and horizontal cells by retinal progenitors. Neuron 43, 795–807. https://doi.org/10.1016/j.neuron.2004.08.041

Li, X., Guo, W., Li, J., Yue, P., Bu, H., Jiang, J., Liu, W., Xu, Y., Yuan, H., Li, T., Wang, A., 2020. Histone Acetylation at the Promoter for the Transcription Factor PuWRKY31 Affects Sucrose Accumulation in Pear Fruit1 [OPEN]. Plant Physiology 182, 2035–2046. https://doi.org/10.1104/pp.20.00002

Li, Y., Chen, X., Lu, C., 2021. The interplay between DNA and histone methylation: molecular mechanisms and disease implications. EMBO reports 22, e51803. https://doi.org/10.15252/embr.202051803

Lindström, E., Shimokawa, T., Toftgård, R., Zaphiropoulos, P.G., 2006. PTCH mutations: distribution and analyses. Human Mutation 27, 215–219. https://doi.org/10.1002/humu.20296

Litingtung, Y., Chiang, C., 2000. Specification of ventral neuron types is mediated by an antagonistic interaction between Shh and Gli3. Nat Neurosci 3, 979–985. https://doi.org/10.1038/79916

Lochab, A.K., Extavour, C.G., 2017. Bone Morphogenetic Protein (BMP) signaling in animal reproductive system development and function. Developmental Biology 427, 258–269. https://doi.org/10.1016/j.ydbio.2017.03.002

Lotfipour, S., Byun, J.S., Leach, P., Fowler, C.D., Murphy, N.P., Kenny, P.J., Gould, T.J., Boulter, J., 2013. Targeted Deletion of the Mouse α2 Nicotinic Acetylcholine Receptor Subunit Gene (Chrna2) Potentiates Nicotine-Modulated Behaviors. J Neurosci 33, 7728–7741. https://doi.org/10.1523/JNEUROSCI.4731-12.2013

Loureiro, J., Peifer, M., 1998. Roles of Armadillo, a Drosophila catenin, during central nervous system development. Current Biology 8, 622–633. https://doi.org/10.1016/S0960-9822(98)70249-0

Ma, Z., Zeng, Y., Wang, M., Liu, W., Zhou, J., Wu, C., Hou, L., Yin, B., Qiang, B., Shu, P., Peng, X., 2023. N4BP1 mediates RAM domain-dependent notch signaling turnover during neocortical development. The EMBO Journal 42, e113383. https://doi.org/10.15252/embj.2022113383

Mahler, J., Filippi, A., Driever, W., 2010. DeltaA/DeltaD Regulate Multiple and Temporally Distinct Phases of Notch Signaling during Dopaminergic Neurogenesis in Zebrafish. J. Neurosci. 30, 16621–16635. https://doi.org/10.1523/JNEUROSCI.4769-10.2010

Mangum, R., Varga, E., Boué, D.R., Capper, D., Benesch, M., Leonard, J., Osorio, D.S., Pierson, C.R., Zumberge, N., Sahm, F., Schrimpf, D., Pfister, S.M., Finlay, J.L., 2016. SHH desmoplastic/nodular medulloblastoma and Gorlin syndrome in the setting of Down syndrome: case report, molecular profiling, and review of the literature. Childs Nerv Syst 32, 2439–2446. https://doi.org/10.1007/s00381-016-3185-0

Martin, B.J.E., Brind'Amour, J., Kuzmin, A., Jensen, K.N., Liu, Z.C., Lorincz, M., Howe, L.J., 2021. Transcription shapes genome-wide histone acetylation patterns. Nat Commun 12, 210. https://doi.org/10.1038/s41467-020-20543-z

Masahira, N., Takebayashi, H., Ono, K., Watanabe, K., Ding, L., Furusho, M., Ogawa, Y., Nabeshima, Y., Alvarez-Buylla, A., Shimizu, K., Ikenaka, K., 2006. Olig2-positive progenitors in the embryonic spinal cord give rise not only to motoneurons and oligodendrocytes, but also to a subset of astrocytes and ependymal cells. Dev Biol 293, 358–369. https://doi.org/10.1016/j.ydbio.2006.02.029

Massagué, J., Seoane, J., Wotton, D., 2005. Smad transcription factors. Genes Dev. 19, 2783–2810. https://doi.org/10.1101/gad.1350705

McCrea, D.A., Rybak, I.A., 2008. Organization of mammalian locomotor rhythm and pattern generation. Brain Res Rev 57, 134–146. https://doi.org/10.1016/j.brainresrev.2007.08.006

Meeker, N.D., Hutchinson, S.A., Ho, L., Trede, N.S., 2007. Method for isolation of PCR-ready genomic DNA from zebrafish tissues. BioTechniques 43, 610–614. https://doi.org/10.2144/000112619

Megason, S.G., McMahon, A.P., 2002. A mitogen gradient of dorsal midline Wnts organizes growth in the CNS. Development 129, 2087–2098. https://doi.org/10.1242/dev.129.9.2087

Melesina, J., Simoben, C.V., Praetorius, L., Bülbül, E.F., Robaa, D., Sippl, W., 2021. Strategies To Design Selective Histone Deacetylase Inhibitors. ChemMedChem 16, 1336–1359. https://doi.org/10.1002/cmdc.202000934

Menelaou, E., McLean, D.L., 2019. Hierarchical control of locomotion by distinct types of spinal V2a interneurons in zebrafish. Nat Commun 10, 4197. https://doi.org/10.1038/s41467-019-12240-3

Merino, R., Gañan, Y., Macias, D., Economides, A.N., Sampath, K.T., Hurle, J.M., 1998. Morphogenesis of Digits in the Avian Limb Is Controlled by FGFs, TGFβs, and Noggin through BMP Signaling. Developmental Biology 200, 35–45. https://doi.org/10.1006/dbio.1998.8946

Milenkovic, L., Scott, M.P., Rohatgi, R., 2009. Lateral transport of Smoothened from the plasma membrane to the membrane of the cilium. Journal of Cell Biology 187, 365–374. https://doi.org/10.1083/jcb.200907126

Miller, R.H., Dinsio, K., Wang, R., Geertman, R., Maier, C.E., Hall, A.K., 2004. Patterning of spinal cord oligodendrocyte development by dorsally derived BMP4. J Neurosci Res 76, 9–19. https://doi.org/10.1002/jnr.20047

Ming, J.E., Roessler, E., Muenke, M., 1998. Human developmental disorders and the Sonic hedgehog pathway. Molecular Medicine Today 4, 343–349. https://doi.org/10.1016/S1357-4310(98)01299-4

Mitra, S., Sharma, P., Kaur, S., Khursheed, M.A., Gupta, S., Chaudhary, M., Kurup, A.J., Ramachandran, R., 2019. Dual regulation of lin28a by Myc is necessary during zebrafish retina regeneration. J Cell Biol 218, 489–507. https://doi.org/10.1083/jcb.201802113

Miyazono, K., Maeda, S., Imamura, T., 2005. BMP receptor signaling: Transcriptional targets, regulation of signals, and signaling cross-talk. Cytokine & Growth Factor Reviews, Bone Morphogenetic Proteins 16, 251–263. https://doi.org/10.1016/j.cytogfr.2005.01.009

Mizoguchi, T., Fukada, M., Iihama, M., Song, X., Fukagawa, S., Kuwabara, S., Omaru, S., Higashijima, S.-I., Itoh, M., 2020. Transient activation of the Notch-her15.1 axis plays an important role in the maturation of V2b interneurons. Development 147, dev191312. https://doi.org/10.1242/dev.191312

Mohedas, A.H., Xing, X., Armstrong, K.A., Bullock, A.N., Cuny, G.D., Yu, P.B., 2013. Development of an ALK2-Biased BMP Type I Receptor Kinase Inhibitor. ACS Chem. Biol. 8, 1291–1302. https://doi.org/10.1021/cb300655w

Moreno-Yruela, C., Zhang, D., Wei, W., Bæk, M., Liu, W., Gao, J., Danková, D., Nielsen, A.L., Bolding, J.E., Yang, L., Jameson, S.T., Wong, J., Olsen, C.A., Zhao, Y., 2022. Class I histone deacetylases (HDAC1–3) are histone lysine delactylases. Science Advances 8, eabi6696. https://doi.org/10.1126/sciadv.abi6696

Mueller, T.D., 2015. Chapter One - Mechanisms of BMP–Receptor Interaction and Activation, in: Litwack, G. (Ed.), Vitamins & Hormones, Bone Morphogenic Protein. Academic Press, pp. 1–61. https://doi.org/10.1016/bs.vh.2015.06.003

Mukai, T., Otsuka, F., Otani, H., Yamashita, M., Takasugi, K., Inagaki, K., Yamamura, M., Makino, H., 2007. TNF-α inhibits BMP-induced osteoblast differentiation through

activating SAPK/JNK signaling. Biochemical and Biophysical Research Communications 356, 1004–1010. https://doi.org/10.1016/j.bbrc.2007.03.099

Muroyama, Y., Fujihara, M., Ikeya, M., Kondoh, H., Takada, S., 2002. Wnt signaling plays an essential role in neuronal specification of the dorsal spinal cord. Genes Dev. 16, 548–553. https://doi.org/10.1101/gad.937102

Myers, P.Z., Eisen, J.S., Westerfield, M., 1986. Development and axonal outgrowth of identified motoneurons in the zebrafish. J. Neurosci. 6, 2278–2289. https://doi.org/10.1523/JNEUROSCI.06-08-02278.1986

Navratilova, P., Fredman, D., Hawkins, T.A., Turner, K., Lenhard, B., Becker, T.S., 2009. Systematic human/zebrafish comparative identification of *cis*-regulatory activity around vertebrate developmental transcription factor genes. Developmental Biology 327, 526–540. https://doi.org/10.1016/j.ydbio.2008.10.044

Nguyen, V.H., Trout, J., Connors, S.A., Andermann, P., Weinberg, E., Mullins, M.C., 2000. Dorsal and intermediate neuronal cell types of the spinal cord are established by a BMP signaling pathway. Development 127, 1209–1220. https://doi.org/10.1242/dev.127.6.1209

Nickel, J., Mueller, T.D., 2019. Specification of BMP Signaling. Cells 8, 1579. https://doi.org/10.3390/cells8121579

Nikaido, M., Tada, M., Saji, T., Ueno, N., 1997. Conservation of BMP signaling in zebrafish mesoderm patterning. Mechanisms of Development 61, 75–88. https://doi.org/10.1016/S0925-4773(96)00625-9

Okigawa, S., Mizoguchi, T., Okano, M., Tanaka, H., Isoda, M., Jiang, Y.-J., Suster, M., Higashijima, S., Kawakami, K., Itoh, M., 2014. Different combinations of Notch ligands and receptors regulate V2 interneuron progenitor proliferation and V2a/V2b cell fate determination. Developmental Biology 391, 196–206. https://doi.org/10.1016/j.ydbio.2014.04.011

Oliveira-Carlos, V. de, Ganz, J., Hans, S., Kaslin, J., Brand, M., 2013. Notch Receptor Expression in Neurogenic Regions of the Adult Zebrafish Brain. PLOS ONE 8, e73384. https://doi.org/10.1371/journal.pone.0073384

Pallucchi, I., Bertuzzi, M., Michel, J.C., Miller, A.C., El Manira, A., 2022. Transformation of an early-established motor circuit during maturation in zebrafish. Cell Reports 39, 110654. https://doi.org/10.1016/j.celrep.2022.110654

Panayi, H., Panayiotou, E., Orford, M., Genethliou, N., Mean, R., Lapathitis, G., Li, S., Xiang, M., Kessaris, N., Richardson, W.D., Malas, S., 2010. Sox1 is required for the specification of a novel p2-derived interneuron subtype in the mouse ventral spinal cord. J Neurosci 30, 12274–12280. https://doi.org/10.1523/JNEUROSCI.2402-10.2010

Panza, P., Sitko, A.A., Maischein, H.-M., Koch, I., Flötenmeyer, M., Wright, G.J., Mandai, K., Mason, C.A., Söllner, C., 2015. The LRR receptor Islr2 is required for retinal axon routing at the vertebrate optic chiasm. Neural Dev 10, 23. https://doi.org/10.1186/s13064-015-0050-x

Papan, C., Campos-Ortega, J.A., 1999. Region-specific cell clones in the developing spinal cord of the zebrafish. Dev Gene Evol 209, 135–144. https://doi.org/10.1007/s004270050237

Papan, C., Campos-Ortega, J.A., 1994. On the formation of the neural keel and neural tube in the zebrafishDanio (Brachydanio) rerio. Roux's Arch Dev Biol 203, 178–186. https://doi.org/10.1007/BF00636333

Park, H.-C., Shin, J., Appel, B., 2004. Spatial and temporal regulation of ventral spinal cord precursor specification by Hedgehog signaling. Development 131, 5959–5969. https://doi.org/10.1242/dev.01456

Patten, I., Placzek*, M., 2000. The role of Sonic hedgehog in neural tube patterning. CMLS, Cell. Mol. Life Sci. 57, 1695–1708. https://doi.org/10.1007/PL00000652

Peng, C.-Y., Yajima, H., Burns, C.E., Zon, L.I., Sisodia, S.S., Pfaff, S.L., Sharma, K., 2007. Notch and MAML Signaling Drives Scl-Dependent Interneuron Diversity in the Spinal Cord. Neuron 53, 813–827. https://doi.org/10.1016/j.neuron.2007.02.019

Petrova, R., Joyner, A.L., 2014. Roles for Hedgehog signaling in adult organ homeostasis and repair. Development 141, 3445–3457. https://doi.org/10.1242/dev.083691

Pierreux, C.E., Nicolás, F.J., Hill, C.S., 2000. Transforming Growth Factor β-Independent Shuttling of Smad4 between the Cytoplasm and Nucleus. Molecular and Cellular Biology 20, 9041–9054. https://doi.org/10.1128/MCB.20.23.9041-9054.2000

Polizio, A.H., Chinchilla, P., Chen, X., Kim, S., Manning, D.R., Riobo, N.A., 2011. Heterotrimeric Gi Proteins Link Hedgehog Signaling to Activation of Rho Small GTPases to Promote Fibroblast Migration *. Journal of Biological Chemistry 286, 19589–19596. https://doi.org/10.1074/jbc.M110.197111

Pond, K.W., Doubrovinski, K., Thorne, C.A., 2020. Wnt/β-catenin Signaling in Tissue Self-Organization. Genes 11, 939. https://doi.org/10.3390/genes11080939

Ravanelli, A.M., Appel, B., 2015. Motor neurons and oligodendrocytes arise from distinct cell lineages by progenitor recruitment. Genes Dev. 29, 2504–2515. https://doi.org/10.1101/gad.271312.115

Rayon, T., Maizels, R.J., Barrington, C., Briscoe, J., 2021. Single-cell transcriptome profiling of the human developing spinal cord reveals a conserved genetic programme with human-specific features. Development 148, dev199711. https://doi.org/10.1242/dev.199711

Resh, M.D., 2021. Palmitoylation of Hedgehog proteins by Hedgehog acyltransferase: roles in signalling and disease. Open Biology 11, 200414. https://doi.org/10.1098/rsob.200414

Rima, M., Lattouf, Y., Abi Younes, M., Bullier, E., Legendre, P., Mangin, J.-M., Hong, E., 2020. Dynamic regulation of the cholinergic system in the spinal central nervous system. Sci Rep 10, 15338. https://doi.org/10.1038/s41598-020-72524-3

Rimkus, T.K., Carpenter, R.L., Qasem, S., Chan, M., Lo, H.-W., 2016. Targeting the Sonic Hedgehog Signaling Pathway: Review of Smoothened and GLI Inhibitors. Cancers 8, 22. https://doi.org/10.3390/cancers8020022

Robbins, D.J., Fei, D.L., Riobo, N.A., 2012. The Hedgehog Signal Transduction Network. Science Signaling 5, re6–re6. https://doi.org/10.1126/scisignal.2002906

Roelink, H., Porter, J.A., Chiang, C., Tanabe, Y., Chang, D.T., Beachy, P.A., Jessell, T.M., 1995. Floor plate and motor neuron induction by different concentrations of the amino-terminal cleavage product of sonic hedgehog autoproteolysis. Cell 81, 445–455. https://doi.org/10.1016/0092-8674(95)90397-6

Roth, S.Y., Denu, J.M., Allis, C.D., 2001. Histone Acetyltransferases. Annual Review of Biochemistry 70, 81–120. https://doi.org/10.1146/annurev.biochem.70.1.81

Ruiz, L., Kaczmarska, Z., Gomes, T., Aragon, E., Torner, C., Freier, R., Baginski, B., Martin-Malpartida, P., de Martin Garrido, N., Marquez, José.A., Cordeiro, T.N., Pluta, R., Macias, M.J., 2021. Unveiling the dimer/monomer propensities of Smad MH1-DNA complexes. Computational and Structural Biotechnology Journal 19, 632–646. https://doi.org/10.1016/j.csbj.2020.12.044

Sagner, A., Briscoe, J., 2019. Establishing neuronal diversity in the spinal cord: a time and a place. Development 146, dev182154. https://doi.org/10.1242/dev.182154

Samuel, G., Miller, D., Saint, R., 2001. Conservation of a DPP/BMP signaling pathway in the nonbilateral cnidarian Acropora millepora. Evolution & Development 3, 241–250. https://doi.org/10.1046/j.1525-142x.2001.003004241.x

Santa, F.D., Barozzi, I., Mietton, F., Ghisletti, S., Polletti, S., Tusi, B.K., Muller, H., Ragoussis, J., Wei, C.-L., Natoli, G., 2010. A Large Fraction of Extragenic RNA Pol II Transcription Sites Overlap Enhancers. PLOS Biology 8, e1000384. https://doi.org/10.1371/journal.pbio.1000384

Santistevan, N.J., Nelson, J.C., Ortiz, E.A., Miller, A.H., Halabi, D.K., Sippl, Z.A., Granato, M., Grinblat, Y., 2022. cacna2d3, a voltage-gated calcium channel subunit, functions in vertebrate habituation learning and the startle sensitivity threshold. PLOS ONE 17, e0270903. https://doi.org/10.1371/journal.pone.0270903

Satou, C., Sugioka, T., Uemura, Y., Shimazaki, T., Zmarz, P., Kimura, Y., Higashijima, S., 2020. Functional Diversity of Glycinergic Commissural Inhibitory Neurons in Larval Zebrafish. Cell Reports 30, 3036-3050.e4. https://doi.org/10.1016/j.celrep.2020.02.015

Schäfer, M., Kinzel, D., Winkler, C., 2007. Discontinuous organization and specification of the lateral floor plate in zebrafish. Dev Biol 301, 117–129. https://doi.org/10.1016/j.ydbio.2006.09.018

Schmierer, B., Hill, C.S., 2007. TGFβ–SMAD signal transduction: molecular specificity and functional flexibility. Nat Rev Mol Cell Biol 8, 970–982. https://doi.org/10.1038/nrm2297

Scott, K., O'Rourke, R., Winkler, C.C., Kearns, C.A., Appel, B., 2021. Temporal single-cell transcriptomes of zebrafish spinal cord pMN progenitors reveal distinct neuronal and

glial progenitor populations. Developmental Biology 479, 37–50. https://doi.org/10.1016/j.ydbio.2021.07.010

Sengupta, M., Daliparthi, V., Roussel, Y., Bui, T.V., Bagnall, M.W., 2021. Spinal V1 neurons inhibit motor targets locally and sensory targets distally. Curr Biol 31, 3820-3833.e4. https://doi.org/10.1016/j.cub.2021.06.053

Seredick, S., Hutchinson, S.A., Van Ryswyk, L., Talbot, J.C., Eisen, J.S., 2014. Lhx3 and Lhx4 suppress Kolmer–Agduhr interneuron characteristics within zebrafish axial motoneurons. Development 141, 3900–3909. https://doi.org/10.1242/dev.105718

Shah, A.N., Davey, C.F., Whitebirch, A.C., Miller, A.C., Moens, C.B., 2015. Rapid reverse genetic screening using CRISPR in zebrafish. Nat Methods 12, 535–540. https://doi.org/10.1038/nmeth.3360

Shah, K., Kazi, J.U., 2022. Phosphorylation-Dependent Regulation of WNT/Beta-Catenin Signaling. Front. Oncol. 12. https://doi.org/10.3389/fonc.2022.858782

Shahbazian, M.D., Grunstein, M., 2007. Functions of Site-Specific Histone Acetylation and Deacetylation. Annual Review of Biochemistry 76, 75–100. https://doi.org/10.1146/annurev.biochem.76.052705.162114

Shimizu, T., Kagawa, T., Wada, T., Muroyama, Y., Takada, S., Ikenaka, K., 2005. Wnt signaling controls the timing of oligodendrocyte development in the spinal cord. Developmental Biology 282, 397–410. https://doi.org/10.1016/j.ydbio.2005.03.020

Shin, J., Poling, J., Park, H.-C., Appel, B., 2007. Notch signaling regulates neural precursor allocation and binary neuronal fate decisions in zebrafish. Development 134, 1911–1920. https://doi.org/10.1242/dev.001602

Shinozuka, T., Takada, S., 2021. Morphological and Functional Changes of Roof Plate Cells in Spinal Cord Development. JDB 9, 30. https://doi.org/10.3390/jdb9030030

Simon, R., Lufkin, T., Bergemann, A.D., 2007. Homeobox gene Sax2 deficiency causes an imbalance in energy homeostasis. Developmental Dynamics 236, 2792–2799. https://doi.org/10.1002/dvdy.21320

Skaggs, K., Martin, D.M., Novitch, B.G., 2011. Regulation of spinal interneuron development by the Olig-related protein Bhlhb5 and Notch signaling. Development 138, 3199–3211. https://doi.org/10.1242/dev.057281

Smith, G.M., Falone, A.E., Frank, E., 2012. Sensory axon regeneration: rebuilding functional connections in the spinal cord. Trends Neurosci 35, 156–163. https://doi.org/10.1016/j.tins.2011.10.006

Song, W., Nadeau, P., Yuan, M., Yang, X., Shen, J., Yankner, B.A., 1999. Proteolytic release and nuclear translocation of Notch-1 are induced by presenilin-1 and impaired by pathogenic presenilin-1 mutations. Proceedings of the National Academy of Sciences 96, 6959–6963. https://doi.org/10.1073/pnas.96.12.6959

Sorrentino, A., Thakur, N., Grimsby, S., Marcusson, A., von Bulow, V., Schuster, N., Zhang, S., Heldin, C.-H., Landström, M., 2008. The type I TGF-β receptor engages TRAF6 to activate TAK1 in a receptor kinase-independent manner. Nat Cell Biol 10, 1199–1207. https://doi.org/10.1038/ncb1780

Starr, D.B., Hawley, D.K., 1991. TFIID binds in the minor groove of the TATA box. Cell 67, 1231–1240. https://doi.org/10.1016/0092-8674(91)90299-E

Steinhart, Z., Angers, S., 2018. Wnt signaling in development and tissue homeostasis. Development 145, dev146589. https://doi.org/10.1242/dev.146589

Tacchelly-Benites, O., Wang, Z., Yang, E., Benchabane, H., Tian, A., Randall, M.P., Ahmed, Y., 2018. Axin phosphorylation in both Wnt-off and Wnt-on states requires the tumor suppressor APC. PLOS Genetics 14, e1007178. https://doi.org/10.1371/journal.pgen.1007178

Tajer, B., Dutko, J.A., Little, S.C., Mullins, M.C., 2021. BMP heterodimers signal via distinct type I receptor class functions. Proceedings of the National Academy of Sciences 118, e2017952118. https://doi.org/10.1073/pnas.2017952118

Tan, X., Shi, S.-H., 2013. Neocortical neurogenesis and neuronal migration. Wiley Interdiscip Rev Dev Biol 2, 443–459. https://doi.org/10.1002/wdev.88

Tan, Z., Qin, S., Yuan, Y., Hu, X., Huang, X., Liu, H., Pu, Y., He, C., Su, Z., 2022. NOTCH1 signaling regulates the latent neurogenic program in adult reactive astrocytes after spinal cord injury. Theranostics 12, 4548. https://doi.org/10.7150/thno.71378

Tanabe, Y., William, C., Jessell, T.M., 1998. Specification of motor neuron identity by the MNR2 homeodomain protein. Cell 95, 67–80. https://doi.org/10.1016/s0092-8674(00)81783-3

Thaler, J., Harrison, K., Sharma, K., Lettieri, K., Kehrl, J., Pfaff, S.L., 1999. Active Suppression of Interneuron Programs within Developing Motor Neurons Revealed by Analysis of Homeodomain Factor HB9. Neuron 23, 675–687. https://doi.org/10.1016/S0896-6273(01)80027-1

Thaler, J.P., Lee, S.-K., Jurata, L.W., Gill, G.N., Pfaff, S.L., 2002. LIM Factor Lhx3 Contributes to the Specification of Motor Neuron and Interneuron Identity through Cell-Type-Specific Protein-Protein Interactions. Cell 110, 237–249. https://doi.org/10.1016/S0092-8674(02)00823-1

Timmermann, S., Lehrmann, H., Polesskaya, A., Harel-Bellan, A., 2001. Histone acetylation and disease. CMLS, Cell. Mol. Life Sci. 58, 728–736. https://doi.org/10.1007/PL00000896

Todd, K.J., Lan-Chow-Wing, N., Salin-Cantegrel, A., Cotter, A., Zagami, C.J., Lo, R., Stifani, S., 2012. Establishment of motor neuron-V3 interneuron progenitor domain boundary in ventral spinal cord requires Groucho-mediated transcriptional corepression. PLoS One 7, e31176. https://doi.org/10.1371/journal.pone.0031176

Tokarska, A., Silberberg, G., 2022. GABAergic interneurons expressing the α2 nicotinic receptor subunit are functionally integrated in the striatal microcircuit. Cell Reports 39, 110842. https://doi.org/10.1016/j.celrep.2022.110842

Turner, B.M., 2000. Histone acetylation and an epigenetic code. BioEssays 22, 836–845. https://doi.org/10.1002/1521-1878(200009)22:9<836::AID-BIES9>3.0.CO;2-X

Umeda, K., Shoji, W., 2017. From neuron to behavior: Sensory-motor coordination of zebrafish turning behavior. Dev Growth Differ 59, 107–114. https://doi.org/10.1111/dgd.12345

van den Brink, G.R., 2007. Hedgehog Signaling in Development and Homeostasis of the Gastrointestinal Tract. Physiological Reviews 87, 1343–1375. https://doi.org/10.1152/physrev.00054.2006

Wang, M.M., 2011. Notch signaling and Notch signaling modifiers. The International Journal of Biochemistry & Cell Biology 43, 1550–1562. https://doi.org/10.1016/j.biocel.2011.08.005

Wang, R., Guo, S., Yang, L., 2023. Tal2 is required for generation of GABAergic neurons in the zebrafish midbrain. Dev Dyn 252, 263–275. https://doi.org/10.1002/dvdy.534

Werner, F., Jain, M.K., Feinberg, M.W., Sibinga, N.E.S., Pellacani, A., Wiesel, P., Chin, M.T., Topper, J.N., Perrella, M.A., Lee, M.-E., 2000. Transforming Growth Factor-β1 Inhibition of Macrophage Activation Is Mediated via Smad3 *. Journal of Biological Chemistry 275, 36653–36658. https://doi.org/10.1074/jbc.M004536200

Williams, K., Ribera, A.B., 2020. Long-lived zebrafish Rohon-Beard cells. Dev Biol 464, 45–52. https://doi.org/10.1016/j.ydbio.2020.05.003

Wine-Lee, L., Ahn, K.J., Richardson, R.D., Mishina, Y., Lyons, K.M., Crenshaw, E.B., III, 2004. Signaling through BMP type 1 receptors is required for development of interneuron cell types in the dorsal spinal cord. Development 131, 5393–5403. https://doi.org/10.1242/dev.01379

Wodarz, A., Nusse, R., 1998. MECHANISMS OF WNT SIGNALING IN DEVELOPMENT. Annual Review of Cell and Developmental Biology 14, 59–88. https://doi.org/10.1146/annurev.cellbio.14.1.59

Xing, L., Anbarchian, T., Tsai, J.M., Plant, G.W., Nusse, R., 2018. Wnt/β-catenin signaling regulates ependymal cell development and adult homeostasis. Proc Natl Acad Sci U S A 115, E5954–E5962. https://doi.org/10.1073/pnas.1803297115

Xing, L., Chai, R., Wang, J., Lin, J., Li, H., Wang, Y., Lai, B., Sun, J., Chen, G., 2022. Expression of myelin transcription factor 1 and lamin B receptor mediate neural progenitor fate transition in the zebrafish spinal cord pMN domain. J Biol Chem 298, 102452. https://doi.org/10.1016/j.jbc.2022.102452

Xu, L., Thali, M., Schaffner, W., 1991. Upstream box/TATA box order is the major determinant of the direction of transcription. Nucleic Acids Research 19, 6699–6704. https://doi.org/10.1093/nar/19.24.6699

Xu, X., Yu, Q., Fang, M., Yi, M., Yang, A., Xie, B., Yang, J., Zhang, Z., Dai, Z., Qiu, M., 2020. Stage-specific regulation of oligodendrocyte development by Hedgehog signaling in the spinal cord. Glia 68, 422–434. https://doi.org/10.1002/glia.23729

Yamashita, H., Ten Dijke, P., Heldin, C.-H., Miyazono, K., 1996. Bone morphogenetic protein receptors. Bone 19, 569–574. https://doi.org/10.1016/S8756-3282(96)00259-1

Yan, X., Liao, H., Cheng, M., Shi, X., Lin, X., Feng, X.-H., Chen, Y.-G., 2016. Smad7 Protein Interacts with Receptor-regulated Smads (R-Smads) to Inhibit Transforming Growth

Factor-β (TGF-β)/Smad Signaling *. Journal of Biological Chemistry 291, 382–392. https://doi.org/10.1074/jbc.M115.694281

Yang, L., Wang, F., Strähle, U., 2020. The Genetic Programs Specifying Kolmer–Agduhr Interneurons. Front. Neurosci. 14. https://doi.org/10.3389/fnins.2020.577879

Yang, Y., Zhang, R., Li, Z., Mei, L., Wan, S., Ding, H., Chen, Z., Xing, J., Feng, H., Han, J., Jiang, H., Zheng, M., Luo, C., Zhou, B., 2020. Discovery of Highly Potent, Selective, and Orally Efficacious p300/CBP Histone Acetyltransferases Inhibitors. J. Med. Chem. 63, 1337–1360. https://doi.org/10.1021/acs.jmedchem.9b01721

Yu, K., McGlynn, S., Matise, M.P., 2013. Floor plate-derived sonic hedgehog regulates glial and ependymal cell fates in the developing spinal cord. Development 140, 1594–1604. https://doi.org/10.1242/dev.090845

Zhang, J., Lanuza, G.M., Britz, O., Wang, Z., Siembab, V.C., Zhang, Y., Velasquez, T., Alvarez, F.J., Frank, E., Goulding, M., 2014. V1 and v2b interneurons secure the alternating flexor-extensor motor activity mice require for limbed locomotion. Neuron 82, 138–150. https://doi.org/10.1016/j.neuron.2014.02.013

Zhang, Q., Xu, H., Zhao, W., Zheng, J., Sun, L., Luo, C., 2020. Zygotic Vsx1 Plays a Key Role in Defining V2a Interneuron Sub-Lineage by Directly Repressing tal1 Transcription in Zebrafish. International Journal of Molecular Sciences 21, 3600. https://doi.org/10.3390/ijms21103600

Zhou, B., Lin, W., Long, Y., Yang, Y., Zhang, H., Wu, K., Chu, Q., 2022. Notch signaling pathway: architecture, disease, and therapeutics. Sig Transduct Target Ther 7, 1–33. https://doi.org/10.1038/s41392-022-00934-y

Zhou, Q., Heinke, J., Vargas, A., Winnik, S., Krauss, T., Bode, C., Patterson, C., Moser, M., 2007. ERK signaling is a central regulator for BMP-4 dependent capillary sprouting. Cardiovascular Research 76, 390–399. https://doi.org/10.1016/j.cardiores.2007.08.003